PORTIONS OF THIS DOCUMENT ARE ILLEGIBLE

NUREG/CR-3069
SAND82-2738/2
Vol. 2

Interaction of Electromagnetic Pulse with Commercial Nuclear Power Plant Systems

Main Report

Prepared by D. M. Ericson, Jr., D. F. Strawe, S. J. Sandberg, V. K. Jones, G. D. Rensner, R. W. Shoup, R. J. Hanson, C. B. Williams

Sandia National Laboratories

Boeing Aerospace Company

Booz-Allen & Hamilton, Inc.

IRT Corporation

Prepared for
U.S. Nuclear Regulatory Commission

GPO Printed copy price $11.00

NUREG/CR--3069-Vol.2

NUREG/CR-3069, Vol. 2
SAND82-2738/2
AN, 1S, 9E, 9U

DE83 007881

Interaction of Electromagnetic Pulse with Commercial Nuclear-Power-Plant Systems

Volume II

MAIN REPORT

Manuscript Completed: December 1982
Date Published: February 1983

David M. Ericson, Jr.
Sandia National Laboratories

David F. Strawe
Steven J. Sandberg
Vincent K. Jones*
Boeing Aerospace Company

Gary D. Rensner
R. William Shoup**
Roy J. Hanson
Booz-Allen & Hamilton, Inc.

C. Brian Williams
IRT Corporation

Sandia National Laboratories
Albuquerque, New Mexico 87185
operated by
Sandia Corporation
for the
U. S. Department of Energy

Prepared for
Office of Nuclear Reactor Regulation
U. S. Nuclear Regulatory Commission
Washington, DC 20555

NRC Fin No. A1118

*Now with Science and Engineering Associates.
**Now with IRT Corporation.

Abstract

This study examines the interaction of the electromagnetic pulse from a high altitude nuclear burst with commercial nuclear power plant systems. The potential vulnerability of systems required for safe shutdown of a specific nuclear power plant are explored. EMP signal coupling, induced plant response and component damage thresholds are established using techniques developed over several decades under Defense Nuclear Agency sponsorship. A limited test program was conducted to verify the coupling analysis technique as applied to a nuclear power plant. The results are extended, insofar as possible to other nuclear plants. Based upon the analysis, it was concluded that: (1) Diffuse fields inside Seismic Class I buildings are negligible; (2) EMP signal entry points are identifiable; (3) Interior signal attenuation can be reasonably modeled; (4) Damage thresholds, even for equipment containing solid state components are high; (5) EMP induced signals at the critical equipment in the example plant are much less than nominal operating levels, but plant topology and cabling practice have a strong influence on responses; (6) The likelihood that individual components examined will fail is small; therefore, it is unlikely that an EMP event would fail sufficient equipment so as to prevent safe shutdown.

CONTENTS

CONTENTS (Continued)

CONTENTS (Continued)

APPENDICES

ILLUSTRATIONS

ILLUSTRATIONS (Continued)

ILLUSTRATIONS (Continued)

ILLUSTRATIONS (Continued)

TABLES

TABLES

Acknowledgments

The authors are indebted to the Tennessee Valley Authority for their cooperation and assistance during the conduct of this study. Special appreciation goes to Mr. Charles Gilliland of the Office of Engineering Design and Construction for his aid in obtaining plant drawings, equipment specifications and other engineering data, and to Mr. James Vineyard of the Watts Bar Nuclear Plant for his aid in defining equipment interfaces and operating procedures during the on-site portions of this study. Mr. Vineyard's knowledge of plant details saved many hours of effort. Our thanks also go to Mr. James Gallacher, Mr. Steve Wilmet, and Mr. Bruce Harlacher of IRT Corporation for their efforts in conducting the verification measurements.

1.0 Introduction

1.1 Background

It has been recognized for many years that the detonation of a nuclear weapon at high altitude ($\geq$ 40 kM) leads to the creation of an intense electromagnetic field of very short duration, the electromagnetic pulse (EMP). The EMP from a single detonation at the proper altitude could induce large currents and voltages in electrical equipment over the entire continental United States. As a result, the U.S. Defense Department has devoted substantial resources to understanding EMP effects on military systems. Based upon these studies, some weapons systems and defense communications systems have been "hardened" against EMP by radio frequency shielding or by installation of protective devices.

At the present time, commercial nuclear power plants are not required to have protection against EMP. The Nuclear Regulatory Commission (NRC) Regulations (10 CFR 50.13) state that license applicants are, "not required to provide for design features or other measures for the specific purpose of protection against the effects of (a) attacks and destructive acts including sabotage, directed at the facility by an enemy of the United States, whether a foreign government or other person, or (b) use or deployment of weapons incident to U. S. defense activities." Therefore, no protection against EMP has been required in nuclear power plant design. Given this situation, the present study was undertaken to address the question: "Could the effects of an EMP due to high altitude nuclear weapon detonation (which produces no significant radiation or physical damage at ground level) adversely affect the safe shutdown capability of commercial nuclear power plants?" A sustained inability to shut down such plants could lead to significant public health effects or impair our national recovery capability in event of an actual nuclear attack. Therefore, the overall objective of this study is to provide the NRC with a basis for considering the need to amend the regulations to include design requirements for the protection of nuclear power plants against the effects of EMP.

The effects of EMP on a nuclear power plant were considered in earlier studies by the Oak Ridge National Laboratory.[1,2] The purpose of the work described in Reference 2 was to determine if EMP is a serious problem for nuclear power plants and, if necessary, recommend means of protecting these plants from potentially unsafe conditions. This was a limited scope study and as a result, zero or first-order estimates were used to define EMP induced transients and their probable effects on the plant. In the Oak Ridge study the emphasis was upon the EMP signal which could be induced directly on plant cabling, given very conservative assumptions on shielding effectiveness. Less effort was directed toward EMP-induced signals induced on cabling penetrating into the plant because for the plant considered all underground ducting had metal conduit over the entire length. Although the study drew upon design information for several

plant types, no single plant was subjected to a detailed analyses. The Oak Ridge study concluded that,

> "The most probable effect of EMP on a modern nuclear power plant is an unscheduled shutdown. EMP may also cause an extended shutdown by the unnecessary activation of some safety related systems. In general, EMP would be a nuisance to nuclear plants, but it is not considered a serious threat to plant safety."

Because the Oak Ridge study did not attempt to analyze any particular plant in depth, some questions persist as to the applicability of the conclusions, and as to whether or not nuclear plants can be safely shutdown subsequent to an EMP interaction. Also, some of the newer operating plants and plants under construction use more electronic devices (semiconductors, transistors, integrated circuits, etc.) considered to be particularly susceptible to the currents and voltages which can be induced by an EMP interaction than do the older plants. Because of the resultant uncertainty about EMP effects on commercial nuclear power plant shutdown capability, this study was undertaken.

The vulnerability of nuclear power plants to sabotage or terrorist acts employing land-based generators which are capable of producing EMP-like effects was also considered early in the study. It was concluded that a serious threat of this type did not exist. This is discussed further in Section 2.4.

1.2 Objectives

This program was established as a scoping study with the following objectives:

1. Determine the vulnerability of systems required for safe shutdown of a specific nuclear plant to the effects of EMP.

2. Establish how any safe shutdown systems vulnerable to EMP may best be hardened against it.

3. Characterize to the extent possible, the effects of EMP on nuclear plants in general based upon the results for systems in the example plant.

An alternate expression of the objectives is that this study assesses the EMP sensitivity of essential features of selected safe shutdown systems on nuclear power plants in order to identify any points which may be unduly exposed or sensitive. Then, where appropriate, proposes remedies for such sensitivity.

1.3 Study Approach

To accomplish these objectives, the program was structured as shown on Figure 1.1. First the systems of concern were identified and defined. Then estimates were made of the currents and voltages which might exist at key points (systems of concern) if the plant

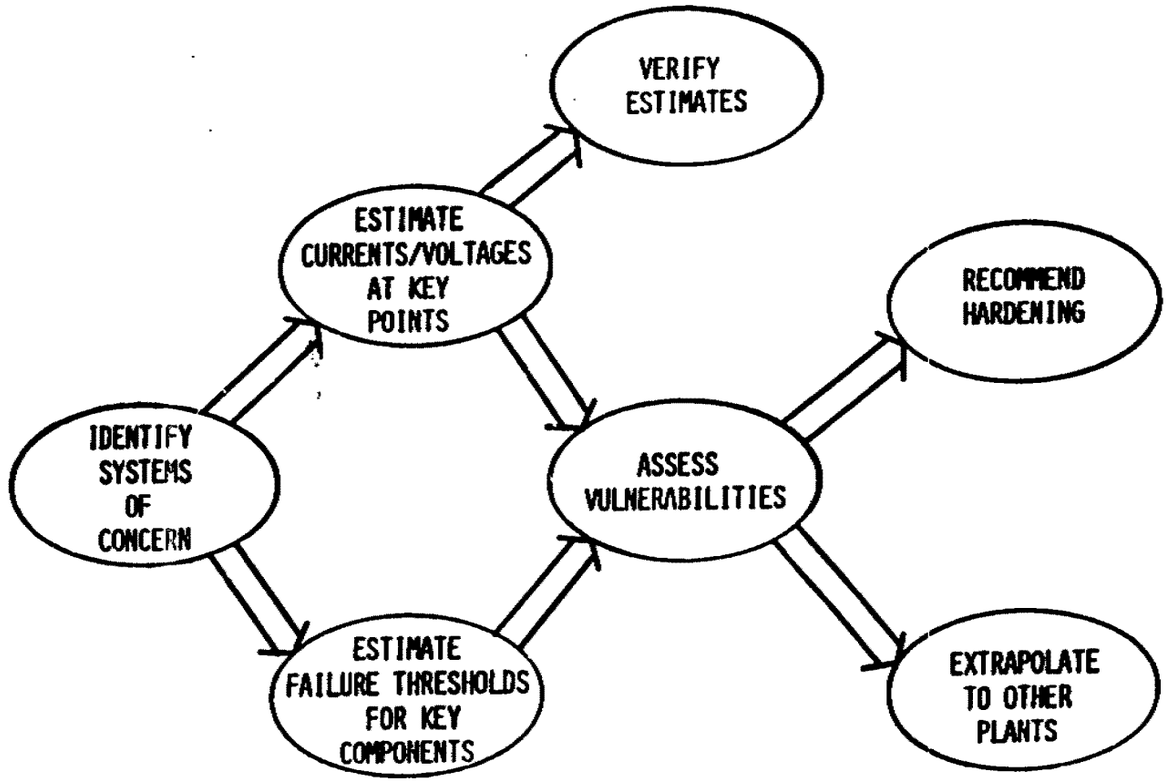

Figure 1.1. Study Approach for EMP Interaction with Nuclear Power Plants.

should be subjected to an EMP. This involves examining the plant in light of the potential interaction mechanisms, and based upon the configuration of the plant systems (that is, what loads are active, what circuits are open, where are cables routed, etc.) analyzing how signals could be induced and distributed. Concurrently, component damage thresholds were estimated. The components of the systems of concern were examined, and based upon circuit configurations and piecepart characteristics, estimates made of the signal levels at the component interconnections which could cause failure of the component. These two sets of estimates were then compared to assess the vulnerability of the selected components. Because nuclear plants, like many military systems, are very complex, a modest experimental program was conducted to provide some verification of the estimated induced signal levels. These measurements were not intended to establish whether the example facility is or is not hard to EMP. Rather they serve to verify (or reject) conclusions reached about signal distribution and attenuation. If vulnerabilities are predicted, recommendations are made for eliminating or reducing them; that is, recommendations are made for hardening. Finally, the results are extrapolated to other nuclear plants. This report describes the study and reports the results and conclusions.

1.4 Study Organization

Any investigation of the potential effects of EMP on commercial nuclear power plants requires a broad range of expertise in nuclear plant systems and nuclear weapons effects. For this reason, a number of government and industry organizations are involved as shown in Figure 1.2. Overall program direction is the responsibility of the NRC Office of Nuclear Reactor Regulation. The program technical monitor is supported by other members of the NRC staff and a Research Review Panel comprised of nationally known authorities on nuclear systems and nuclear weapon effects. The Defense Nuclear Agency (DNA) of the Department of Defense (DOD) participated in the planning of the program and is represented on the review panel. The day-to-day technical management has been handled by Sandia National Laboratories. In this capacity, Sandia provided the necessary nuclear systems analyses and the interfaces between the subcontractors conducting specific portions of the study. The EMP response and vulnerability analyses were prepared by Boeing Aerospace Co. using the techniques and expertise developed over a number of years in various programs done for the DOD. The verification measurements were made by IRT Corporation, again using techniques, equipment, and expertise developed in various DOD programs. The damage threshold estimates were developed by Booz-Allen & Hamilton. Although similar work has been sponsored by the DOD, the equipment used in nuclear power plants contains components which are not included in current damage threshold data bases. This required Booz-Allen to do some extrapolation.

Subsequent sections of this report outline the boundary assumptions and constraints, the implementation of the approach, described above, and the results of the study.

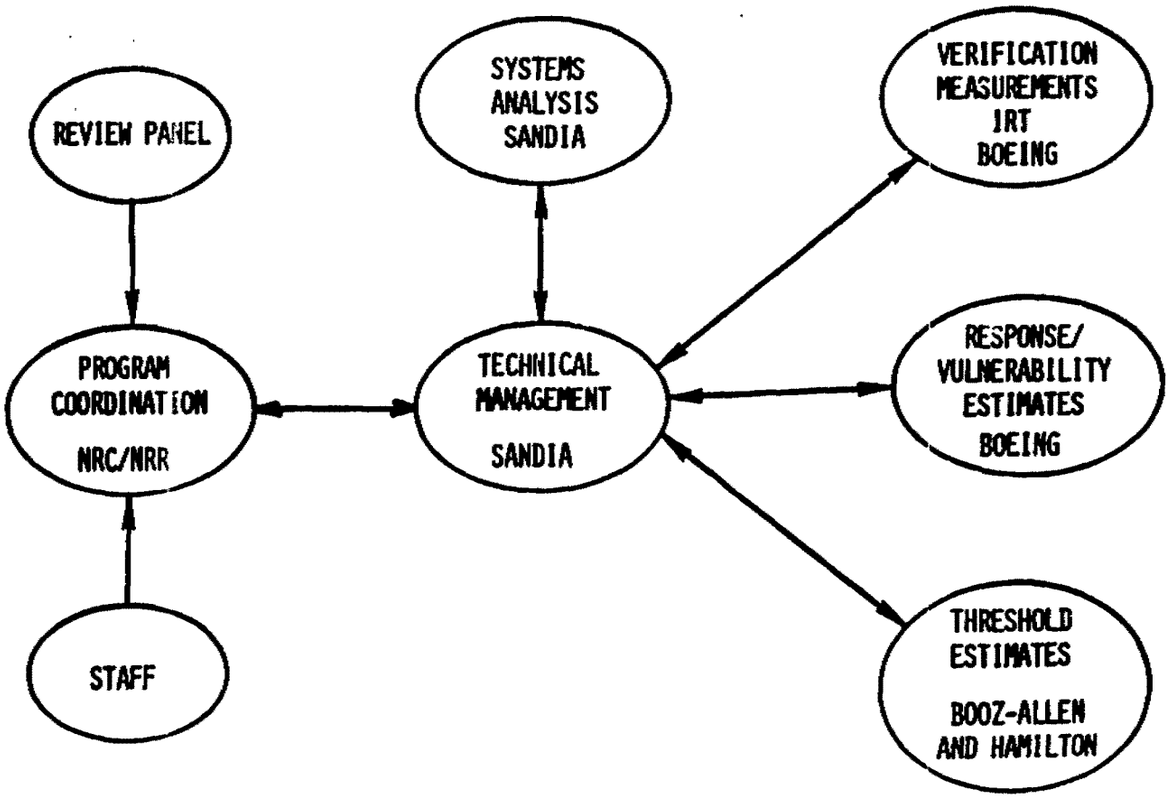

Figure 1.2. EMP Study Organization.

1.5 Study Constraints and Assumptions

Certain constraints and assumptions were adopted early in the work to keep the problem tractable. These bounding conditions are discussed in more detail where they appear in the report. However, they are assembled here because they effect the conduct of the study and the conclusions drawn, and so that they may be more readily identified by the reader.

1. The study is limited to those systems required for safe shutdown of the nuclear plant. It is focused on particular systems and on components representative of classes of equipment used in plant systems so that a detailed analysis provides insight into potential vulnerabilities.

2. The study is based on a "worst case" EMP threat situation. That is, it was assumed that the incident EMP threat embodied a bounding peak field intensity and an orientation relative to the plant system such as to optimally excite every point of interaction.

3. The magnetohydrodynamic (MHD) EMP was not considered extensively in the study for reasons cited in Section 2.3.

4. Permanent damage failure is the criterion used to assess system vulnerability. That is, signal upset effects were not considered in the study.

5. No attempt was made to estimate damage thresholds for cables, power and distribution transformers and rotating machinery. This was not deemed necessary because of considerations cited in Section 7.1, however, estimates of such thresholds based upon available data are used in Section 8.0.

6. The damage threshold calculations were analytical only, i.e., no supporting component test program was conducted as is traditionally done by the EMP effects research community. However, the data base used included experimental data from previous programs, published threshold data, and data derived using empirical models and published device electrical parameters.

7. Because semiconductor devices generally have been shown to be more susceptible to EMP induced failure than passive components, the failure threshold analysis focused upon those devices and excluded the passive components.

8. The failure threshold analysis was conducted at 1 MHz, chosen as a median value for the predicted dominant responses. Coupling data subsequently developed (Figure 6.11) indicates that this was a reasonable choice.

9. Internal interfaces within individual modules or equipment cabinets were not included in the damage threshold analysis. That is, on equipment items analyzed, only those pins that serve as interfaces to the "outside world" were considered. More specifically, the threat parameter (voltage or current) is traced from its source in the external circuitry to the module interface pin, the individual component damage threshold parameter is reflected back from the component through the module circuitry to the same interface pin, and the parameter valves are then compared.

2.0 EMP Phenomena of Interest

2.1 High-Altitude EMP

When a nuclear weapon is detonated at very high altitudes (≥40 kM), the prompt radiation travels substantial distances before significant interactions occur in the upper atmosphere. Eventually, however, the energy in the form of gamma radiation that is radiated toward the earth begins to interact with air molecules, primarily through Compton scattering. Because the gamma energies are high there is a net "forward" motion of the Compton electrons. That is, a net movement of charge in the same direction as the gamma photons. However, because the negatively charged electrons are moving in the geomagnetic field, they are turned. The acceleration associated with this turning produces radiation which is propagated earthward. Because the gamma photons travel at light speed and the electrons travel in the same direction, the radiation from the turning interferes constructively, with the net result that a large radio frequency signal is generated. This is the high-altitude electromagnetic pulse (HEMP). A more complete technical descrption of this phenomena may be found in a review article by Longmire.[3]

The EMP signal generated by the interaction described above is characterized by intense electric fields with peak values approaching 10-50 kilovolts per meter. The pulse has a very short rise time, on the order of 5-10 nanoseconds with a duration of 0.5-1 microsecond. The peak power density is high, approaching several megawatts per square meter. However, because of the very short pulse duration and because only a very small fraction of the total weapon energy is converted to EMP, the total energy density is modest, on the order of a few tenths of a joule per square meter (see Table 2.1).

Table 2.1.

Typical EMP Values

Peak Electric Fields	~10-50 kV/ M
Pulse Rise Time	~ 5-10 nsec
Pulse Duration	~ 0.5-1 μsec
Peak Power Density	~ 1-5 MW/m^2
Total Energy Density	~ 0.1-0.9 J/m^2

With weapon burst heights of 100 kilometers the area covered by the pulse is very large. In fact, a single megaton size detonation can cover most of the North American Continent with fields of tens of kilovolts per meter as illustrated in Figure 2.1. The field strengths near the outer limit of coverage will be about half that of the maximum which occurs in the vicinity of surface zero in Figure 2.2.

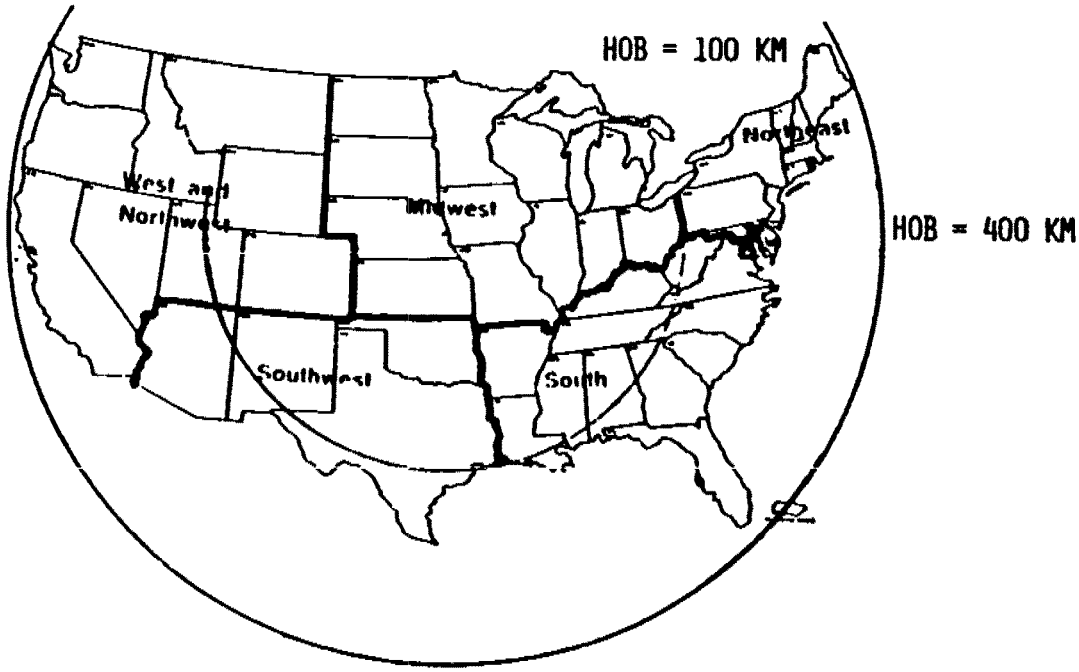

Figure 2.1. Tangent Radius (Surface Area Covered by EMP) for Two Burst Heights.

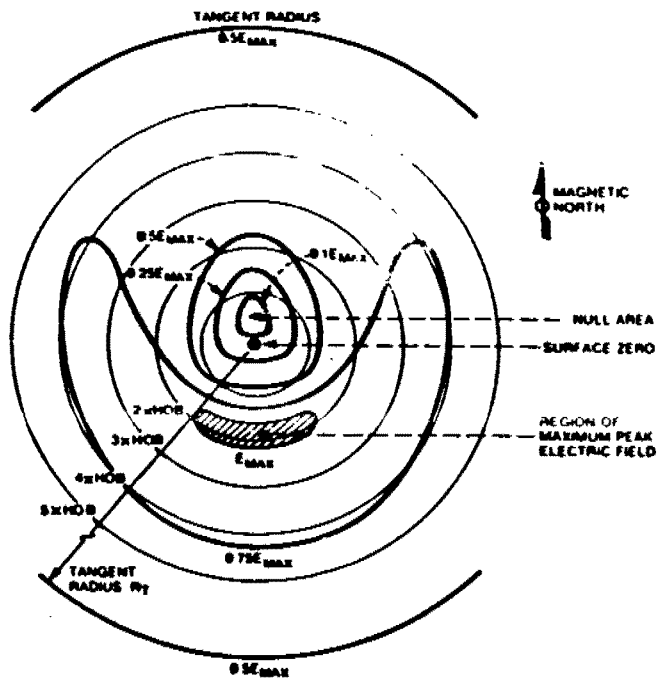

Figure 2.2. Variations in High Altitude EMP Peak Electric Field on Surface of Continental United States (Reference 4).

2.2 EMP Interactions

The HEMP, being a broad-band radio frequency signal, can interact with a variety of electrical networks which are specifically designed as antennas or which act as an antenna when subjected to such a signal. For land-based facilities, such as nuclear power plants, we can identify three potential interaction paths. The EMP signal may penetrate directly into the plant interior, the so-called diffused field, and then couple with interior plant cabling to induce currents on those cables. The EMP can interact with the external power grid to which the plant is connected, and currents induced on the external distribution system in close proximity to the plant could penetrate into the plant on power lines feeding plant systems. Finally, the EMP might induce currents on power and instrumentation lines which interconnect various plant buildings and systems. All of these potential mechanisms are addressed in this study.

2.3 EMP Threat

In any vulnerability study one of the first questions of concern is, what is the threat? Because defining an EMP threat to the continental U.S. involves many factors and transcends problems associated with just the nuclear power industry, the decision was made that this study would look at a "worst case" situation. That is, it was assumed that the threat is such as to optimally excite each and every potential point of interaction. Clearly, in any actual scenario, no single weapon could be so targeted as to do that, therefore the results establish an upper bound to the threat to the plant.

The actual EMP threat waveform used later in the coupling analyses is the commonly recognized double exponential, high altitude EMP waveform[4] characterized by an electrical field time history of:

$$E(t) = E_o(e^{-\alpha t} - e^{-\beta t})$$

where

$$E_o = 5.25 \times 10^4 \text{ V/m}$$
$$\alpha = 4.0 \times 10^6 \text{ sec}^{-1}$$
$$\beta = 4.76 \times 10^8 \text{ sec}^{-1}$$

The frequency spectrum of this pulse can be obtained by taking the Fourier transform of the time domain wave form. The significant frequencies extend out to about 150 MHz with the bulk of the energy (99.9 percent) below about 100 MHz.[4]

Because EMP susceptibility questions are of particular concern to the DOD, there is continuing research and investigation designed to better define the EMP environment. In the early stages of this study there was some discussion between the study team and the Defense Nuclear Agency as to the appropriate threat waveform. When some of the newer formulations were compared to the standard double exponential cited above, it was observed that in the frequency domain the double exponential threat bounds all other threats. Likewise, none of the other suggested threats had peak field intensities (E_o) greater than the 5.00×10^4 V/M cited. Therefore, because there was no compelling reason to change, the double exponential waveform was used.

It is known that a magnetohydrodynamic (MHD) pulse, persisting for tens to hundreds of seconds, follows the early time HEMP. A typical normalized waveform derived from atmospheric nuclear test data is shown in Figure 2.3. The MHD-EMP waveform can have peak electric field intensities of 10 to 100 V/km over large areas. In order to be a threat to nuclear plant equipment, two conditions must be present:

1. Transmission lines must be sufficiently long to allow for large potential differences to exist between end points.

2. A low impedance dc ground must exist at both ends of the transmission line to allow dc currents to flow.

These two conditions are typically present in the bulk distribution system of electric power systems. In particular, wye-connected transformers or auto-transformers are usually used at this level of distribution which allows for the required dc earth connection.

At Watts Bar the 24 kV/500 kV transformers are delta-wye connected with the wye connection on the 500 kV distribution side. This seems to be true for most plants. Thus MHD-EMP currents induced on the 500 kV transmission lines can be expected to flow to earth ground via the 500 kV secondary windings of the transformers. Due to the inherent dc isolation of the delta-connected transformer primaries, dc currents will be blocked at the transformer and not coupled further into the plant. The major consideration, then, is the reaction of the main power tranformers to dc biasing currents on the outputs.

Electric utilities in norther latitudes have been concerned about solar-induced currents and their effect on bulk power distribution for many years. For solar-induced currents of less magnitude than may be expected from MHD-EMP, some of the following effects have been observed:[5,6]

1. The crest of the transformer magnetizing flux rises above the saturation level resulting in increased magnetizing current.

2. Reactive power increases.

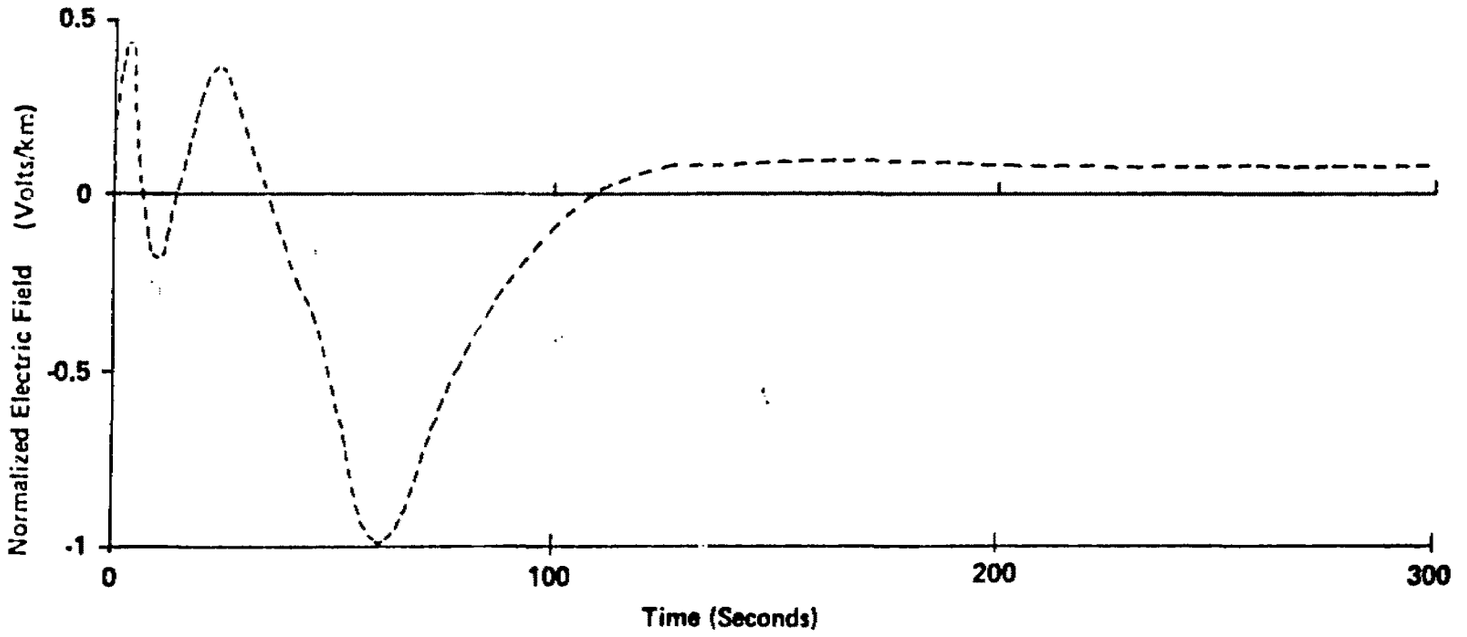

Figure 2.3. Magneto-hydrodynamic EMP Waveform.

3. Significant levels of 60 Hz harmonics are generated.

4. Heating may occur.

5. Protection circuitry may be initiated by the unusally large magnitude of the exciting current.

The MHD-EMP threat, then, is expected to be confined to the main output transformers. The most drastic response of the power system to MHD-EMP would likely be a disconnection of the transformer from the transmission grid as a result of either damage to the transformer itself by thermal effects or initiation of the transformer protective circuitry. Neither of these occurrences would affect the ability of safety systems to shutdown the plant. The Department of Energy and the DOD intend to address the MHD-EMP effect on power system equipment in a program currently being conducted.[7] That program will likely provide better estimates of MHD-EMP effects on transformers.

2.4 EMP Generators

Land based generators capable of being transported by truck have been developed in connection with EMP vulnerability testing of military systems. These generators are capable of producing localized EMP-like effects. Concerns have been expressed regarding the vulnerability of commercial nuclear power plants to sabotage or terrorist acts employing such generators. This type of EMP threat was considered early in the study by the government and industry participants involved, including the Research Review Panel established to monitor the study and provide peer review of its results. It was concluded that a threat did not exist because of the difficulty of deploying and operating such equipment in the vicinity of a plant without being detected, and because the effects of this type of equipment are low level and highly localized. Therefore, no further analysis of this type of EMP threat was included in this study.

3.0 Example Plant Description

3.1 General

The Watts Bar Nuclear Plant of the Tennessee Valley Authority was selected as the example plant for this study. This selection was predicated upon several factors. This plant was used in an earlier study on systems interactions in nuclear power plants,[8] therefore a significant amount of information was already available in the form of system descriptions and system fault trees. In addition, the design and construction of the plant had progressed to the point where final configurations were known, but at the same time it was "open enough" so that details of system arrangements could be observed visually.

The Watts Bar Nuclear Plant is a two-unit Westinghouse, pressurized water reactor plant located on the Tennessee River, approximately midway between Knoxville and Chattanooga. Each unit is rated at 1177 MWe (3425 MWt). Located in close proximity to the nuclear plant are the Watts Bar coal-fired Steam Plant and the Watts Bar Hydroelectric Dam. Figure 3.1 is a plan view of the area around the plant and Figure 3.2 provides two photographic views.

Offsite electrical power is supplied to the common station service transformers at the nuclear plant from two 161 kV feeders from the switchyard adjacent to the dam powerhouse. This 161 kV feed is required to power both reactor startup and shutdown systems. On-line operational power is derived from the 24 kV output of the nuclear plant turbine generators through the unit station service transformers. The plant main transformers supply 500 kV to the TVA transmission grid from the same 24 kV turbine outputs. Figure 3.3 is a plot plan of the nuclear plant showing the location of the various transformers and identifying the buildings and structures associated with the operation of the plant.

The plot plan shows the locations of the various plant buildings, the routing of conduit duct banks, and a partial layout of earth grounding cables. Only a rough layout of grounding is included to show the magnitude of the grounding arrangement. The extensive network of buried mechanical piping is not shown on the plot plan due to its complexity. Because this is an "integrated" two unit plant, there are a number of shared facilities. The auxiliary and control buildings, the diesel generator building and the intake pumping station house systems for both units. However, separation is maintained between units and between redundant safety trains for each unit.

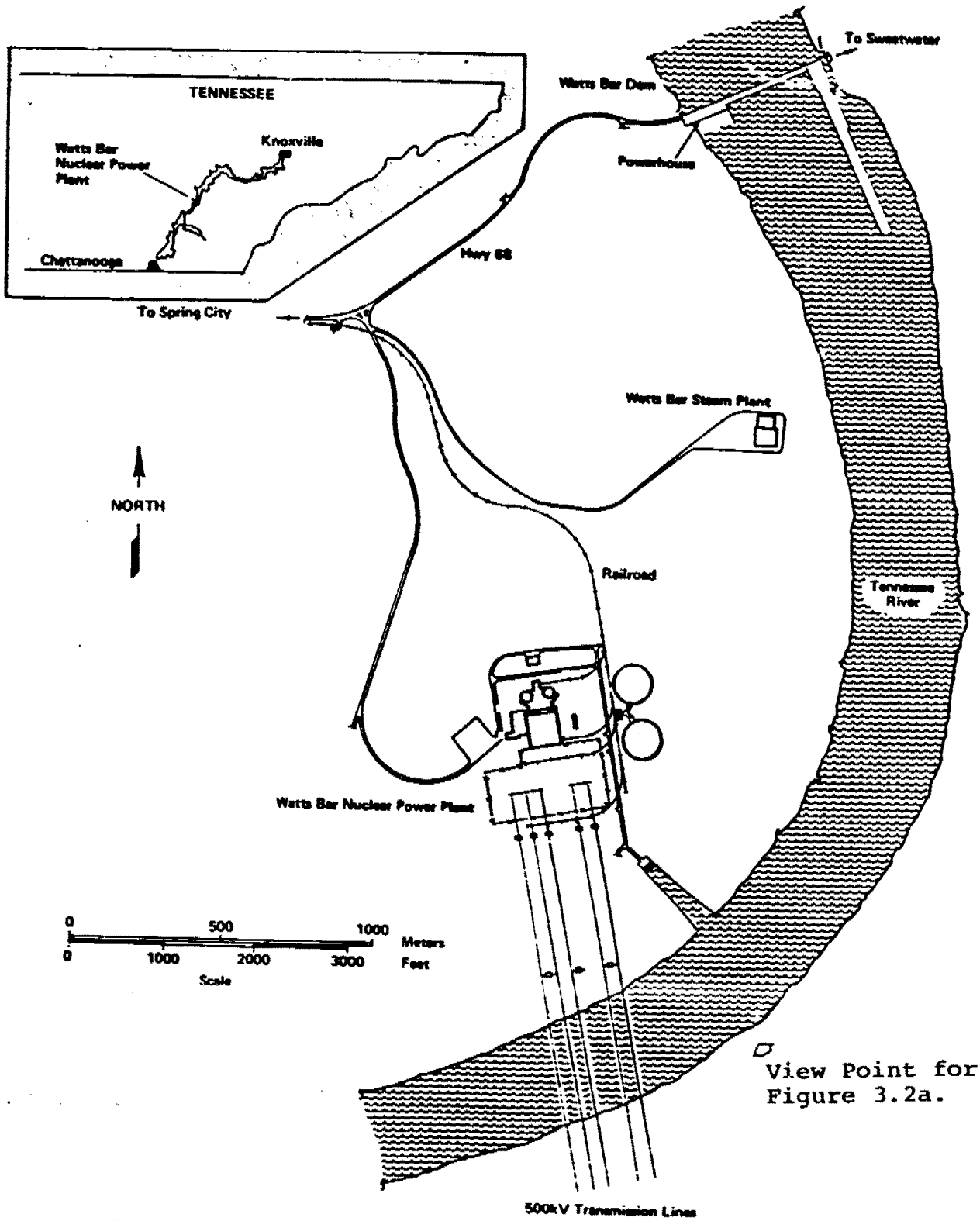

Figure 3.1. Watts Bar Nuclear Plant and Environs.

(See Area Plan in Figure 3.1 for Photograph Orientation.)

Figure 3.2a. Photographic View of Watts Bar Nuclear Plant (Looking Northwest).

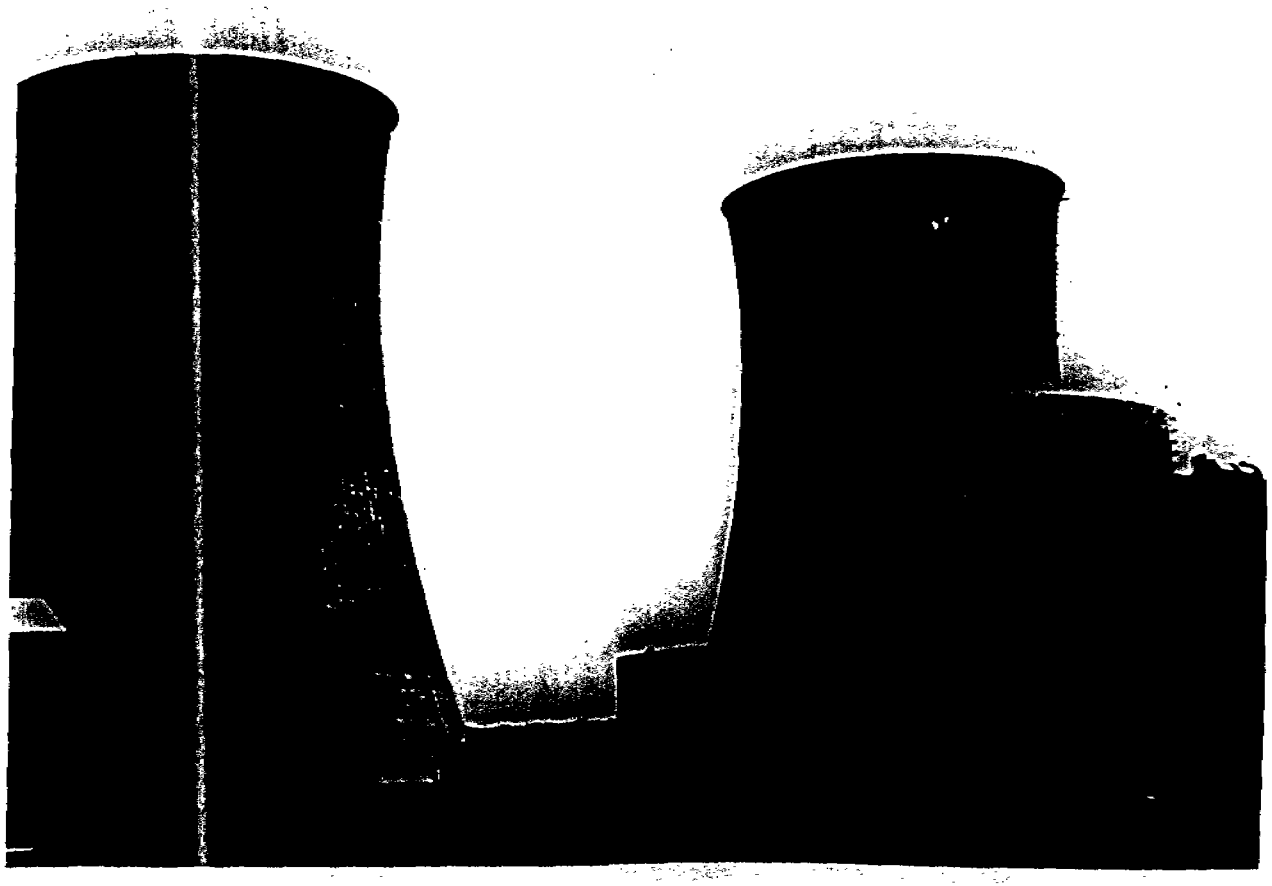

(See Site Plan in Figure 3.3 for Photograph Orientation.)

Figure 3.2b. Photographic View of Watts Bar Nuclear Plant (Looking Southeast).

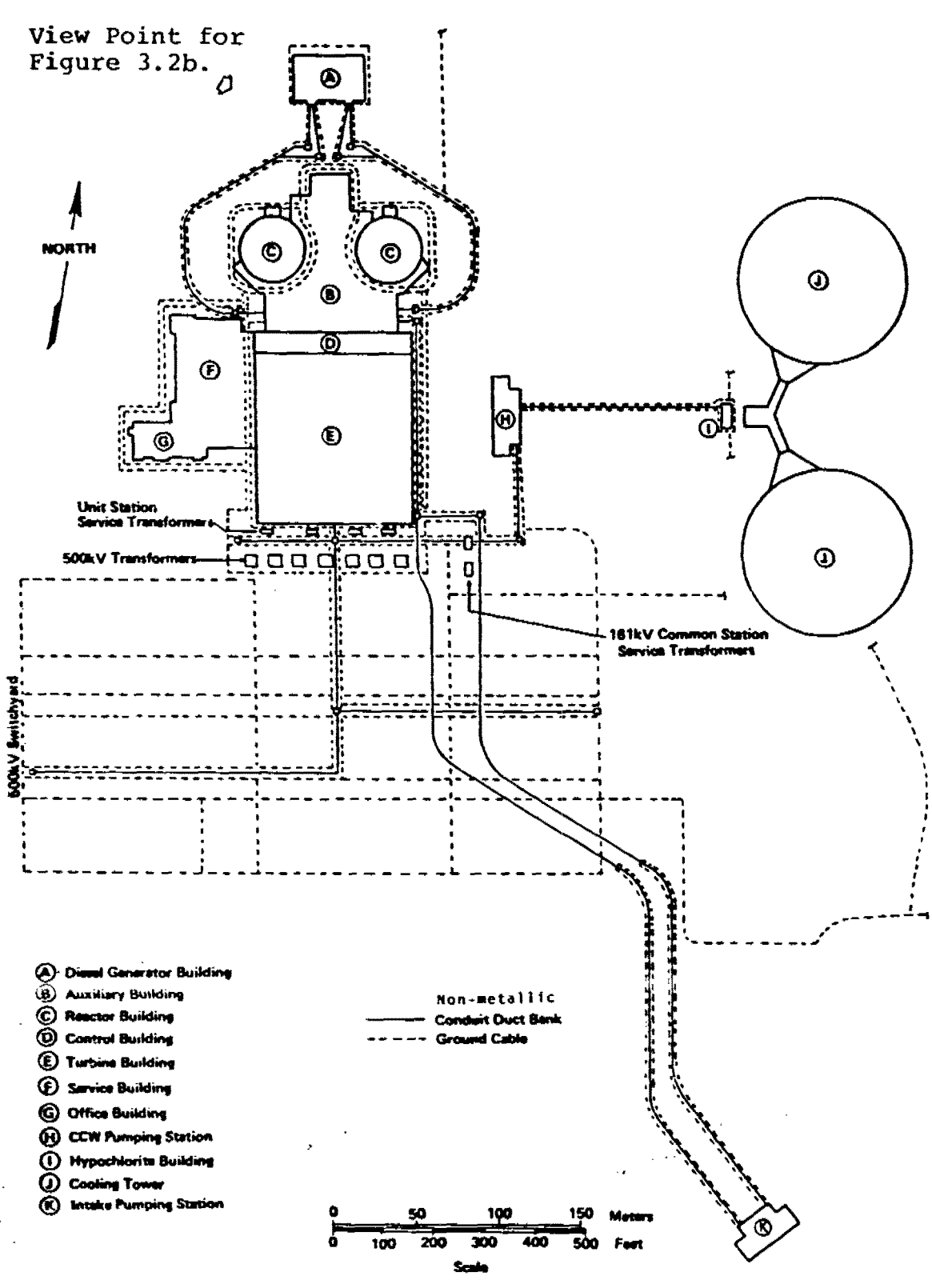

Figure 3.3. Plot Plan Watts Bar Nuclear Plant.

All buildings housing safety-related equipment are constructed to seismic Category I specifications. The walls of the Auxiliary Building, for example, are approximately 2 feet thick with a double course of reinforcing bars. Other Category I structures include the Diesel Generator, Control, and Intake Pumping Station Buildings. The reactor building is even more massive because of its containment function. Figure 3.4 shows some of the plant construction features in a cross sectional view of the Auxiliary, Control, and Turbine Buildings. The Turbine Building, because it does not house safety-related equipment, is not constructed to Category I specifications but is built of structural steel beams with a sheet steel and glass outer shell.

3.2 Design Features of Special Interest

Conduit duct banks (see Figure 3.3) interconnect plant buildings and provide seismic Category 1 protection for power, control, and signal cables that connect to various plant systems. A detail of a duct bank section that connects the Auxiliary Building to the Intake Pumping Structure is shown on Figure 3.5. The duct bank consists of an array of plastic conduits encased in concrete. Steel conduits are used instead of plastic from the final manhole to the actual penetration of a building, but this represents a short distance compared to the overall length of the duct bank.

Cables are pulled into the conduits in functional groupings based on power levels. In general, the high-voltage, high-power cables are routed along the top ducts of the bank and the low voltag , low-power cables are routed along the bottom. The duct banks are buried as deeply as 20 feet and, in general, slope to a depth of 5 to 10 feet at the building penetrations. Ground cables are run parallel to the duct banks in order to provide lightning protection.

Within the buildings, cables typically run on ladder and ventilated louver-type cable trays. As with the conduit duct banks, cables are separated on trays as to functional type based on voltage and power levels. When a variety of cable types share a coincident routing, the trays are arranged into levels as shown in Figure 3.6. The high-voltage, high-power cables are physically at the top of the stack and the low-voltage, low-power cables are at the bottom. Physical separations of about 1 foot are typicaly maintained between levels.

With the exception of certain low-level signal and control cables, most cabling within and between buildings is unshielded. High-voltage, three-phase 6.9 kV power cables consist of an individual cable per phase, each wrapped with an overlapping helical foil shield which is locally grounded at each point of distribution or termination. All 480 V cables are unshielded and consist of both three-phase-per cable and individual-cable-per-phase cable types. Medium-level signal and control cables are usually unshielded-twisted pair or multiconductor cables.

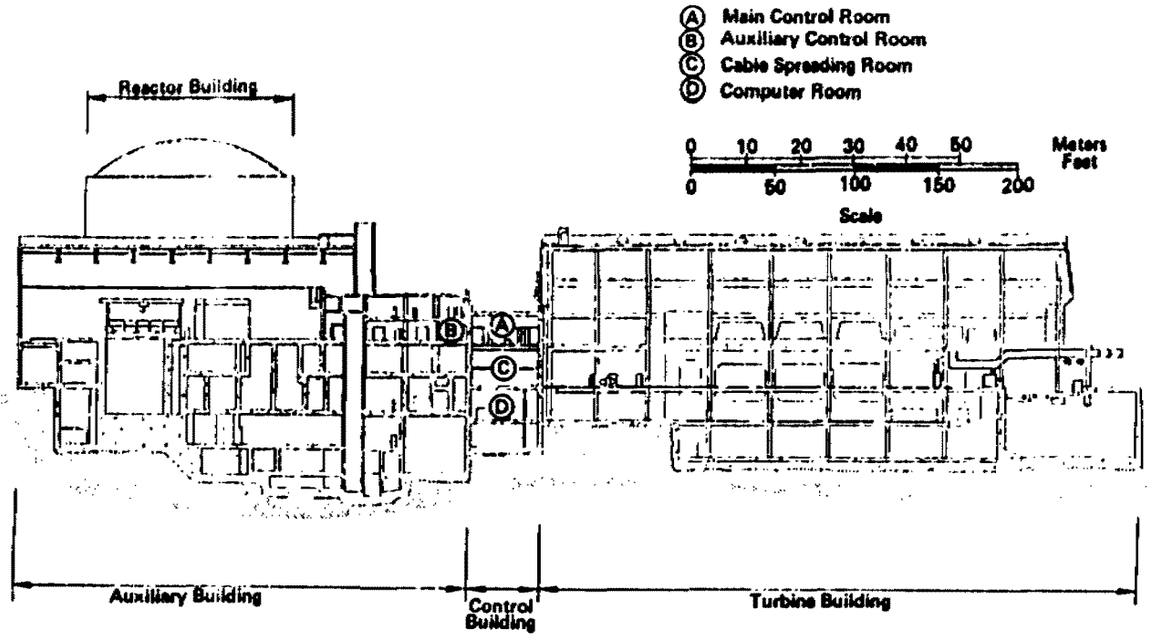

Figure 3.4. Cross-sectional View Watts Bar Nuclear Plant.

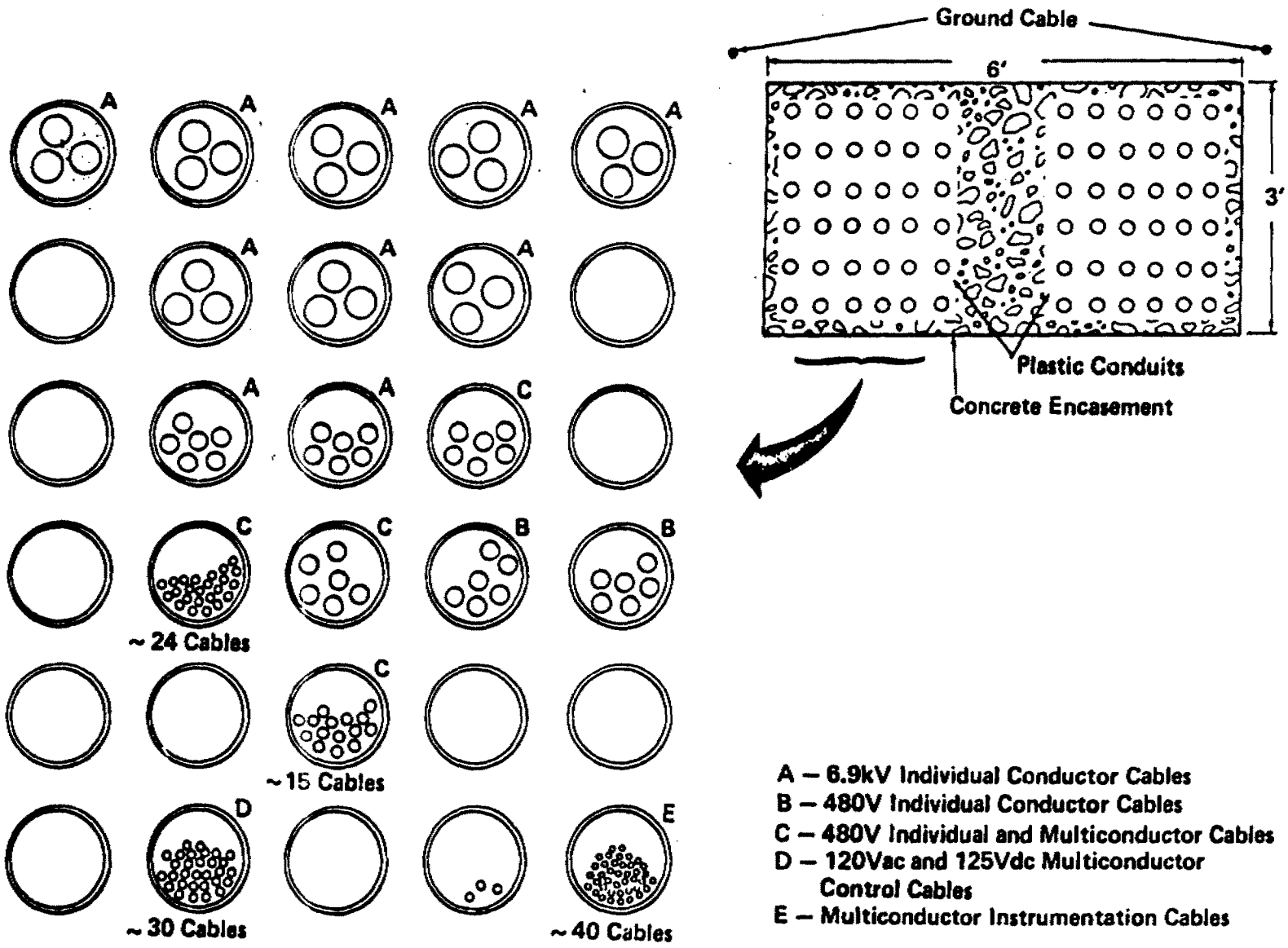

Figure 3.5. Conduit Duct Bank Details.

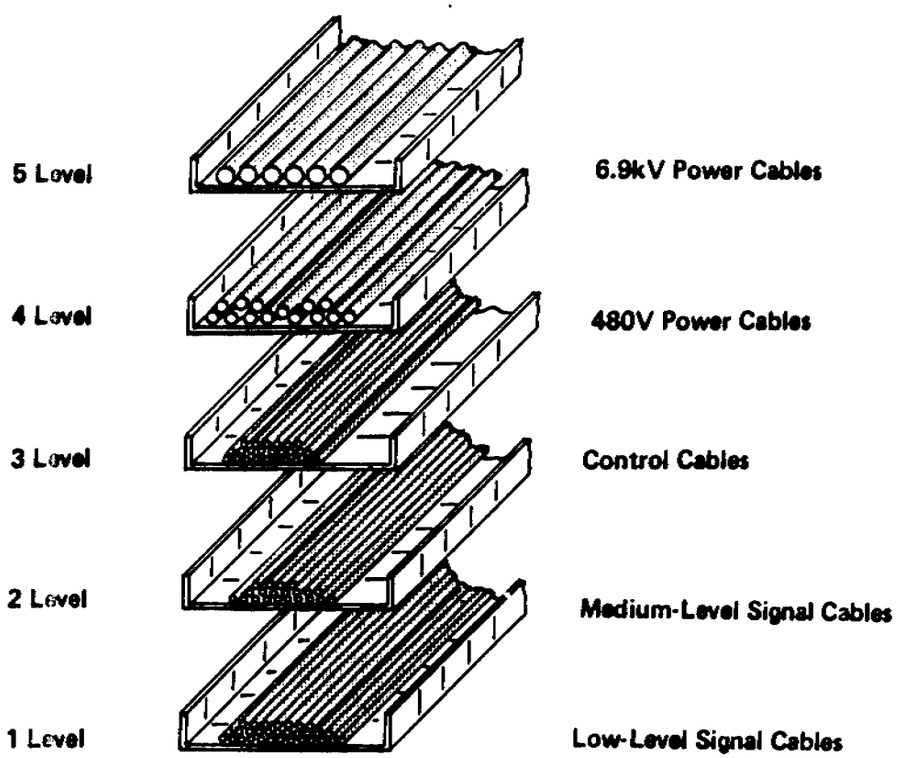

Figure 3.6. Cable Tray Details.

4.0 Nuclear Systems Analysis

4.1 Critical Systems

This investigation is limited to selected systems required for safe shutdown of a nuclear power plant, therefore the systems of interest must be defined. Three essential functions must be accomplished to safely shut down a nuclear plant.

The fission process must be terminated, i.e., the reactor must be shutdown.

The coolant inventory must be maintained so that the core remains covered.

The heat generated from the radioactive decay of fission products must be removed.

Given the functions which must be carried out, it is a relatively straightforward task to define the systems of interest. In fact, this is normally done by each licensee in the Safety Analysis Report. For the example plant, the systems required for safe shutdown include:

The reactor protection system (at least a manual scram capability).

The ac/dc emergency power systems (required for power, control, and instrumentation).

The auxiliary feedwater system (first path for decay heat removal if the main condenser is not available and there is no major loss of coolant).

The residual heat removal system (required for primary system cooling to take plant to cold shutdown).

Chemical and volume control system (necessary to make up coolant loss from seal leakage, volume shrink on cooling, etc.).

Component cooling water system (the intermediate loop between equipment being cooled and the ultimate heat sink).

Essential raw cooling water system (the ultimate heat sink for a wide range of support systems).

Portions of the heating, ventilating and air conditioning system.

Instrument air (for instrumentation and in some instances valve control).

These systems may carry other titles in other plants but similar functions will be performed.

Based upon other studies conducted by Sandia there are several observations which can be made about this list. First, not every system is required at the instant of shutdown. And, in fact, some systems may not be needed until many hours after shutdown is initiated. This can have an important bearing on the effects of a system failure. Second, as shown below, there is a "common denominator" present and that is the dependence upon emergency electrical power. For example, in most instances, even the steam turbine powered auxiliary feedwater system requires dc power for control purposes.

4.2 Initial Analyses of Safe Shutdown Systems

As indicated above, a number of system level fault trees were prepared previously for the Watts Bar Plant. Because the Auxiliary Feedwater System can be extremely important for decay heat removal, this system was analyzed first. The fault trees prepared under the Systems Interaction Methodology Applications Program[8] were used as the starting point for the EMP analysis. However to adequately treat the questions of EMP susceptibility, it was necessary to further develop the fault trees. Because there is widespread interest in the methods and techniques of probabilistic risk assessment, there is active research in the area of fault tree development. In fact, standardized procedures are being developed to provide consistency in the fault trees generated. These standardized techniques[9] were used here. An example of the results follows.

The Auxiliary Feedwater Systems are typically designed so that even if failures occur in the emergency electrical power system, feedwater can be provided by means of a steam turbine driven pump. However, if the motor operated valve (MOV) in the steam supply line fails to open to supply steam to the turbine then that system is inoperative. Figure 4.1 shows the development of the event, MOV 1 Fails Closed, using the IREP procedures.[9] The valve fails closed if there is no electrical power, which can result if circuit breakers fail open, if cables fail or if there is a loss of power on the bus. This latter loss of power can be further defined as indicated in the subsequent development of the tree. The obvious conclusion is that the emergency electrical power systems are indeed crucial to the operation of the auxiliary feedwater systems. It was quickly apparent from a brief review of other systems that this was indeed the "common denominator" throughout the safe shutdown systems. Therefore, the subsequent analyses focused on the ac/dc emergency power systems and control and instrumentation systems for the critical systems.

4.3 Electrical Distribution System

A simplified one line diagram for the internal electrical power systems is shown in Figure 4.2. The Station Service Transformers provide 6.9 kV power to the Unit Boards which in turn feed the 6.9 kV Shutdown Boards and also some non-safety loads through

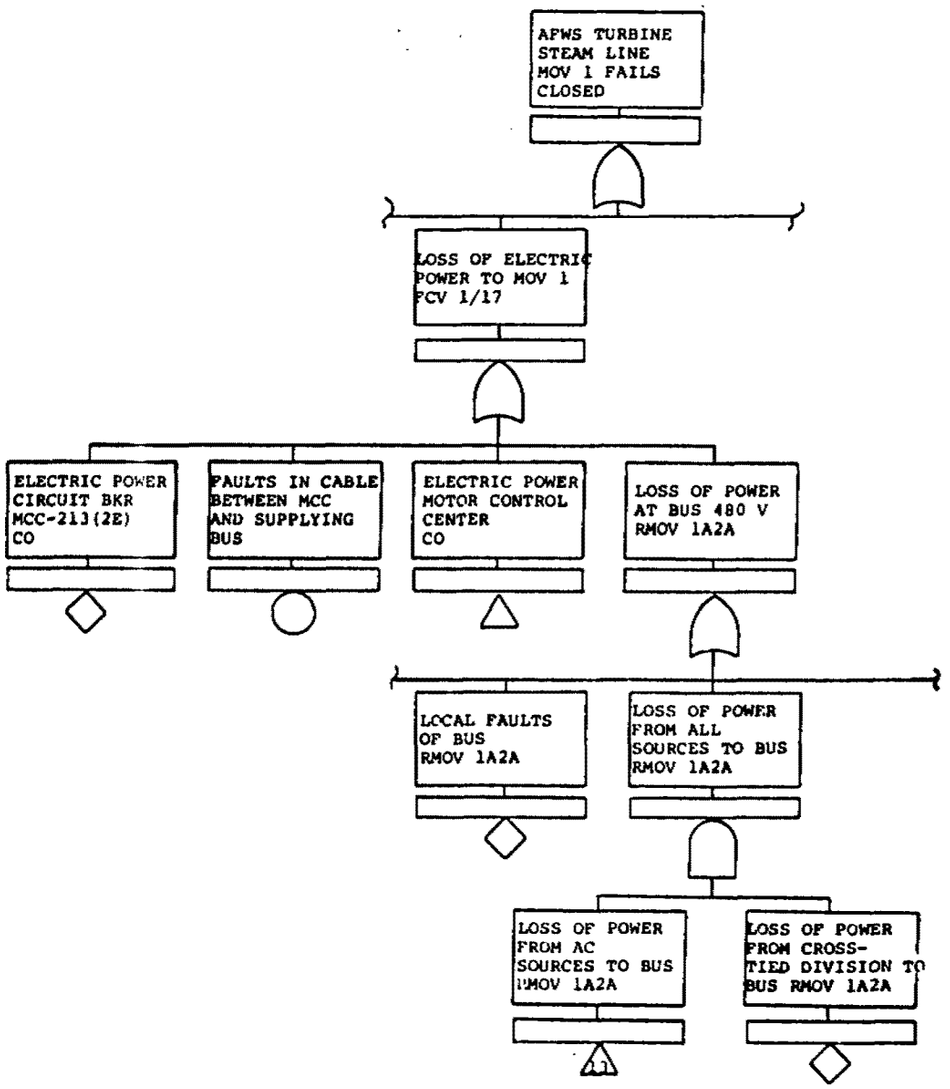

Figure 4.1. Portion of AFWS Fault Tree.

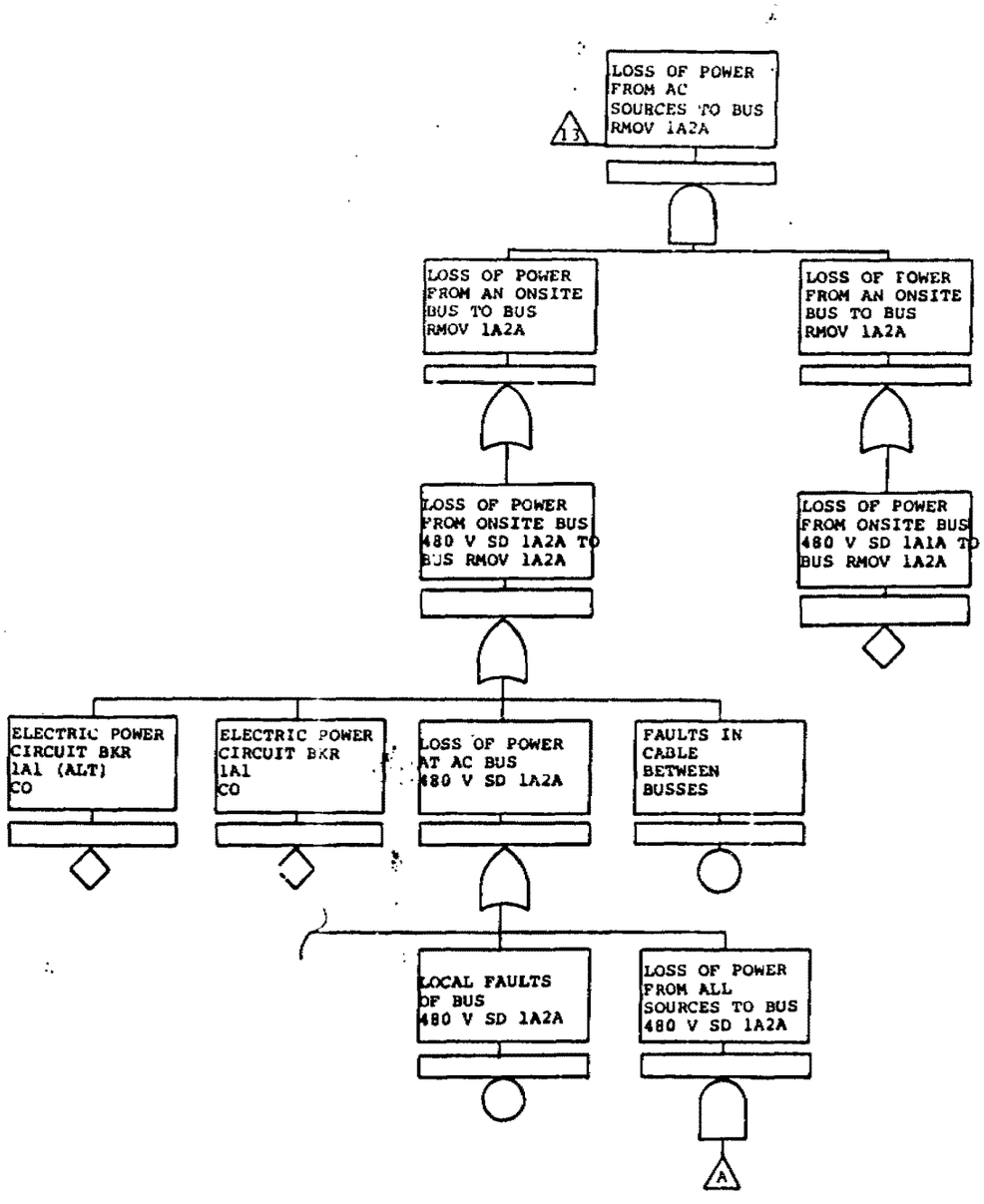

Figure 4.1. Portion of AFWS Fault Tree (Continued).

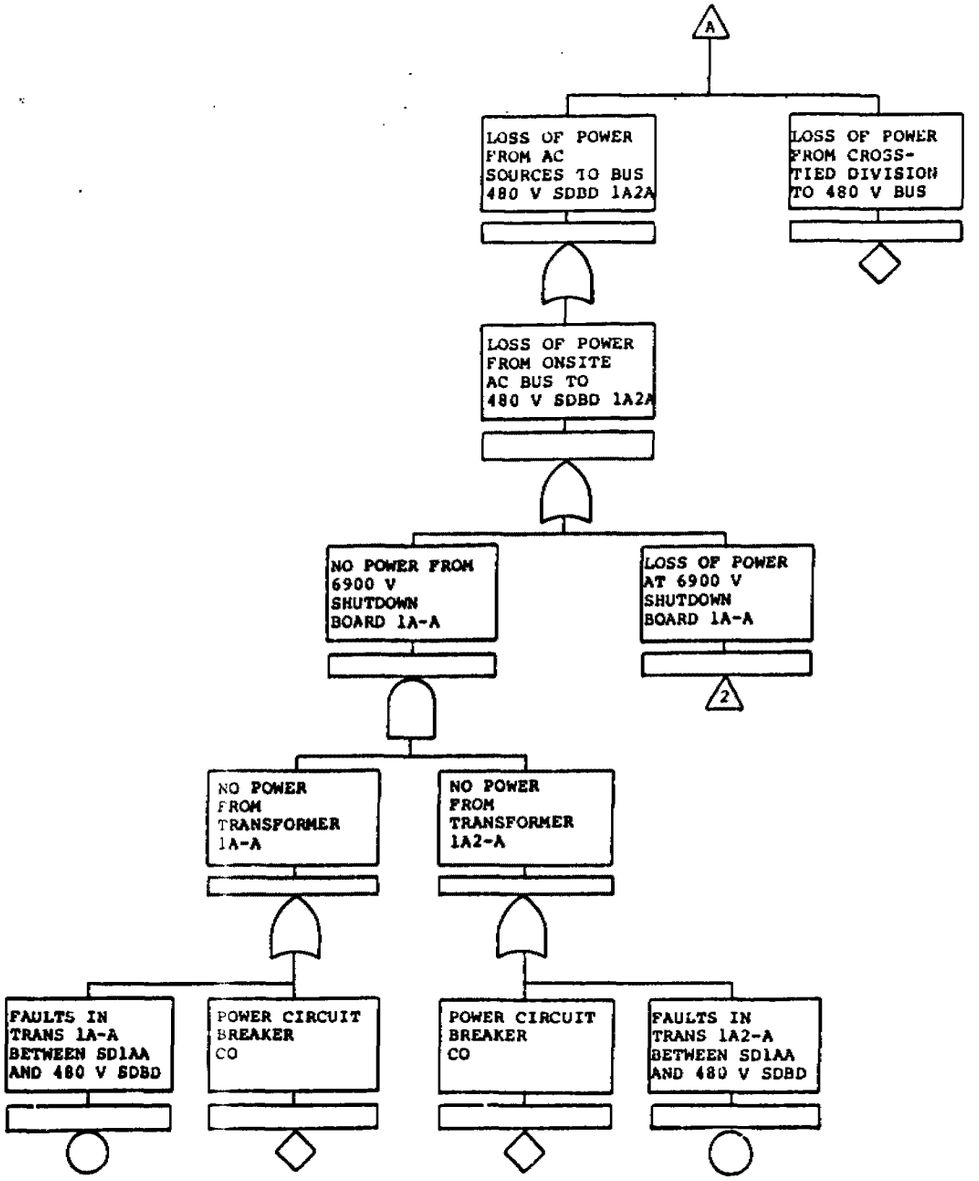

Figure 4.1. Portion of AFWS Fault Tree (Continued).

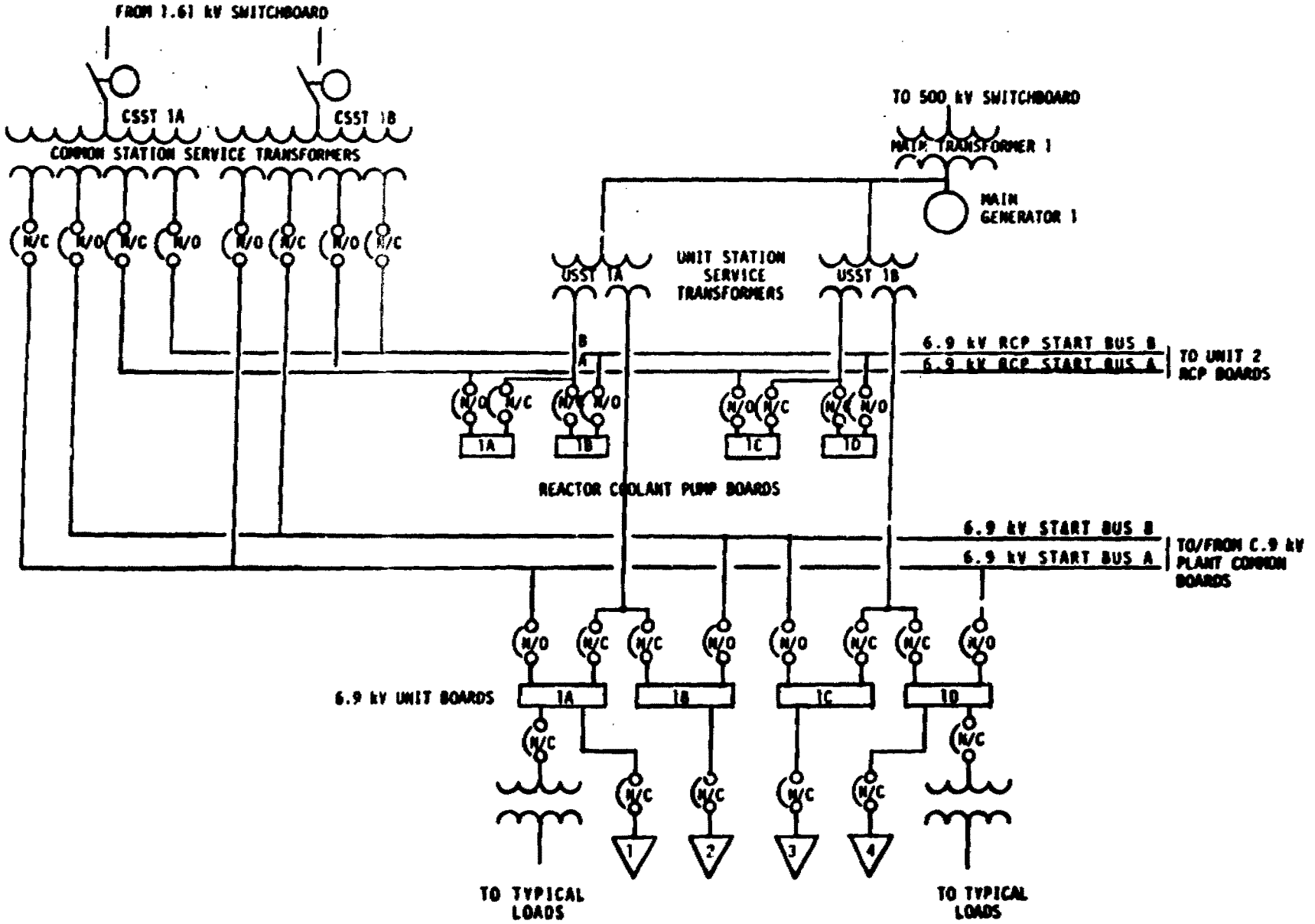

Figure 4.2. Simplified One-Line Diagram Watts Bar Nuclear Plant Electrical Power System.

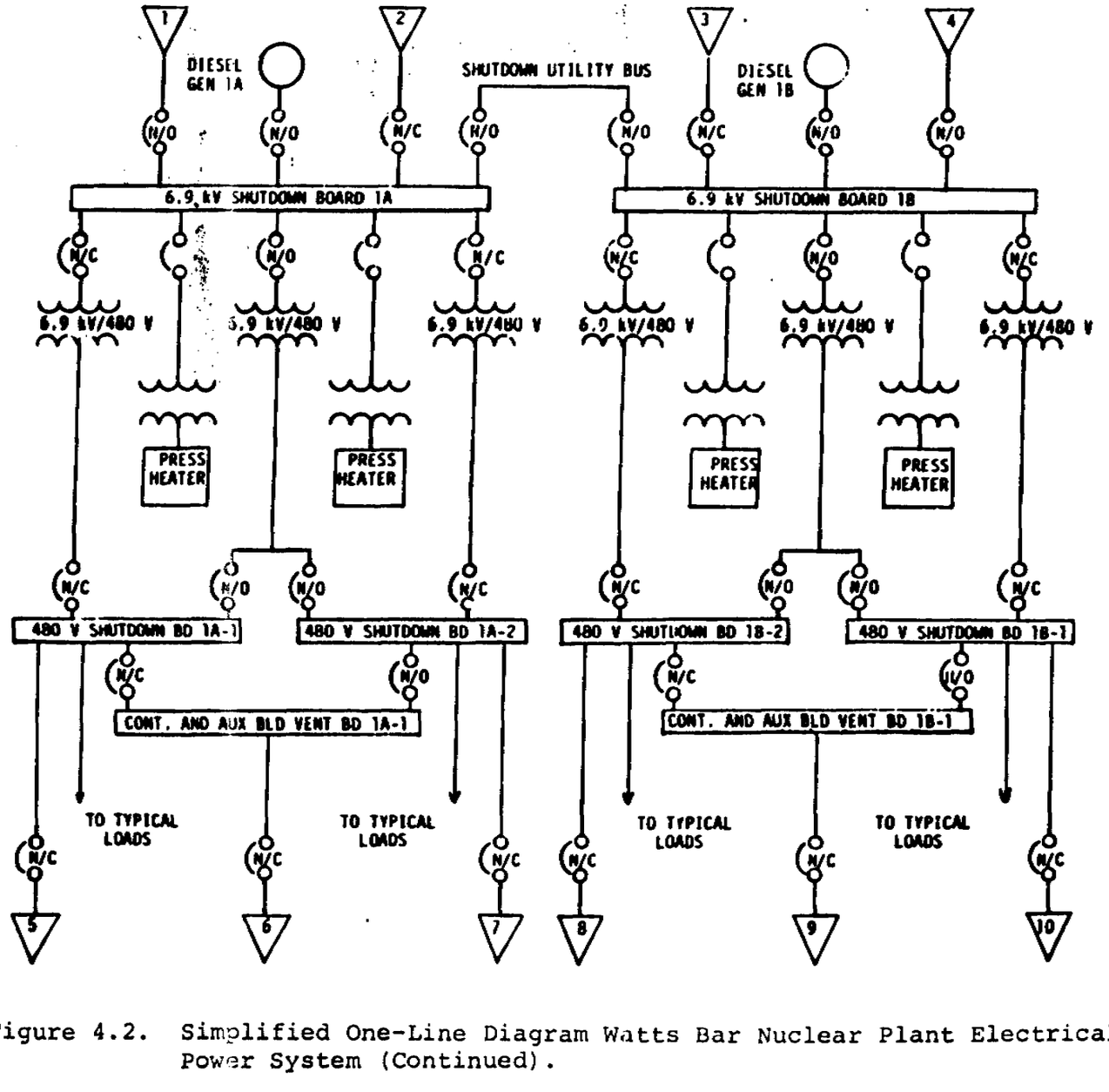

Figure 4.2. Simplified One-Line Diagram Watts Bar Nuclear Plant Electrical Power System (Continued).

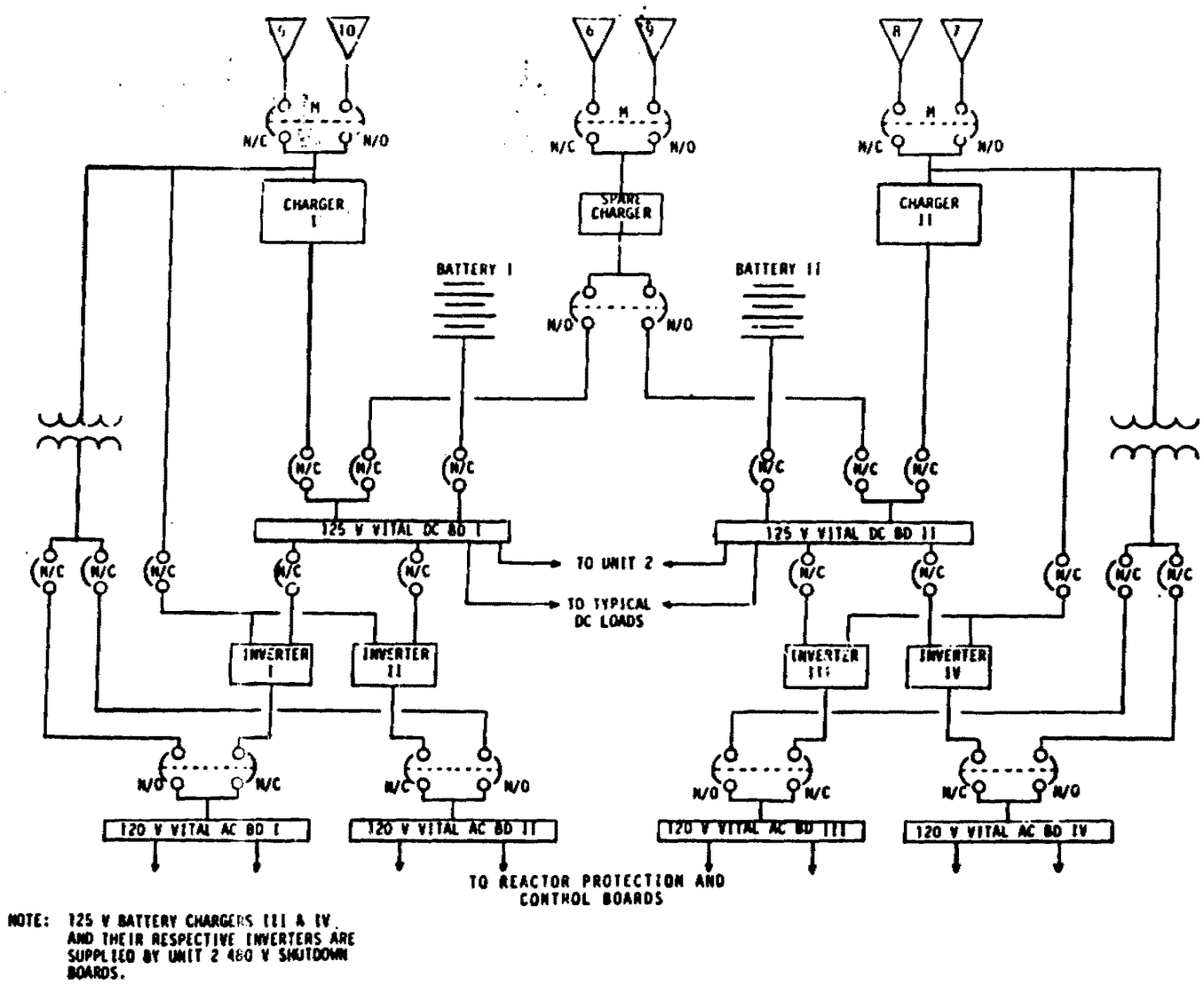

Figure 4.2. Simplified One-Line Diagram Watts Bar Nuclear Plant Electrical Power System (Continued).

6.9 kV/480 V transformers and provide 6.9 kV power. The 6.9 kV Shutdown Boards may also be supplied from the Standby Diesel Generators. Power is passed to the 480 V Shutdown Boards via 6.9 kV/480 V transformers. The 480 V power is then fed to a number of motor control centers (e.g., the Containment and Auxiliary Building Ventilation Board). The 480 V Shutdown Boards also provide power to the battery chargers and inverters and thus to the vital dc and ac boards.

The actual loads associated with each of the shutdown boards and subsequent load centers were established by a detailed examination of the one-lines for each board. Such a one-line is shown in Figure 4.3. This permitted us to define the loads, the control systems (ac or dc), the location of switches (control room, motor control center, local). This information was combined with estimates of the length of cable runs interconnecting the load and the bus, a decision as to load status assuming the plant was at normal full power operation (normally energized, normally open, etc.), a decision as to load criticality, and tabulated as shown in Table 4.1. These tables were then used by the analysts to establish the points in the system at which predictions of EMP-induced signals were to be made. The typical prediction points are summarized in Table 4.2.

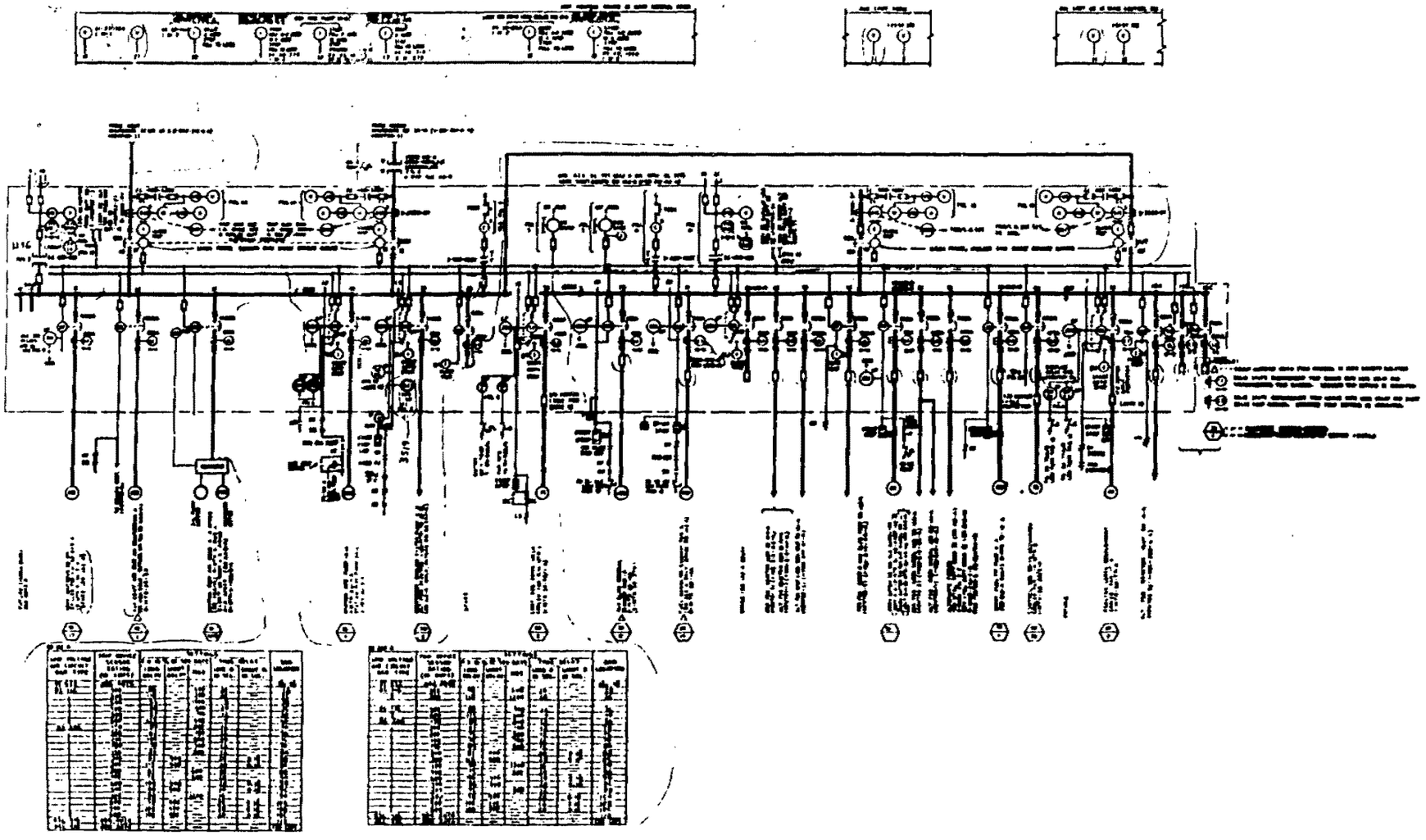

Figure 4.3. Typical One-Line Diagram for 480 V Shutdown Board

Table 4.1

Typical Load Worksheet for EMP Analyses

480 V Shutdown Board 1A1-A (TVA Drawing 45W749-1)

Prediction Required	Connectivity Code[1]	Cable Length (Ft)	Outside Connection	Item/Component	Switch Location[2]
	A	50		Aux Bldg General Supply Fan	MCR-Local-Interlocks
Yes	A	75		CCS Pump 1A-A	MCR-MCC-Local-Interlocks
	D	25		Alt Fdr-Cont and Aux Bldg Vent Bd	MCC-Local
	A	225		CRDM Cooler Fan 1A-A Motor 1	MCR-MCC-Local-Interlocks
	A (intermit)	75		Electric Board Room AHU A-A	Local-Interlocks
	A (intermit)	225		Cont Air Return Fan 1A-A	MCR-Local
	A	225		CRDM Cooler Fan 1A-A Motor 2	Interlocks
Yes	A	100		Norm Fdr 480V Reactor MOV Bd 1A-A	Local
Yes	A	125		Norm Fdr Reactor Vent Bed 1A-A	Local
Yes	A	25		Norm Fdr Cont & Aux Bldg Vent Bd 1A1-A	Local
Yes (Source)	A	750	Yes	Norm Fdr Diesel Aux Bd 1A1-A	Local
Yes (Source)	D	750	Yes	Alt Fdr Diesel Aux Bd 1A2-A	Local
	B	225		SF Pit Pump C-5	Local
	D	175		Alt Fdr 250V Charger	Local
	C	---		Spare	
Yes	A	100		Norm Fdr 125V Charge I	Local
	B	225		Reactor Lower Comp Cooler Fan	MCR-MCC-Local-Interlocks

(1) A-load on normally, B-circuit open at board, C-no connection, D-circuit open at load.
(2) MCR-Main Control Room, MCC-Motor Control Center, Local-at/on equipment, Interlocks-Ties via relays to other equipment.

Table 4.2.

Typical Current/Voltage Prediction Points

6.9 kV Shutdown Boards

Pumps (ERCW, RHR, AFW, CHG)
Pressurizer Heaters

480 V Shutdown Boards

CCS Pumps
Battery Chargers
Inverters
Air Compressors

Reactor MOV Boards

Valves (ERCW, AFW, CCS, RHR, CVCS)
Oil Circulating Pumps (AFW, CHG)
Boric Acid Tank Heaters

Diesel Auxiliary Boards

Battery Chargers
Pumps (Fuel Oil, Lube Oil)
Cooling System Valves

125 VDC Vital Boards

Shutdown Board Control Busses
Battery Chargers
Vital Instrument Inverters
AFW Controls
Relief/Isolation Valve Controls
Reactor Trip Switchgear

120 VAC Vital Instrument Boards

Process Control Groups
SSPS Relays/Power
NIS Power
NSSS Relays

5.0 EMP Interaction Analysis

5.1 Abbreviated Analysis Technique

The analysis technique employed during the EMP assessment of the example plant (Watts Bar) is an outgrowth of analysis procedures developed by Boeing to assess the EMP vulnerability of various military weapon and communication systems.[10] In an effort to reduce the level of effort, and thus the expense, required to perform detailed analyses, abbreviated analysis methods have been devised that allow vulnerability estimates to be made in an onsite environment. Although the technique outlined below is straightforward, abbreviated analyses rely heavily on the experience of the analysts and the confidence previously gained by producing predictions that have been verified by testing programs. Typically, the following tasks are performed in an abbreviated assessment:

1. Cabling attached to the critical equipment is traced to the penetrations of EMP energy which can drive it.

2. EMP-induced signals (short circuit currents) are estimated for the relevant penetration cables.

3. The penetration currents are traced back to the critical equipment taking into consideration ohmic, cross-coupling, and distribution fan-out losses.

4. If the cables under consideration are unshielded, their source impedances and the equipment load impedances are used to derive reflection coefficients at the cable-equipment interfaces. The voltages at the equipment are computed from

$$V_\ell = V_o \left[\frac{2Z_\ell}{Z_o + Z_\ell}\right] \qquad (5.1)$$

where Z_ℓ is the load impedance, Z_o is the source impedance, and V_o is the traveling voltage wave on the cable. Since $V_o = I_o Z_o$ and $I_o = I_{sc}/2$, where I_{sc} is the short circuit current.

$$V_\ell = \frac{I_{sc} Z_o Z_\ell}{Z_o + Z_\ell} \qquad (5.2)$$

For the typical case where the load impedance (particularly in the common mode) is much larger than the source impedance,

$$V_\ell \simeq I_{sc} Z_o \qquad (5.3)$$

If differential mode (wire-to-wire) responses are required, it is assumed that sufficient unbalance exists in conductor topology to allow approximately half of the common mode threat to appear in the differential mode.

5. If the cables are shielded, the responses at the equipment inputs are dependent on the quality of the shields and the treatment of the shields at the cable terminations. This requires a more detailed anaysis involving pigtail effects and coupling through braided shields.

In performing the above tasks during the electromagnetic analysis, coupling model diagrams were developed that detail the connectivity of the critical equipment to sources of EMP excitation. Figure 5.1 is an example of such a model diagram, the remainder are included in Appendix A. These diagrams also serve as worksheets to trace the penetration currents back to the equipment.

The tracing of the penetration currents back to the critical equipment generally requires special consideration at points of fan out such as at distribution boards or cable bundle break-outs. For example, consider N loads or cable conductors connected to a distribution bus being driven by one or more current carrying conductors. The instantaneous currents on all the conductors connected to the bus obey Kirchoff's current law; that is, the instantaneous current out of the bus sums to the instantaneous current into the bus. Due to varying cable lengths and load impedances, the peaks of the output currents will not occur simultaneously; thus, the sum of the individual output time domain peak current levels will not necessarily be equal to the input time domain peak current. In general, the sum of the individual time domain peak currents is greater than the input peak current.

When the N loads are identical, the individual conductor current out of the distribution bus is the input current, I_{in}, reduced by the number of conductors (I_{in}/N).

For non-identical loads there will be a distribution of individual peak current values, above and below I_{in}/N, with an average in the distribution occurring above I_{in}/N. For typical non-identical cable runs with N greater than five and cables of substantial electrical length ($\sim 10\lambda$ where λ is the wavelength of the frequency of interest), experience has shown that the peak of the distribution is usually bounded by the limits I_{in}/N and $I_{in}/\sqrt{N}$. The geometric mean of these two limits, $I_{in}/N^{3/4}$, yields a reasonable estimate of the average peak value of the current distribution.

Two basic configuration types were identified for estimating purposes. In the first case, essentially identical cable types and lengths connect to similar or very remote terminations. Here, the appropriate choice for the average cable current is I_{in}/N. In the second case, generally unknown or differing loads connect to cables of differing types and lengths. The average cable current here is best estimated by $I_{in}/N^{3/4}$.

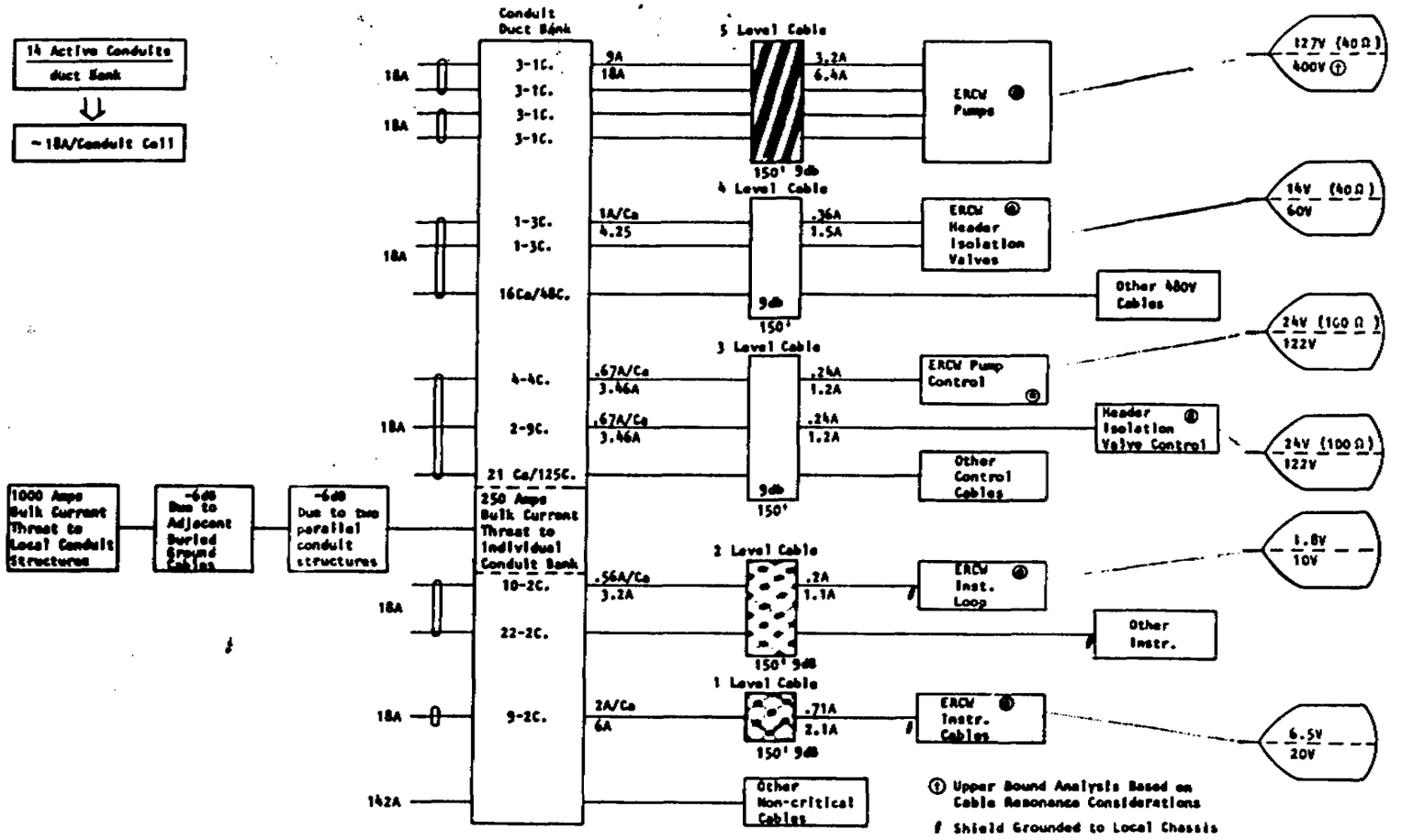

Figure 5.1. Response Model Diagram for Intake Structure.

In the computation of cable losses due to ohmic and cross-coupling effects, experience* has shown that five to six dB of attenuation can be expected for each 100 feet of cable.

5.2 Electromagnetic Features and Analyses

The construction practices employed at the example plant provide a great deal of inherent electromagnetic shielding to the areas of the plant housing safety-related critical systems. The multiple courses of steel rebar in the building walls, the extensive steel mechanical support system, and the large array of interior electrical equipment racks, panels, and cable trays all serve to greatly reduce the level of electromagnetic fields diffusing through the building structure. The least attenuated field component would be the magnetic field near the outside walls and on the upper floors near the roof. Steel-reinforced buildings of this type have exhibited magnetic field shielding effectiveness of 30 dB or more to frequencies ranging up to 75 MHz. In the central regions of the plant, diffusion field strengths are expected to be attenuated 50 dB or more below external incident fields.

Due to the consistent use of continuously connected metal conduits and cable trays within the plant, internal cabling and the associated electrical equipment will be largely decoupled from the attenuated diffusion fields. Responses due to this local excitation are expected to be below an ambient level established by the general dispersion throughout the plant cabling system of penetration currents conducted into the plant on externally excited cabling such as those in the buried conduit systems, the grounding cables and even piping. This general level of ambient response is estimated to be about 1 volt.

The onsite survey and review of plant configuration drawings identified the major penetrations of externally conducted EMP energy to critical systems. The penetrations themselves, while composed of large numbers of individual cables, are discrete, readily identifiable and well controlled. At Watts Bar, the following penetrations were investigated in detail for coupling potential to critical equipment and are depicted in Figure 5.2 by a simplified penetration connectivity diagram.

1) 500 kV overhead transmission lines to the Turbine Building. (At startup and during shutdown the 161 kV feed replaces the 500 kV source.)

2) Buried conduit duct bank cables to the Intake Pumping Station.

3) Buried conduit duct bank cables to the Diesel Generator Building.

---

*Tests which are described in Section 6 were conducted to verify that this experience is also applicable to the example plant.

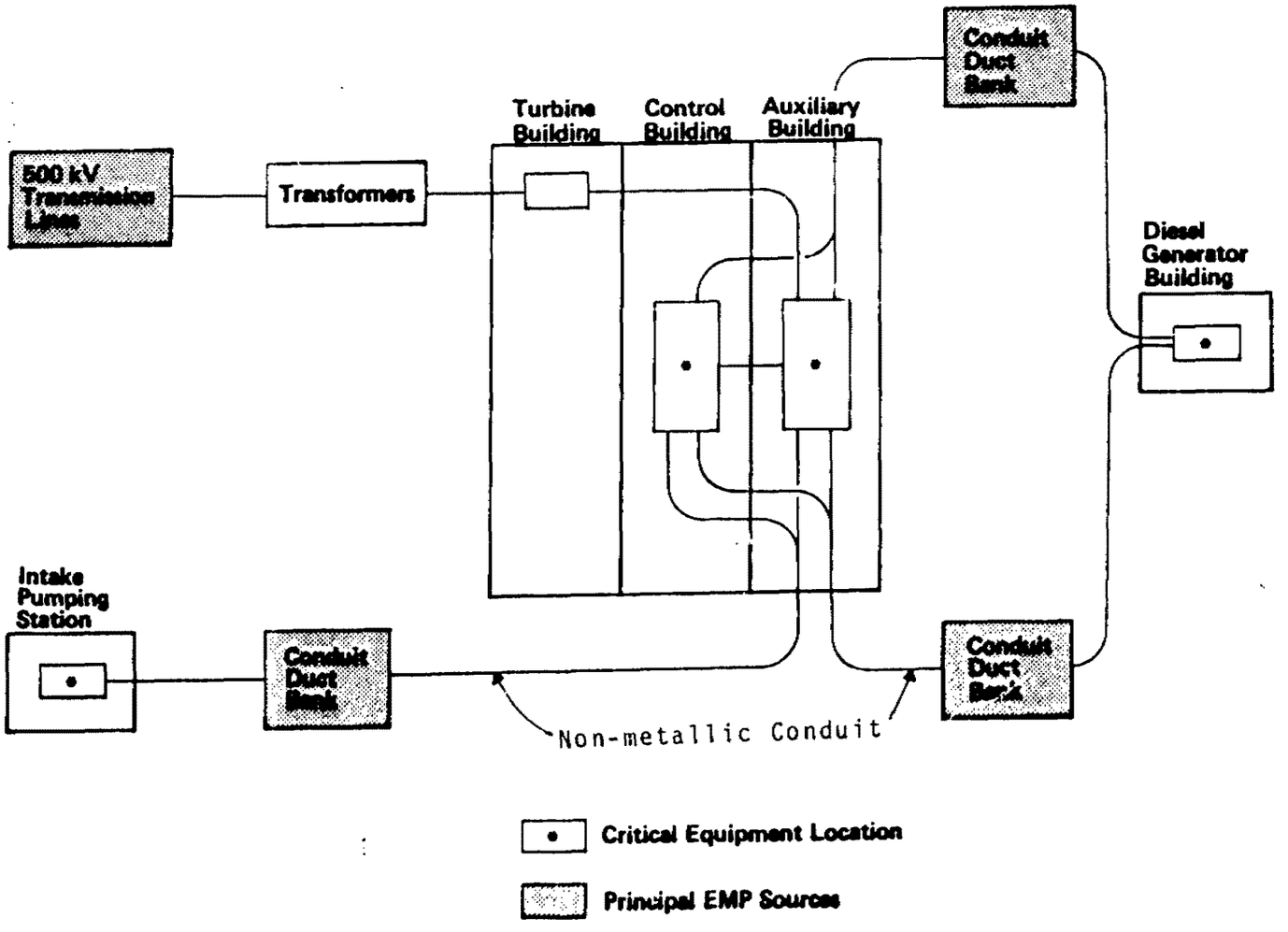

Figure 5.2. Simplified Connectivity Diagram.

4) Buried conduit duct bank cables from the Diesel Generator Building to the Auxiliary Building.

5) Buried conduit duct bank cables from the Intake Pumping Station to Auxiliary Building.

The principal source of EMP energy coupled to critical circuits in the plant is current induced on cables in the external buried conduit systems which penetrate the buildings. The level of the current induced in these conduit systems can be estimated from a model of an infinitely-long buried wire with an incident EMP in the form of a parallel-polarized plane wave of 50 kV/m amplitude. With optimum incidence angles, the response to the commonly accepted high altitude EMP waveform used here is a peak bulk current of approximately 1000 amps on the buried conduit systems. The current time history is roughly double-exponential in character, rising to a peak value in about 500 nanoseconds, and falling to half-peak value in tens of microseconds.[4] Due to the finite length of the buried conduit systems, reflections or oscillations will occur in the actual conduit current responses. Also, the existence of neighboring conduit systems, ground cables, and various mechanical piping systems as well as non-optimum relative orientation of the incident EMP will reduce the bulk current on an individual conduit system to well below that of the idealized, isolated buried conductor. The design philosophy at the plant basically assures that all metal conducting media such as trays, support structures, equipment chassis, and mechanical piping are connected together by the internal ground system. Transient current that would be conducted into the plant on mechanical piping or external buried ground cables would quickly disperse among divergent conducting paths. While the possibility of these transient currents coupling to critical equipment cannot be completely dismissed, no configurations were observed during the survey of the plant that would suggest such an occurrence. Such considerations are indicated on the model diagrams (see Figure 5.1) and serve to reduce the bulk current on the conduit systems studied to approximately 250 amps.

The 250 ampere bulk current induced on a conduit system at a building penetration is shared by the various parallel cables and conductors comprising the cabling in the conduits. Each conduit system carries hundreds of cables, most of which are multiconductor. Because of its larger conductor diameter and isolated routing in separate conduits, power cabling tends to have the largest current per conductor (5 to 10 amps per conductor). Because control cables commonly have hundreds of conductors per conduit, the individual current per conductor is significantly diminished (0.5 amps per conductor).

Power and control cables from the buried conduit systems are routed inside the plant for substantial distances in cable trays with other plant cabling that is not similarly excited. These coincident runs diminish the current response on the penetrating cables by cross-coupling energy to the other cabling in the trays. Energy is also lost through ohmic losses in the conductor resistance. When cabling is brought to a point of distribution such as a

bus board, incoming current tends to divide (fan-out) among the conductors attached to the bus. Therefore, as it propagates inward from a point of penetration the EMP energy tends to be dispersed throughout the interior cabling system, attenuated by ohmic loss, and distributed at bus distribution boards.

In general, only the first or second stages of fan-out distribution will experience a substantial EMP threat. This is the case for the penetration of the 500 kV overhead transmission lines which are capable of producing a bulk current threat on the order of 15,000 amperes at the outputs of the plant main transformers. While this level of current appears formidable, it is attenuated by transformer losses, ohmic and cross-coupling losses, and distribution fan-out to the degree that only milliampere levels remain to threaten system critical equipment. This analysis appears in more detail in the 500 kV transmission line model shown in Appendix A. During periods of reactor shutdown and startup, the 500 kV transmission line connection to the plant unit boards is replaced by a connection to a 161 kV source. In this latter situation there is one less transformer in the circuit to provide attenuation. However, the topology of the connection is such that the bulk current threat is lower (approximately 10,000 A) and there is a longer cable run from the transformer to the Unit Boards. The net result is that the threat to critical systems from the 161 kV transmission lines is comparable to that from the 500 kV transmission line source. A model diagram from the 161 kV source is included in Appendix A.

5.3 EMP-Induced Signal Predictions

The predictions for the various portions of the safety-related systems are detailed on the response model diagrams in Appendix A and in Table 8.1. However it is also convenient to summarize these predictions as shown in Figure 5.3. Here the responses have been grouped according to the nominal operational levels of the equipment involved. It is observed that except for the instrumentation the predicted voltages are much less than the nominal operating levels. Furthermore, a significant fraction of the higher predictions (circled points on Figure 5.3) are observed to occur on systems in the outlying structures. Although the analysis indicates numerous signals less than 1 volt, all such predictions have been summarized as 1 volt in the subsequent vulnerability analysis. This is based upon the earlier observation that the general level of ambient response is on the order of 1 volt.

5.4 Verification Test Predictions

In order to gain confidence in the analytical techniques used to predict the response of the example plant in an EMP environment and to characterize prediction uncertainties (i.e., errors) introduced by using these techniques, it is desirable to perform verification testing. Such testing was performed on the example plant to a limited extent and involved the verification of certain assumptions used in computing the EMP responses including:

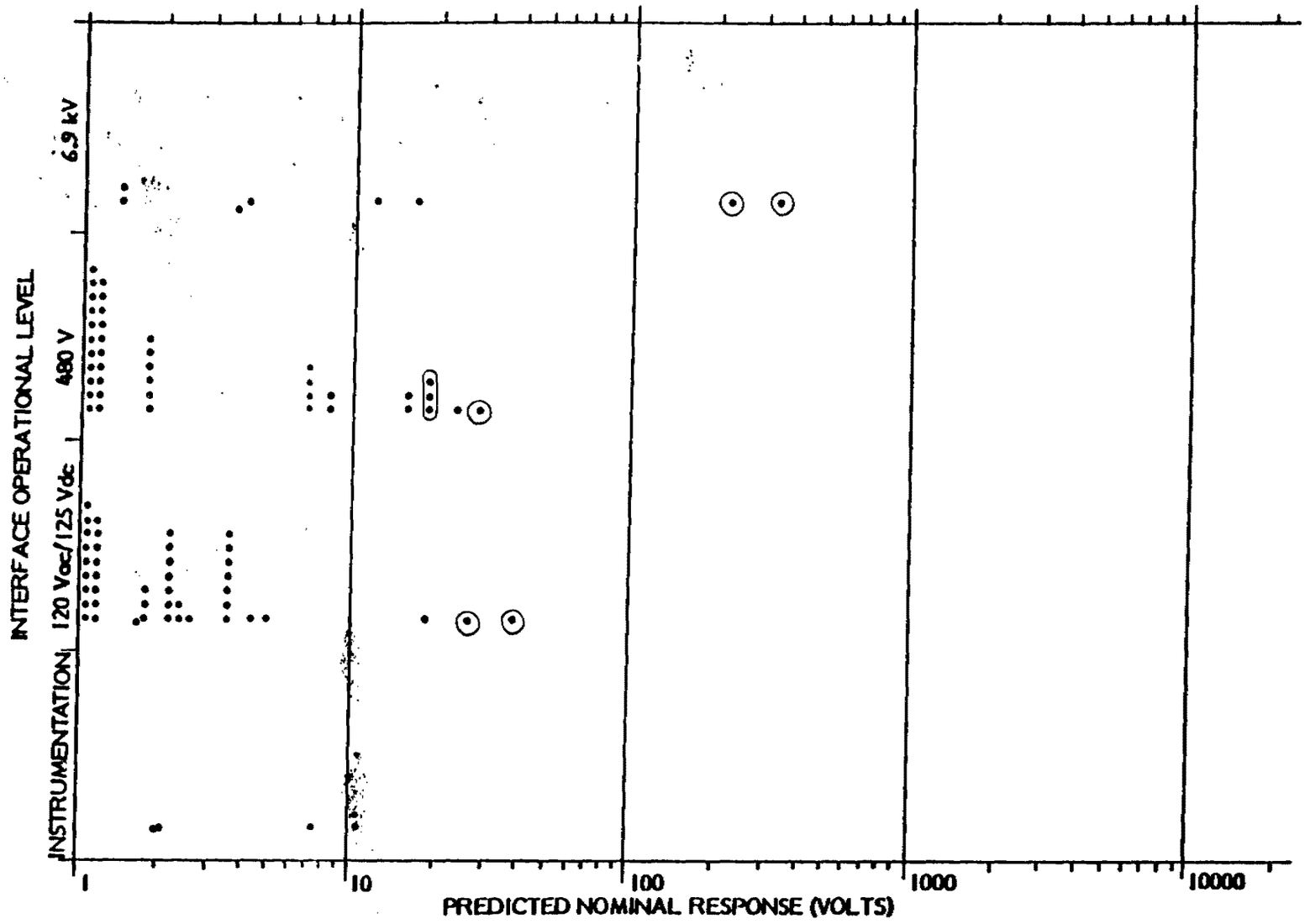

Figure 5.3. Summary of Predicted Nominal Responses.

1. Distribution of fanout currents at bus boards.

2. Attenuation of currents coupled to plant cables.

3. Shielding effectiveness of the building structure.

To accommodate verification testing, it was necessary to test at the plant during its construction phase and as such, the plant configuration did not mirror the operational configurations that were assumed in producing the EMP predictions. However, for the electrical configurations of the systems that were available at the time of testing, test configurations were devised that would allow the modeling assumptions to be checked. Because this configuration was different than the configuration assumed for EMP response predictions, test configuration predictions were performed using the same techniques and assumptions that were used to produce the EMP predictions.

The basic test configurations involved the injection of current onto plant cables or busses interfacing with cables running within the buried conduit structures outside the plant. Measurements were then made on the transmission and distribution of the induced current down into the various levels of the electrical distribution system. In this instance, the signal predictions at the test points assume a drive point bulk current of 1 ampere time-domain amplitude and a spectral content similar to that of the standard EMP double exponential pulse, but with frequencies above 10 MHz attenuated significantly (as would the spectral content of pulses conducted into the plant on buried conduit structure). The predictions are summarized in Table 5.1 with a portion of the prediction point (also the test point) locations illustrated on Figure 5.4. These predictions are also summarized in Tables 6.2 and 6.3 along with the test results.

Table 5.1

Predictions for CW Direct Injection Tests

Test Point	Predicted Response*
D	270 mA
E	90 mA
F	90 mA
G,I,J	270 mA
K,L,U	67 mA
X	11 mA
Y,Z	5.5 mA
AA,BB	11 mA
CC	9.6 mA
DD,EE,FF,GG	1.1 mA
HH	4.5 mA
II,JJ,KK,LL	0.43 mA
MM,NN	0.44 mA
VV,WW,XX	2.9 V
YY	3 mV
ZZ	5 mV
AAA	8 mV
BBB	16 mV
EEE	11 mV
C-E	2.7 V
C-G,E-G	8 V

*Assumes one ampere peak current at drive point.

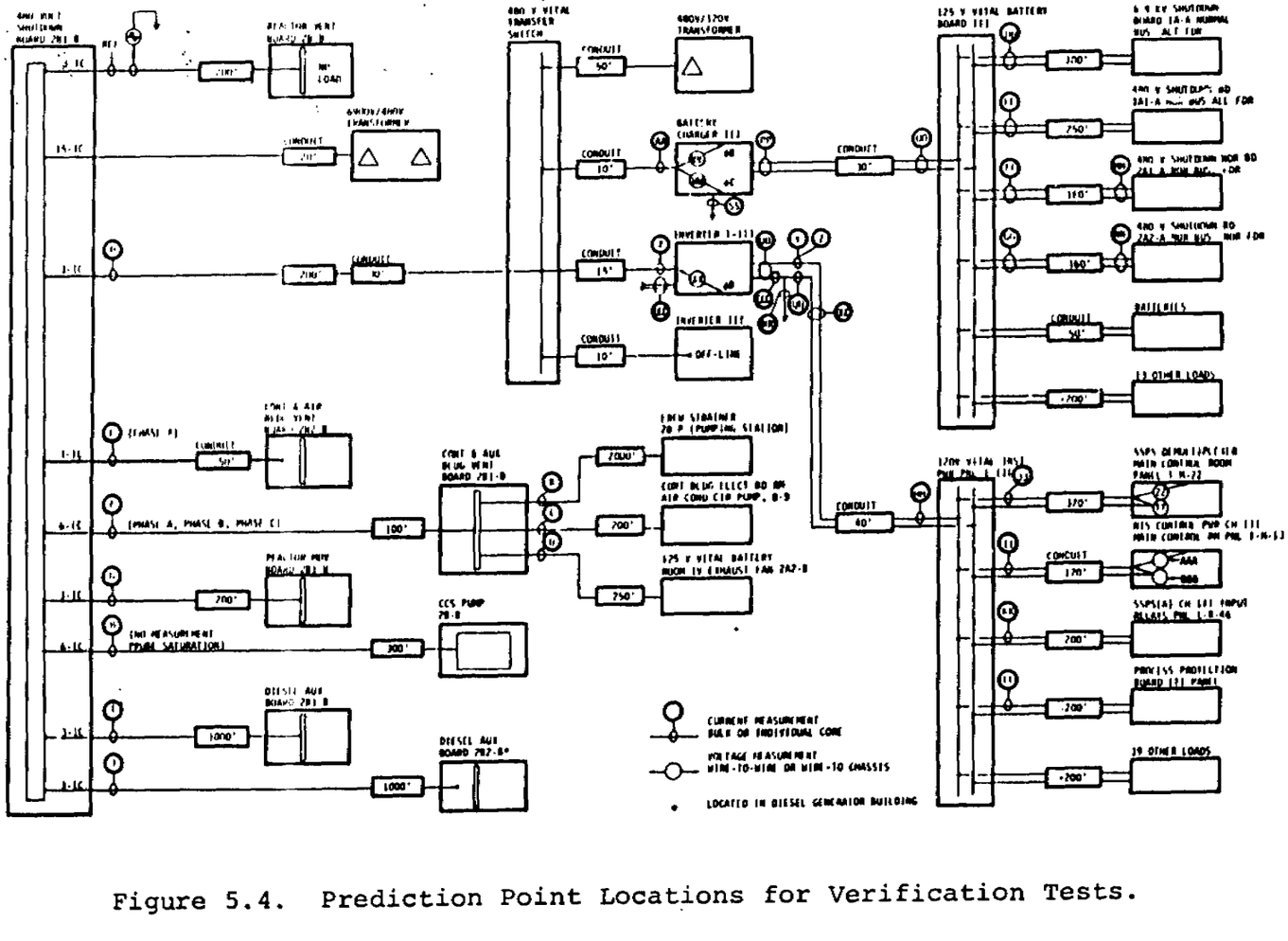

Figure 5.4. Prediction Point Locations for Verification Tests.

6.0 Verification Measurements

6.1 Introduction

Whenever a facility as complex as a communications terminal or a nuclear power plant is analyzed for EMP vulnerabilities, the question arises, "How good is the assessment?" Such concerns are frequently addressed, at least in part, by conducting experimental measurements. This program is no exception to that practice. However, it is impractical to subject a facility as large as a nuclear power plant to "threat level" simulation signals. On the other hand, it is possible to conduct a program of specialized verification measurements. Such tests were conducted at the Watts Bar Nuclear Plant and those measurements are discussed in detail in the following sections.

6.1.1 Direct Injection Tests. A test plan[11] was prepared and distributed to the NRC staff and the NRC Research Review Panel for this program to acquaint them with the test procedures and objectives, and to outline the impact of the tests on the facility operations. After review and subsequent discussions between the study team and the panel, the test objective was finalized as follows:

> "The objective of this test is to conduct a series of CW direct injection measurements on a selected sample of those points for which predictions have been made. The results of these measurements will then be used to compute the amplitude of the induced signals at the selected points. A comparison of the measured and predicted values may then be made to check the assumptions and analytical techniques used in the assessment."

It should be noted that these direct injection tests serve only as a check on the validity of the internal coupling models used and do not serve as a verification of the external to internal, i.e., incident field to facility penetration coupling mechanism.

6.1.2 CW System Description. The tests described in this section were carried out using equipment owned by the U.S. Defense Nuclear Agency and operated under contract by the IRT Corporation.

The DNA CW measurement system was built to provide a low-cost, time-efficient system to obtain estimates of EMP response at operational Command, Control and Communications (C^3) facilities, on a non-interferring basis. It has often been noted that there is an indispensible dependency of analysis on tests and tests on analysis. The CW system was built to help meet this need and to make it economically possible to obtain experimental data on the electromagnetic response of facilities at far more locations than would otherwise be possible. The designing of the system was an exercise in automation and efficiency of gathering, correcting,

formatting, and outputting data. The design was not, however, intended to be a fundamental advance in the design of simulators. In that regard it is basically no better nor worse than what the EMP community has used in the past for operational, ground-based C^3 facilities.

This hybrid CW measurement system consists of two basic subsystems--the Defense Nuclear Agency (DNA) Continuous Wave Measurement system designed by Boeing and modified by EG&G, and the Data Acquisition subsystem consisting of a PDP-11 computer system and software by EG&G. These two subsystems communicate with each other to produce, detect, display, and reduce CW data in the frequency range of .01 MHz to 100 MHz. The system is designed to test facilities either by CW electromagnetic radiation or CW direct injection, collecting the response function or transfer function data, removing the effects of the instrumentation involved, plotting the results and saving the data on cassette for future processing. The system modules consist of the measurement system--a transmitter subsystem and receiver system, the command link which synchronizes the two, sensors, power supplies and generator; and the data acquisition system--a PDP-11/34 CPU, five asynchronous interfaces (RS-232), two 5-megabyte disk drives, disk packs, a Tektronix plotter, system console, and cassette tape subsystem.

Equipment Description. The major equipment items used in the CW system are listed in Table 6.1.

Table 6.1.

Major Equipment Items

Transmitter System

Frequency Synthesizer	Systron Donner 1702
Computer Clock	Data-Chron 3170-114
Power Generator	ONAN 9AD74
Power Amplifier	Amplifier Research AR 500L

Receiver System

Network Analyzer	HP8407A
Phase-Magnitude Display	HP8412A
Frequency Synthesizer (2 ea)	Systron Donner 1702
Digital Multimeter (2 ea)	Data Precision 3400
Computer Clock	Data-Chron 3170-114
Digital Plotter	Tektronix 4662
Attenuators	Wavetek Turret 5010/5070
Fiber Optics System	HDL
Wide-Band Amplifier	HP8447A

The system configuration of the CW system is shown in Figure 6.1. The block diagram for the transmitter indicates that the unit can be used in either a radiated or direct inject mode. There is essentially no restriction on the kind of antenna to be used with the system thus leaving open the possibility of using different antennas for different applications. Direct injection testing is done using a specially designed, single-turn multi-core transformer shown schematically in Figure 6.2.

The receiver block diagram shows the system being used with a reference and measurement sensor, which in practice is some combination of a current probe, voltage probe, or field sensor. In the radiated mode, the nominal operating configuration is with a B field sensor as the reference and a current or voltage probe for the measurement sensor. In the direct inject configuration, a current probe is normally used at the reference with a current or voltage probe at the measurement point. The signals detected by these sensors are amplified and then transmitted to the network analyzer via a fiber optic system.

The receiver and transmitter subsystems are supplied with three synthesizers which are used in a variety of ways. The local RF synthesizer is used as a signal source for system calibrations and also provides a stable reference for ambient noise measurements. The receiver VTO synthesizer is synchronized with the activities of the transmitter RF synthesizer via the program control units (PCUs) to ensure that the receiver and transmitter are operating at the same frequencies.

The receiver DVMs perform A/D conversion of the raw magnitude and phase data generated by the network analyzer as well as providing a front panel check point to monitor the incoming data stream.

Raw data is sent to the DEC computer via the PCU where all computations using the data and all manipulation on the data sets are performed. Storage is available on the computer disk units with long-term storage being provided on cassette tape. Hard copy plots of measured data, corrected for system instrumentation effects as well as predictions of transient time domain responses based on the measured data are available in a hard copy plot via the Tektronix flat-bed plotter, an example of which is shown in Figure 6.3.

6.1.3 The Predicted Time Domain Response. The data output from the CW system which is of primary interest is the predicted time domain response. To produce this response, the computer uses measured transfer function data, corrected for system instrumentation effects, in conjunction with the spectrum of a given time domain signal driving function. This data is used to predict what the response to the time domain signal driving function would be at the test point if the given signal was incident at the reference point. In order to accomplish this task, the computer requires that a frequency domain description of the incident time domain signal be generated and stored. This spectral data is then multiplied by

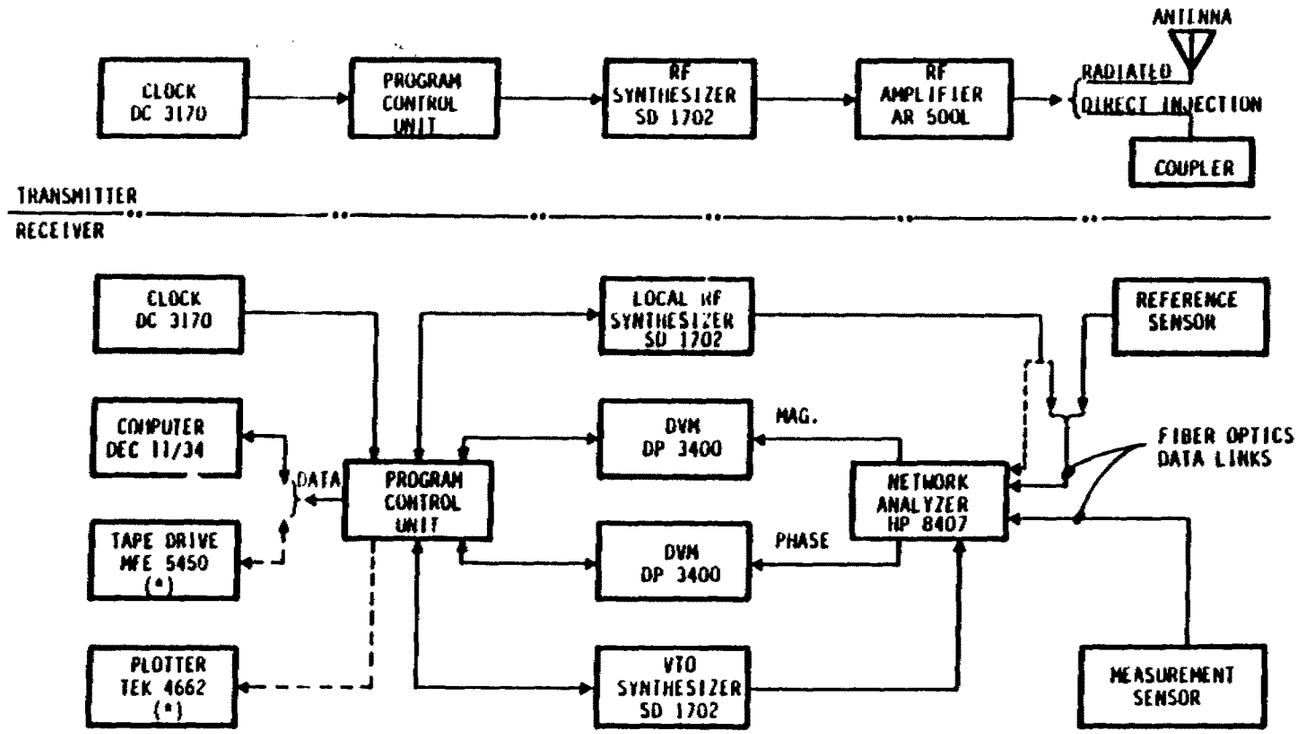

Figure 6.1. DNA CW Receiver and Transmitter Subsystems

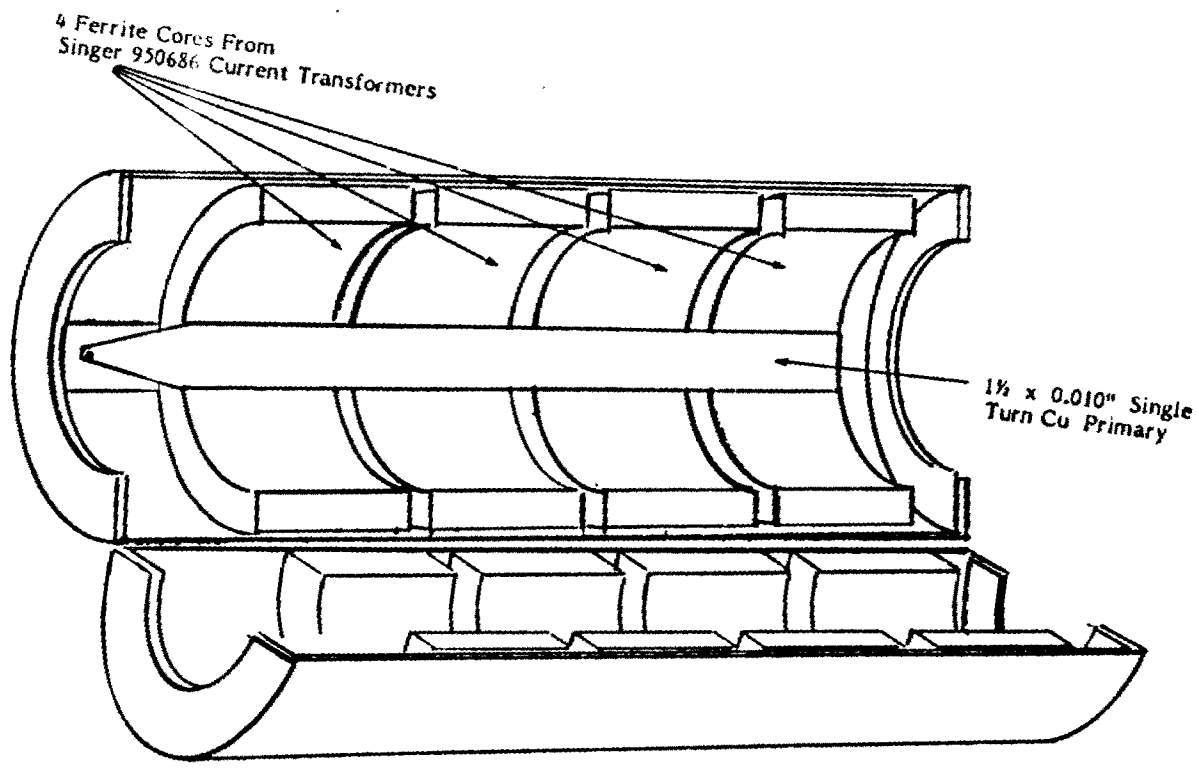

Figure 6.2. Direct Injection Current Transformer in Open Position

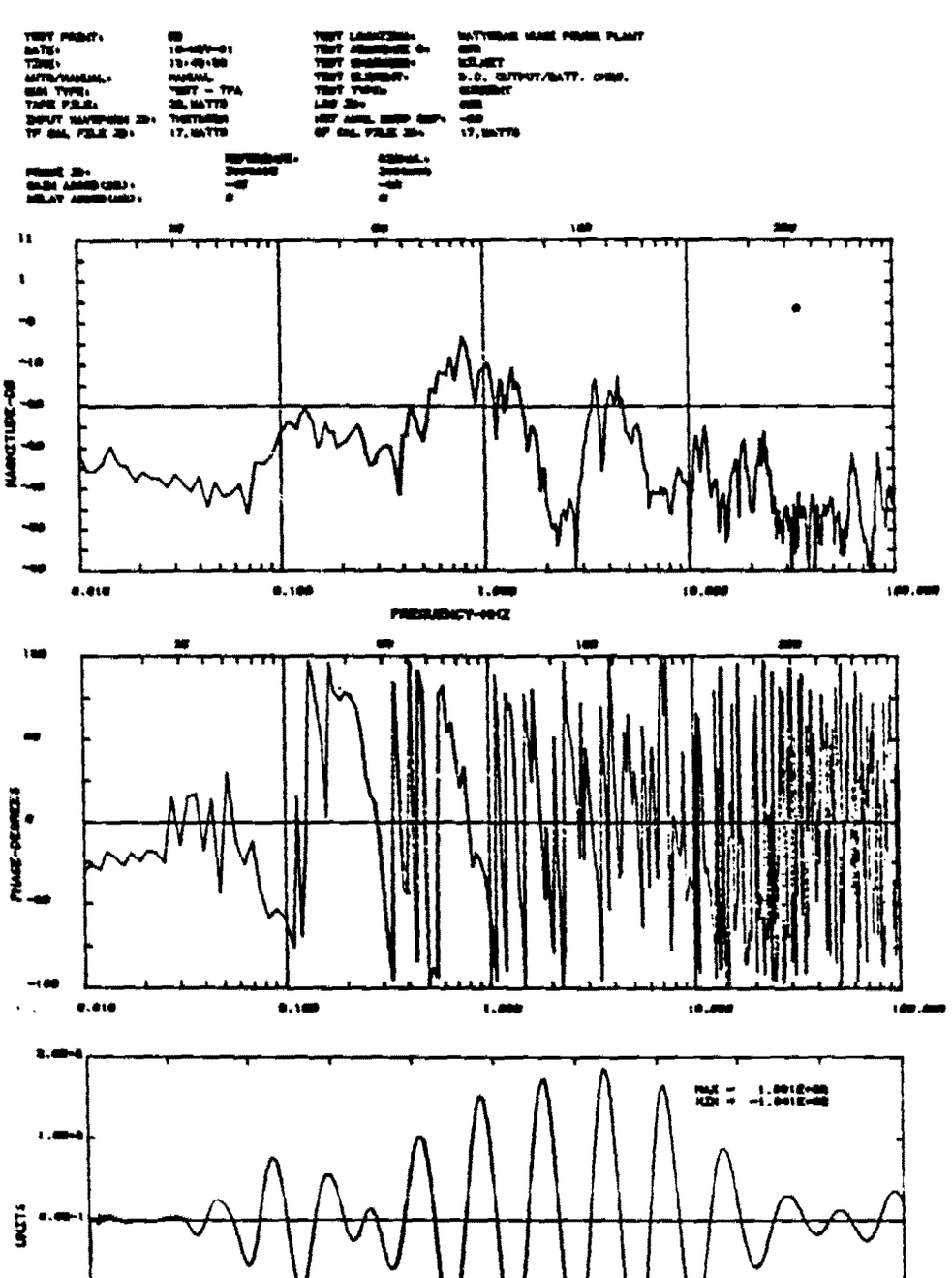

Figure 6.3. Example of Hard Copy Plot from Tektronix Plotter

the transfer function of interest and passed to a program which computes the inverse Fourier transform of the composite data set.

The Driving Function. The driving function is referred to in the CW literature as the "threat" while the computer file containing its description is referred to as the "threat file." There are a variety of mechanisms for creating or inputting the threat file. A digitized description of a time domain waveform can be inputted and transformed inside the computer or a suitably formatted file can be input directly. In many cases the threat file is generated internally from analytical expressions. A brief discussion of the process involved in generating threat files internally illustrates this commonly used feature of the system as well as illustrating the general structure of all threat files.

The analytic threat file is defined by the following time domain expressions convolved with the impulse response of a ninth-order bandpass Butterworth filter.

$$E_i(t) = A(e^{-\alpha t} - e^{-\beta t}) \text{ V/m} \quad 0 < \alpha < \beta \qquad (6.1)$$

where

$$A = 5 \times 10^4 \ \frac{\alpha + \beta}{\alpha} \left[\left(\frac{\alpha}{\beta} \right)^{\left(\frac{\beta}{\alpha + \beta} \right)} \right] \text{V/m} \ .$$

The Fourier transform of this function is given by

$$E_i(f) = \frac{A(\alpha - \beta)}{[(\alpha^2 + \omega^2)(\beta^2 + \omega^2)]^{1/2}} \text{ V-sec/m} \qquad (6.2)$$

$$\phi_i(f) = -\tan^{-1} \left(\frac{\omega(\alpha + \beta)}{\alpha\beta + \omega^2} \right) \text{ rad}$$

where α and β are operator-specified variables. The expressions in Equation 6.2 are stored in the computer, evaluated at all test frequencies, and then multiplied by the transfer function of a unity amplitude, ninth-order bandpass Butterworth filter. The upper and lower cutoff frequency of the filter are also operator-specified variables.

The primary purpose for including the Butterworth filter function is to reduce the effect of truncation error. The fact that the measured transfer function is not measured from dc to infinity, but is instead truncated at some finite frequency introduces an

oscillatory type of behavior in the predicted time domain response. This effect is attenuated by using a function which terminates the data set in a more gradual manner but only at the expense of suppressing some of the real data. The Butterworth filter is simply a "windowing" function, and as such, it represents a compromise as do all windowing functions.

The threat file which results from the evaluation of equation 6.2 and the Butterworth filter function is a table of complex values with the magnitude and phase of the composite function defined at every possible test frequency that the system can use. This means that the threat function is defined at 4000 frequencies in the range of 10 KHz to 100 MHz, 1000 frequencies in each decade. Regardless of how the threat file is created, be it internally or through the transform of some waveform read into the computer, the final result has to be a table of look up values defined at a predetermined set of 4000 frequencies.

The Inverse Fourier Transform. The method used to perform the inverse transform is a variation of the Guilleman impulse train technique. In this particular application it is more accurate to say that the Guilleman algorithm is equivalent to the inverse, Fourier-integral transform, performed on a contiguous, straight line approximation, of the imaginary part, of the frequency domain data set.[12]

6.2 Prediction and Measurement Comparison

6.2.1 Data Treatment and Test Point Locations. Computing the time domain transient response at a given point, once the transfer function has been measured, requires a knowledge of the incident spectrum at the reference point, i.e., the "threat" referred to in Section 6.1.3.

The threat on the plant cabling can generally be considered broad spectrum up to about 10 MHz because earth losses on the buried penetration cables severely attenuate the higher frequency content of the EMP spectrum. Given this threat spectrum and the lengths of the cabling in the plant, the abbreviated analysis technique employed by Boeing results in the prediction of the response peak amplitudes and limited characterizations of the time histories of the response waveforms. The response waveforms are expected to be damped sinusoids (or sums of several damped sinusoids) with resonant frequencies ranging from 500 kHz to 10 MHz.

In choosing the waveform to be used for current injection on facility cables, two characterizations were considered. One threat characterization uses a 2 MHz damped sinusoid (an average value of the expected range of response resonant frequencies) for the threat signal and the other, the EMP spectrum, attenuated above 10 MHz. During on-site testing most of the transfer function data was processed with the 2 MHz damped sinusoidal threat spectrum (identified by THRTDS2M) as originally proposed. The transfer function data was subsequently reprocessed using the standard EMP double exponential

soectrum that had been Butterworth filtered above 10 MHz (identified by THRTWATT).

Since the transient time domain response for the data processed with THRTDS2M is critically dependent on the amplitude of the transfer function in the vicinity of 2 MHz, the data processed with the EMP spectrum (THRTWATT) should be used to compare the test measurements to the predictions computed by Boeing. Typical formats of the measured data using THRTDS2M and the recomputed time domain transient using the threat file THRTWATT with the following characteristics:

THRTDS2M - 2 MHz Damped Sine Wave (Q = 8)
THRTWATT - Double Exponential $\alpha = 4 \times 10^6$, $\beta = 4.76 \times 10^8$
(Butterworth $f_l = 10^4$ Hz and $f_u = 10^7$ Hz)

are shown in Figures 6.4 and 6.5, respectively.

A comparison of measured and predicted responses for a total of thirty-seven test points has been made and consist of twenty-seven current points and ten voltage points.

The measurements were divided among the 480V distribution system, the 120V ac control system and the 120V dc control system located in the control room and adjacent equipment and board rooms.

The test point locations at which measurements were made and their identifiers are shown schematically in Figures 6.6 through 6.10. It should be noted that predictions were not made for all points at which measurements were made and consequently comparisons will only be presented for a subset of the measurement points shown in the above referenced figures.

6.2.2 Format for Presentation of Data. For each point for which a prediction and measurement exists, the following ratio is computed:

$$R(t) = 20 \log_{10} \frac{\text{Peak Amplitude Measured Response}}{\text{Peak Amplitude Predicted Response}} \qquad (6.3)$$

The responses are the maximum values in the time domain with no regard being paid to the sign of the peak.

The measured responses are normalized to a one ampere peak, double exponential pulse ($\alpha = 4 \times 10^6$ and $\beta = 4.76 \times 10^8$) filtered by a ninth order, unity amplitude Butterworth filter with a lower cut-off frequency of 10 kHz and an upper cut-off frequency of 10 MHz (THRTWATT).

As noted earlier, the purpose of these tests was to provide some verification of the Boeing analytical and thus to provide additional confidence in their analytical predictions. Therefore, a convenient

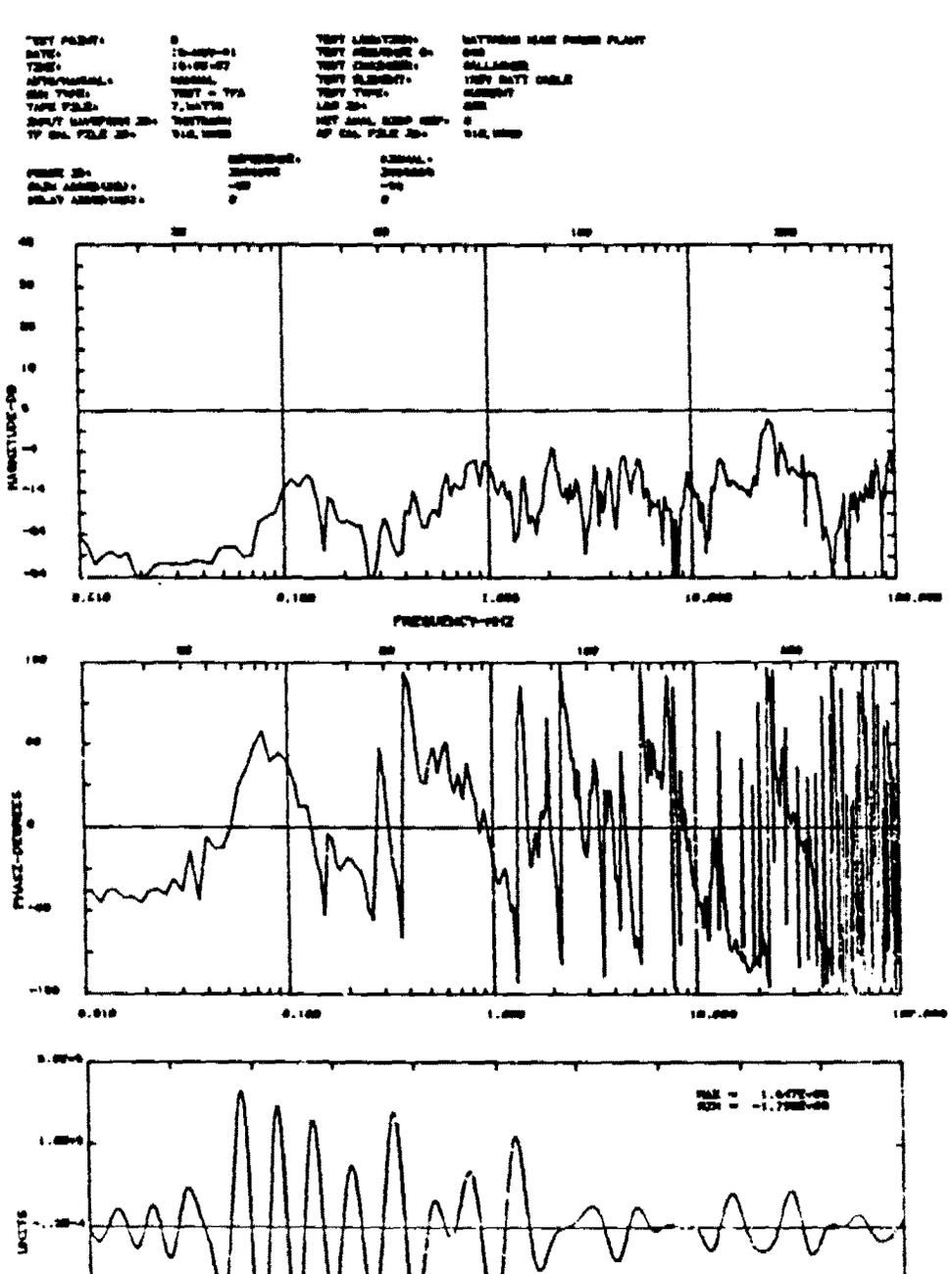

Figure 6.4. Measured Data and Computed Time Domain Response for Test Point 7 Using THETDS2M

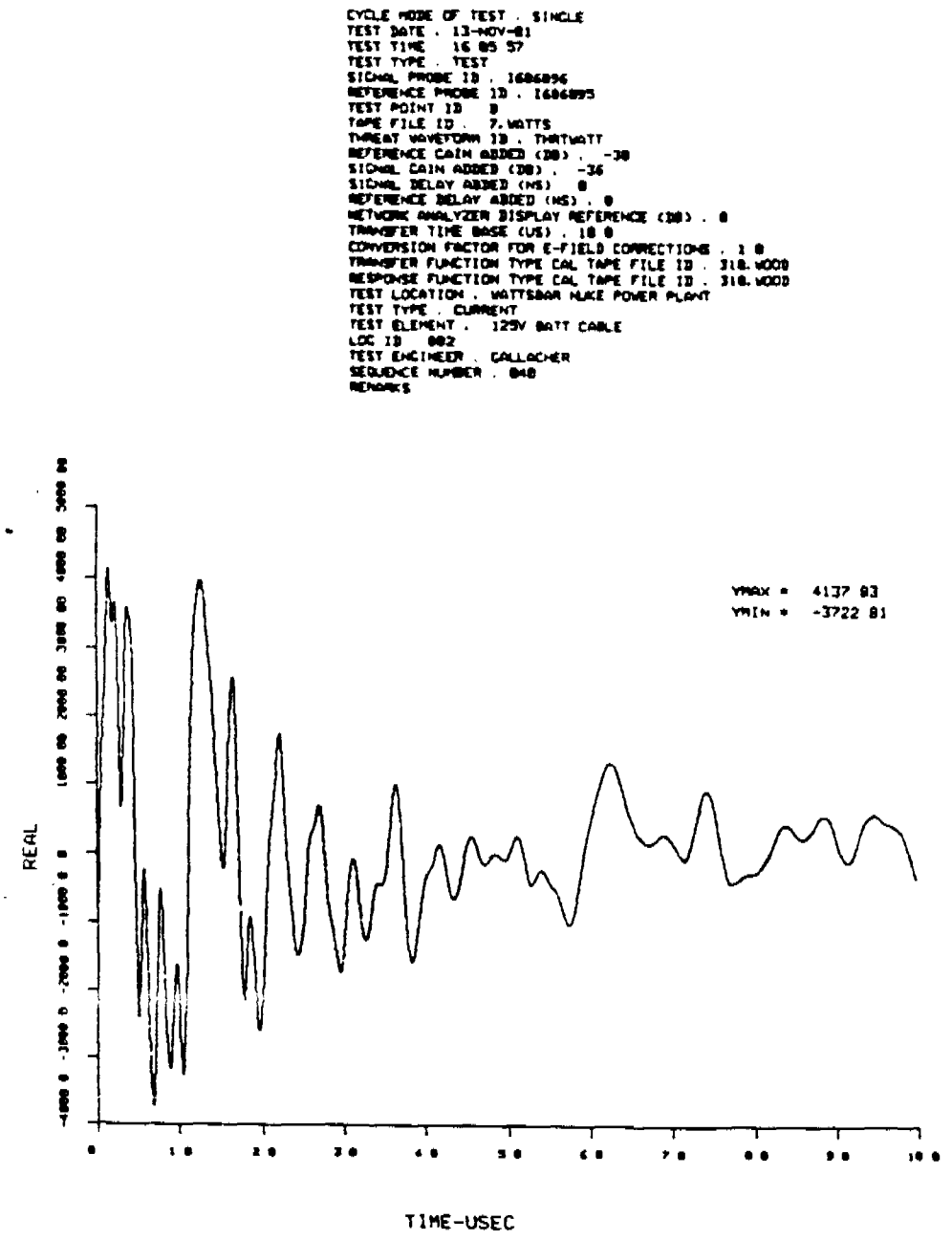

Figure 6.5. Recomputed Transient Time Domain Response for Test Point D Using Threat File THRTWATT

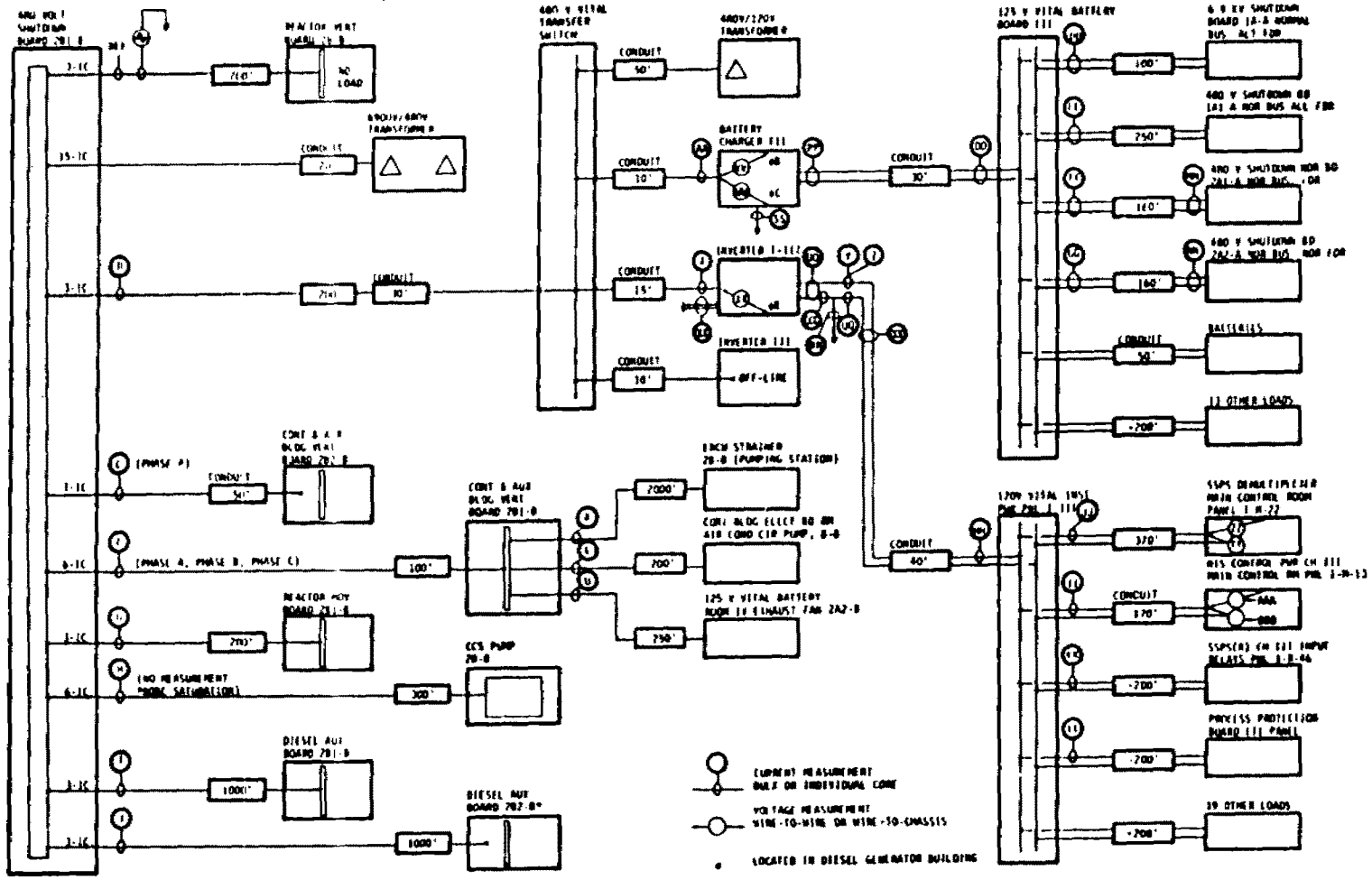

Figure 6.6. Test Point Location From 480V Shutdown Board to 125V Vital Battery Board

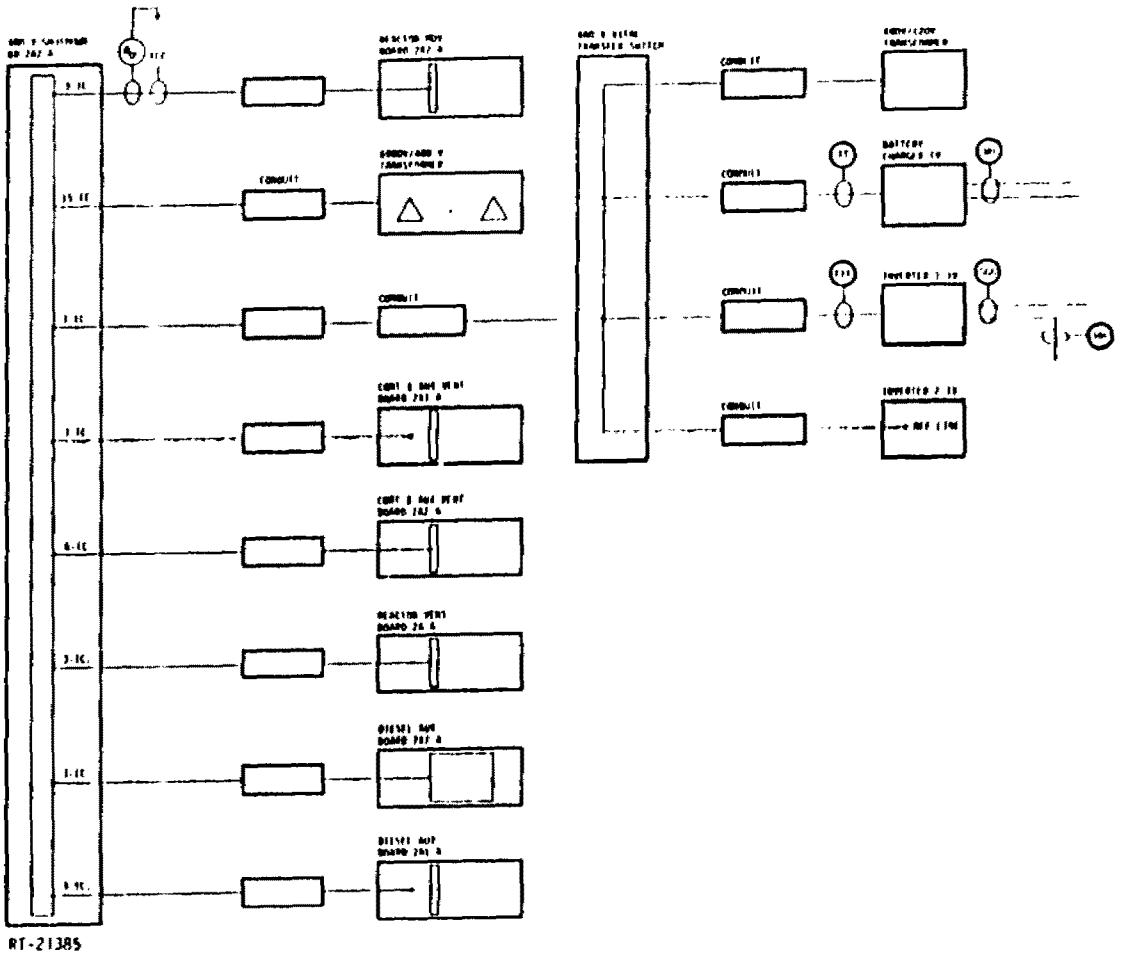

Figure 6.7. Test Point Locations Vicinity of 480V Vital Transfer Switch

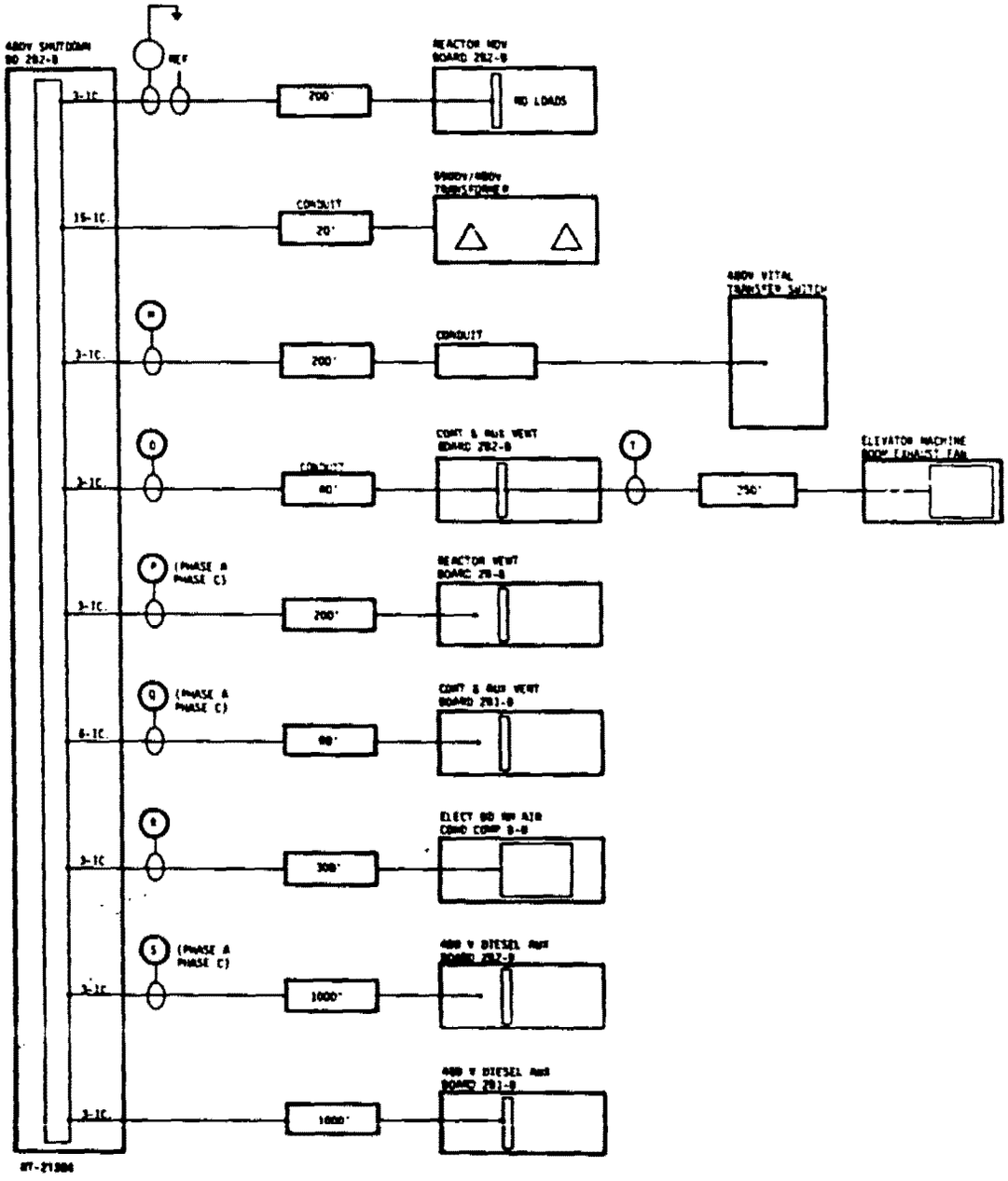

Figure 6.8. Test Point Locations Vicinity of 480V Shutdown Board

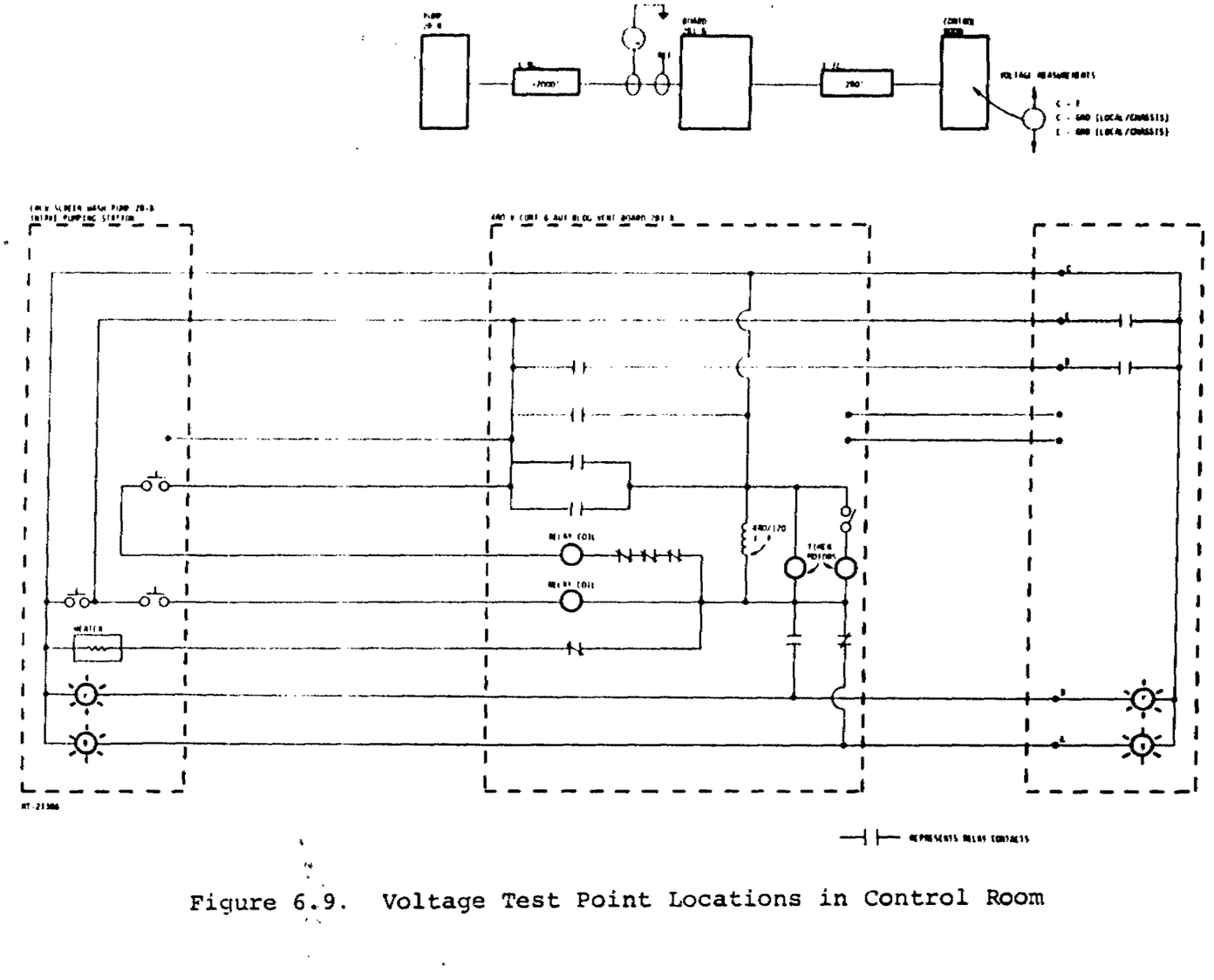

Figure 6.9. Voltage Test Point Locations in Control Room

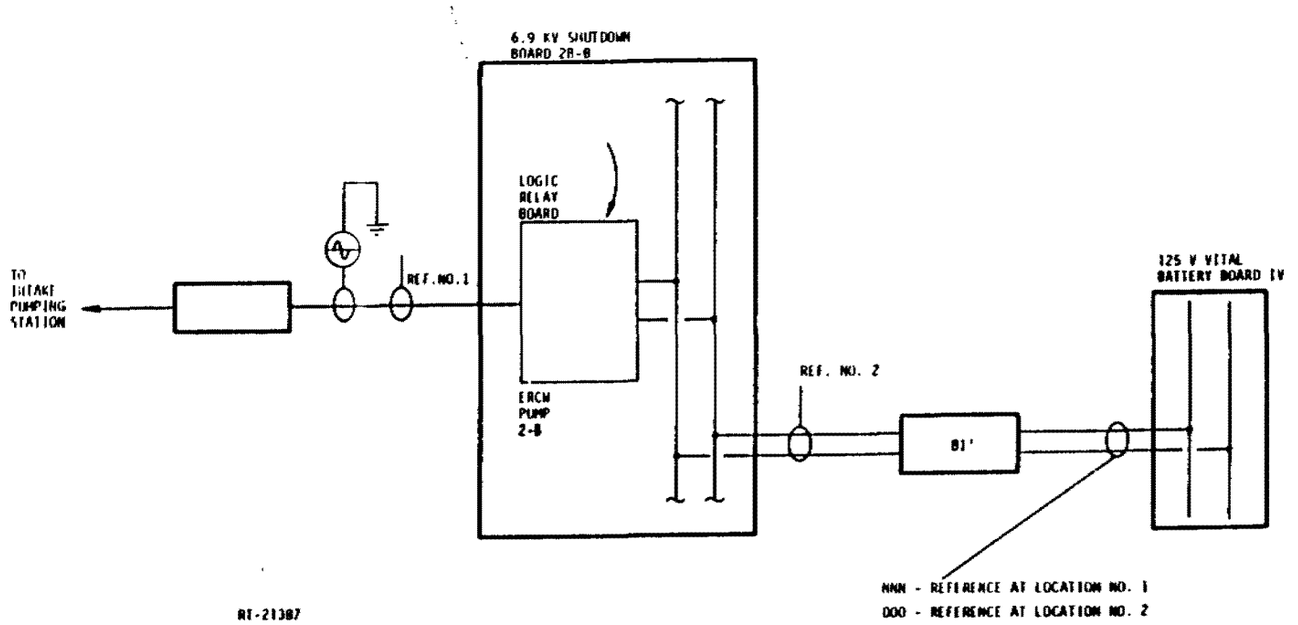

Figure 6.10. Test Point Locations at Output of 6.9kV Shutdown Board

way to summarize the overall quality of the prediction and measurement set, is to compute a mean, $\bar{X}$, of the individual ratios R(t) defined in Equation 6.3 and a sample standard deviation, that is

$$\bar{X} = \frac{1}{n} \sum_{i=1}^{n} R_i(t) \qquad (6.4)$$

and

$$\sigma = \sqrt{\frac{\Sigma R^2 - (\Sigma R)^2/n}{n - 1}} \qquad (6.5)$$

Using this approach, a negative value for $\bar{X}$ would imply that, on the average, the analysis is conservative in that it generally predicts larger currents (or voltages) than measured, a positive value of $\bar{X}$ would imply a generally non-conservative analysis.

6.2.3 Comparison of Measured and Predicted Response. Comparison of the individual measured to predicted response at the 27 current points and 10 voltage points are given in Tables 6.2 and 6.3, respectively.

These reduce to

$\bar{X}$ = - 1.75 dB and σ = 8.4 dB (27 Current Points)

$\bar{X}$ = +13.2 dB and σ = 13.2 dB (10 Voltage Points)

and overall

$\bar{X}$ = + 2.3 dB and σ = 11.8 dB (37 Points)

These results and their implications are discussed further in Section 6.5.1.

6.2.4 Discussion of Measurement Accuracy. Probe and system calibrations (PROBCAL, TCAL and RCAL) were conducted each day during the test when measurements were made and no abnormalities were detected.

Repeatability of results were checked by repeating measurements at two test points over a three-day period. The results of these gave a sample standard deviation (nine measurements) of 0.8 dB.

Table 6.2.

Detailed Comparison of Measured and Predicted Responses

Current Points

Test Point Identifier	Predicted Response (mA)	Measured Response (mA)	Meas. Resp. / Pred. Resp. (dB)
D	270	82.7	-10.3
E	90	83	- 0.7
F	270	216	- 1.9
G	270	270	0.0
I	270	156	- 4.7
J	270	122	- 6.9
K	67	17.5	-11.7
L	67	15.5	-12.7
U	67	14.4	-13.3
X	11	22.9	6.4
Y	5.5	1.0	-14.8
Z	5.5	1.1	-13.9
AA	11	30.6	8.9
BB	11	21.1	5.7
CC	9.6	24	8.0
DD	1.1	6.7	15.7
EE	1.1	2.5	7.1
FF	1.1	2.1	5.6
GG	1.1	3.6	10.3
HH	4.5	1.7	- 8.5
II	0.43	0.35	- 1.8
JJ	0.43	0.14	- 9.7
KK	0.43	0.37	- 1.3
LL	0.43	0.4	- 0.6
MM	0.44	0.45	0.19
NN	0.44	0.48	0.8
EEE	11	7.5	- 3.3

$\bar{X}$ = -1.75 dB σ = 8.4 dB

Table 6.3.

Detailed Comparison of Measured and Predicted Responses

Voltage Points

Test Point Identifier	Predicted Response (V)	Measured Response (V)	Meas. Resp. / Pred. Resp. (dB)
AAA	8×10^{-3}	144×10^{-3}	+25
BBB	16×10^{-3}	140×10^{-3}	+18.8
VV	2.9	3.1	+ 0.58
WW	2.9	2.8	- 0.30
XX	2.9	2.77	- 0.4
YY	3×10^{-3}	166×10^{-3}	+34.8
ZZ	5×10^{-3}	147×10^{-3}	+29.3
C-E	2.7	3.4	+ 2.0
C-G	8.0	26	+10.2
E-G	8.0	32	+12.0

$\bar{X}$ = +13.2 dB σ = 13.2 dB

Ambient noise levels were made in the frequency domain from 10 kHz to 100 MHz at five test points within the facility, namely, I, G, DD, NN and GG. These ambient noise measurements were made with the probe in position on the test point and using a -10 dbm signal from the synthesizer as reference. For all points and at all frequencies the minimum level of the signal above ambient noise was > 65 dB.

6.2.5 Supplementary Measured Data. Additional measurements were made in an attempt to provide further understanding of the interaction of an EMP with a commercial type nuclear power plant. These are presented in the following sections.

Cable Attenuation Measurements. Values for cable attenuation were computed from two sets of response measurements as shown in Table 6.4.

Table 6.4.

Cable Attenuation

Test Point Identifier	Cable Length	Measured Response at GG/FF	Measured Response at NN/MM	Total Att. dB	Total Att. dB/100'
GG-NN	160'	3.6×10^{-3}	0.48×10^{-3}	17.5	10.9
FF-MM	160'	2.1×10^{-3}	0.45×10^{-3}	13.4	8.3

The measured responses are peak values of the transient time domain response. The resultant average attenuation 9.6 dB/100' compares favorably to the values assumed in the analysis of 6 dB/100'.

Transfer Function From Exterior to Interior. In order to investigate the nature of the coupling from the facility exterior to some internal point, a measurement was made of the transfer function on cable 1-4PL-215-4975A running from manhole #22 on the west side of the facility (see Figure 6.14) to the auxiliary room adjacent to the control room. The measured transfer function is shown in Figure 6.11. This transfer function is multipled by the assumed double exponential threat driving function (see Section 6.1.3) and the corresponding time domain transient is shown in Figure 6.12.

Offset and Standard Deviation by Groupings of Test Points. A measure of offset and standard deviation for test points located on the same distribution board is given in Table 6.5. These are the same test points reported in Table 6.2.

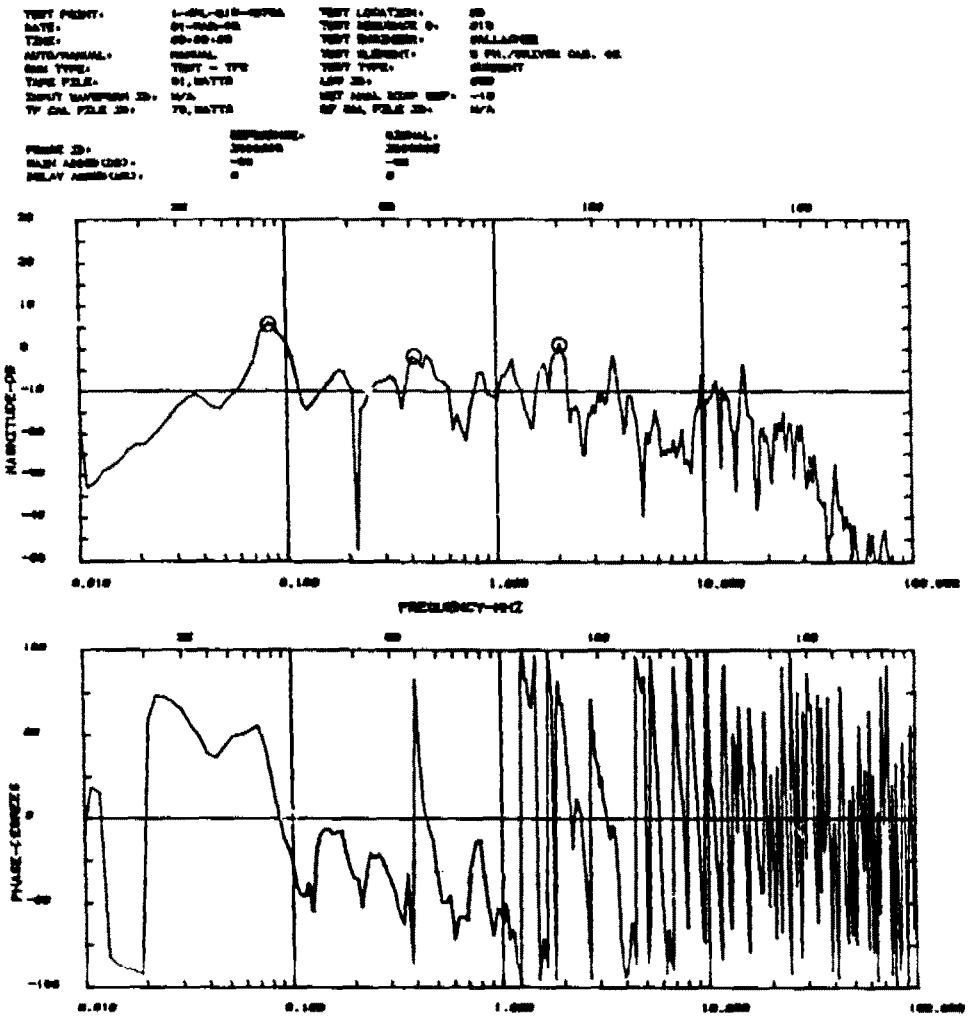

Figure 6.11. Measured Transfer Function from Manhole #22 to Auxiliary Building, Cable 1-4PL-215-4975A

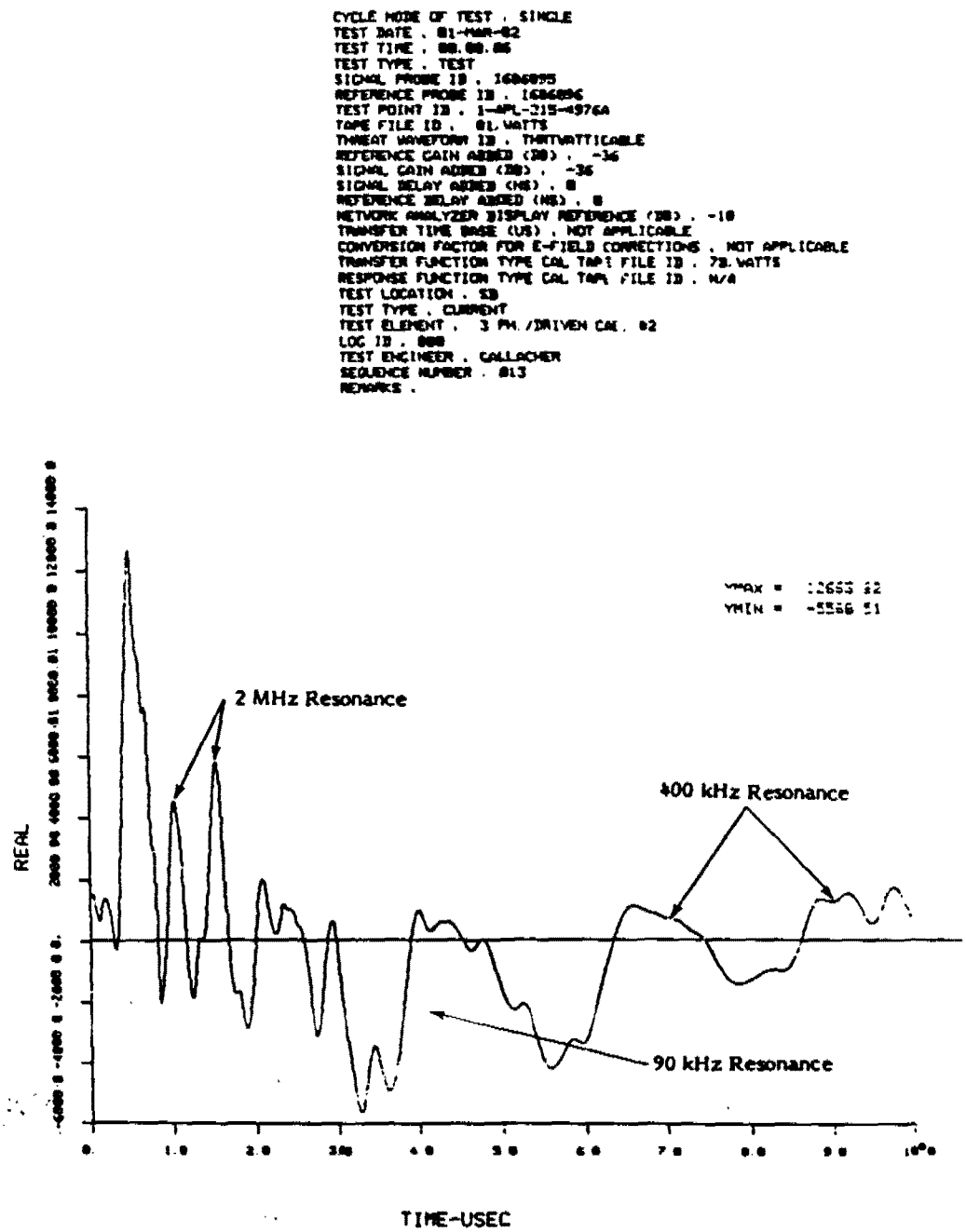

Figure 6.12. Predicted Time Domain Response from Exterior to Interior of Facility

Table 6.5.

Offset and Standard Deviation by Test Point Location

480V Shutdown Bd. 2B1-B

Test Point Identifier	Pred. Response (mA)	Meas. Response THRTWATT	Meas. Resp. / Pred. Resp. (dB)
D	270	82.7	-10.3
E (Single ϕ)	90	83	- 0.7
F (Single ϕ)	90	72	- 1.9
G	270	270	0.0
I	270	156	- 4.7
J	270	122	- 6.9

$\bar{X}$ = -4.1 dB σ = 4.0 dB

Cont. and Aux. Bldg. Vent Bd. 2B1-B

K	67	17.5	-11.7
L	67	15.5	-12.7
U	67	14.4	-13.3

$\bar{X}$ = -12.5 dB σ = 0.8 dB

125V Vital Battery Bd. III (18 Loads)

DD	1.1	6.7	15.7
EE	1.1	2.5	7.1
FF	1.1	2.1	5.6
GG	1.1	3.6	10.3

$\bar{X}$ = +9.7 dB σ = 4.4 dB

INPUT = CC
= 24×10^{-3} A

120V Vital Inst. Power Panel 1-111 (23 Loads)

JJ	0.43	0.14	- 9.7
KK	0.43	0.37	- 1.3
LL	0.43	0.4	- 0.6
II	0.43	0.35	- 1.8

$\bar{X}$ = -3.3 dB σ = 4.2 dB

INPUT = HH
= 1.7×10^{-3}A

6.3 Inadvertent Penetration Tests

In predicting the response of the Watts Bar NPP to an EMP event, the major contribution to the coupling of energy to the facility interior was determined by Boeing to be the cabling from the Diesel Generator Building and the Intake Structure to the Auxiliary Building. The question of the existence of other "inadvertent" or "unknown" penetrations which could contribute to the internal coupling was raised by the panel. Subsequently a test plan was developed which had as one of its objectives the determination of whether or not significant inadvertent or unknown penetrations had been overlooked in the analysis.

In the test the following procedure was adopted. First, a current probe was attached to a test point in the facility that was known to be connected directly to a known external to internal penetration. The external penetration was then excited at a given frequency by means of a multi-turn, one meter diameter loop and the response of the test point recorded. The loop was then moved around the building exterior, first parallel to the facility exterior wall and then at right angles to the facility exterior, while observing the test point response. In this way any inadvertent or unknown penetration excited by the loop, and coupling directly or indirectly to the monitored test point will be detected. This procedure is shown figuratively in Figure 6.13.

6.3.1 Search Procedures. The external penetrations were driven from a 240 turn, one meter diameter loop. The test point response was monitored using a Stoddart (#93686-3) current probe and an Ortholoc-SC 9505 Two Phase Lock-in Analyzer.

Test point response as a function of transmitter (i.e., loop) frequency was as follows:

Test Point Response	Frequency
330 μV	15 kHz
230 μV	45 kHz
180 μV	90 kHz

Since only one frequency was to be used, all measurements were carried out at the frequency giving maximum response, i.e., 15 kHz.

The location of the external manholes and the runs over which the transmitter was taken are shown in Figure 6.14. Ongoing construction activity on the east side of the facility during the testing prevented the transmitter from being moved into that location.

In order to estimate the sensitivity of the test point response to the proximity of the transmitter with respect to the external penetration, the response of the test point as a function of transmitter position with respect to the penetration was measured and is shown in Figure 6.15. It should be noted that the test point

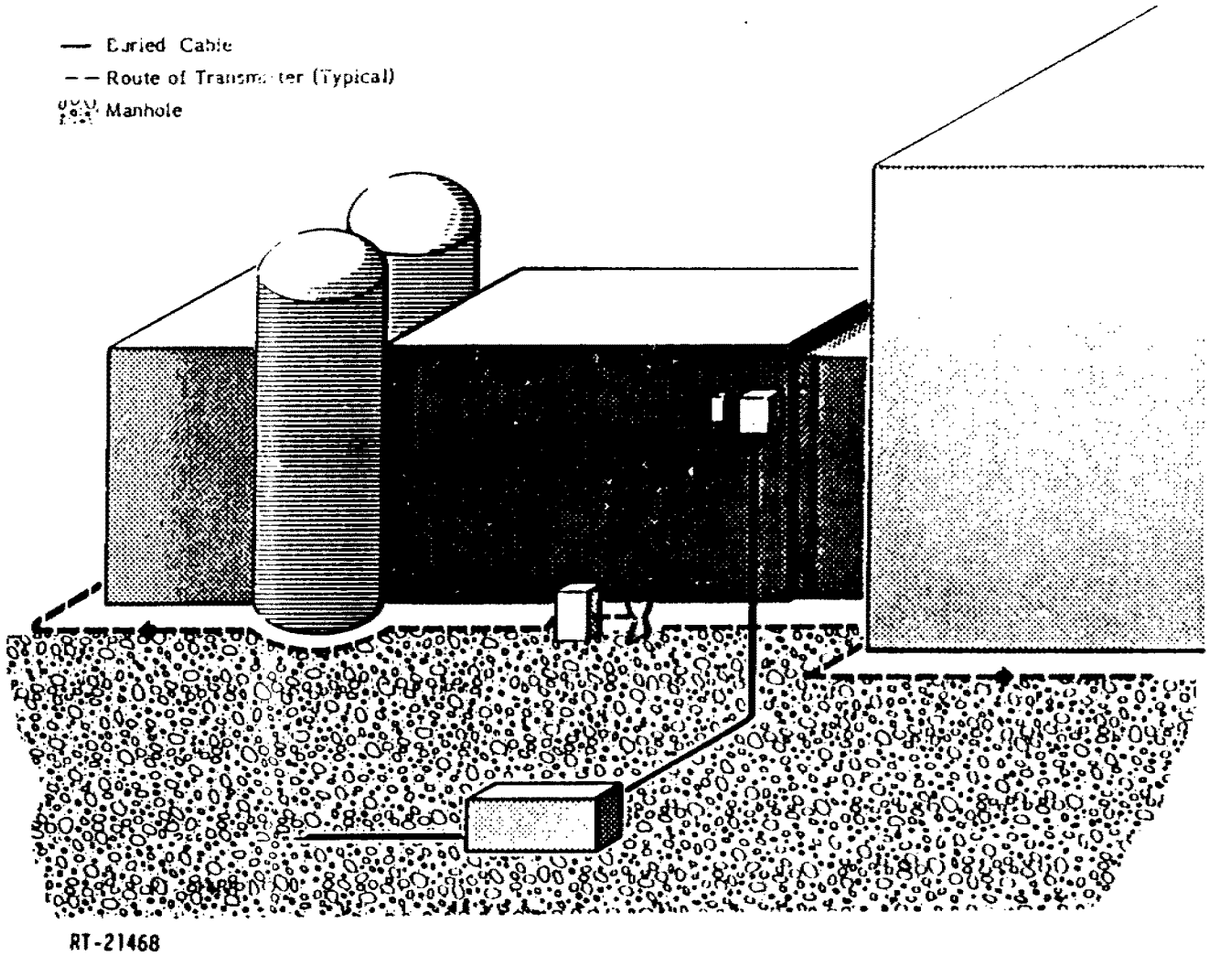

Figure 6.13. Search for Inadvertent Penetrations--Equipment Location

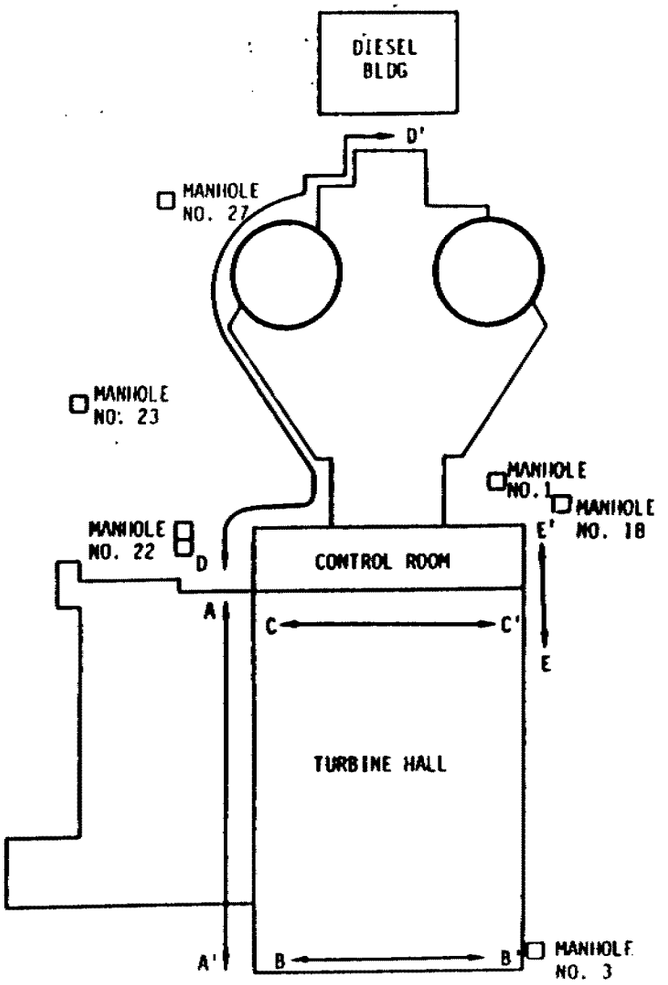

Figure 6.14. Transmitter Locations Used in Search for Inadvertent Penetrations

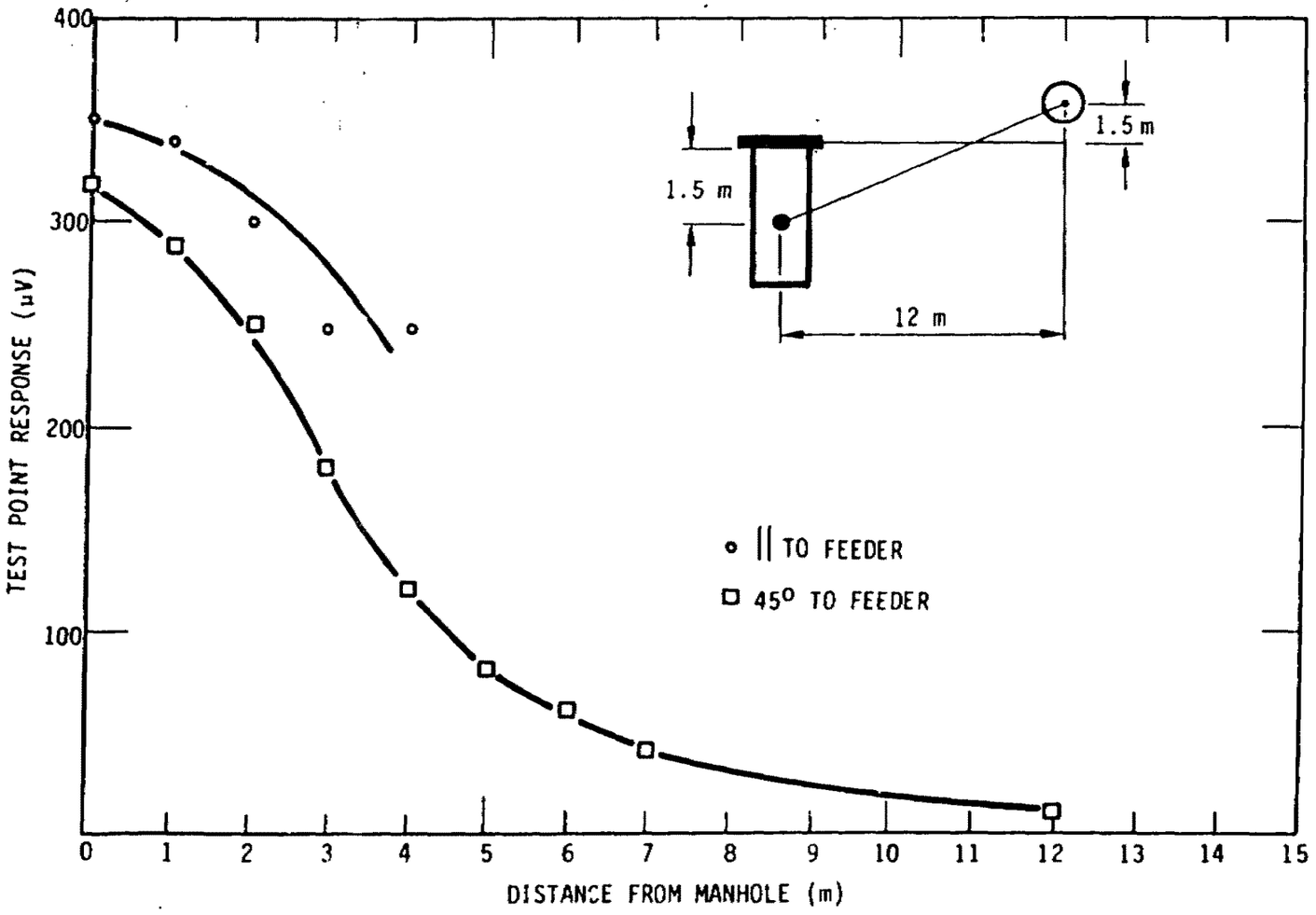

Figure 6. 15. Test Point Response as a Function of Transmitter Location

response is 6 dB above the ambient noise level with the transmitting antenna 12 meters from the penetration at an angle of 45° with respect to the penetration.

6.3.2 Search Results. In the search for inadvertent penetrations, five test point locations were chosen. A sixth point was instrumented but because the circuit breakers were open at the distribution board, the test point was not energized. The initial excitations were via manholes #1, 18 and 22.

A summary of the results of the search are given in Table 6.6.

6.4 Facility Insertion Loss Measurements

As part of a second series of tests, a measurement of the insertion loss present in the facility was undertaken. This was implemented in order to verify the Boeing assumption that the contribution to induced internal currents and voltages from diffused fields is negligible compared to the induced currents and voltages resulting from coupling to external to internal penetrations.

Two types of measurements were conducted. The first was identical in almost all respects to MIL-STD-285, in which local values of electric and magnetic insertion loss at selected frequencies are measured using electric and magnetic dipoles. The second was a measurement using a radiated CW source and the CW system described in Section 6.1.2 in order to assess the influence of penetrations and apertures on insertion loss. The radiated source in this case was a top-loaded monopole described in detail in Section 6.4.1.

6.4.1 Details of the Measurement Technique. The amplitude of the insertion loss produced by an enclosure is a function not only of the materials used in the construction of the enclosure but is also dependent on the characteristics of the fields themselves. Thus, it has become common practice to define both a magnetic and electric field shielding effectiveness or insertion loss. In essence, this represents the two practical extremes that are encountered in an operational environment. Magnetic field shielding effectiveness is the shielding associated with an electromagnetic field whose magnetic or $\bar{H}$ field component is much larger than its associated electric or $\bar{E}$ field component. The type of source that produces this field (the small loop in this case) is often referred to as a low impedance source. Electric field shielding effectiveness refers to the shielding associated with an electromagnetic field whose $\bar{E}$ field is much larger than its associated $\bar{H}$ field. This type of field is produced by a high impedance source such as short electric dipole.

Numbers which are stated as a measure of a shield's effectiveness can vary because of differences in equations used to define the term. For this reason, defining equations for magnetic and electric field SE are included in this document. It should be noted that any SE number is only meaningful when related to its defining equation and to the system used to measure the quantities in the equation.

Table 6.6.

Results of Search for Unknown or Inadvertent Penetrations

Excitation Manhole Number	Test Point	Manhole Excitation Level	Noise Level	Signal Level	Remarks
22	1-4PL-215-4976A feed from DG building	320 μV	1-10 μV	1-10 μV	30 μV response parallel to building on Run DD' - excitation of manhole #27
22	0-3FE-39-668 120V AC board 4G	420 μV	2-4 μV	2-4 μV	120 μV response Run CC' - excitation of CO_2 fire protection Cct. Feeds bus adjacent to test point. 30 μV response Run EE' - excitation of CO_2 fire protection Cct.
1	ERCW screen wash pump B-B cont. and aux. building vent BD2B1-B from cable 2-4PL-67-3905B	1-5 μV	1-5 μV	N.A.	Breaker open at vent board
1	ERCW screen wash pump B-B control cable cont. and aux. building vent board 2B1-B. From cable 2-3PL-67-3907B	30 mV	0.5 mV	0.5 mV	Preamp in (40 dB). At B' parallel to back wall 0.70 mV due to excitation of cable at manhole #3
18	Normal fdr diesel aux BD B2-B from cable 2-4PL-215 4985B	130 μV	1-5 μV	1-5 μV	
1	ERCW Strainer XMTR 67-9A cont. and aux. building vent bd. driven from cable 2-4PL-67-3913A	180 μV	1-4 μV	1-5 μV	150 μV response ⊥ to E, wall turbine hall due to excitation of cable 2-4PL-67-3913A at manhole #3

* Background noise level at test point with transmitter off.

** Observed signal level at test point with transmitter on and away from manhole except as noted under Remarks.

The expressions used for computing electric and magnetic field SE are

$$S_E = 20 \log_{10} \frac{E_1}{E_2} \qquad (6.6)$$

and

$$S_H = 20 \log_{10} \frac{H_1}{H_2} \qquad (6.7)$$

where E_1 = electric field in absence of enclosure; E_2 = electric field within the enclosure; H_1 = magnetic field in absence of enclosure; H_2 = magnetic field within the enclosure.

The equations themselves along with the definitions associated with the field quantities imply the method used for measuring SE, a method often referred to as the "insertion-loss" method.

Ideally the way to measure shielding effectiveness is by the "insertion-loss" technique.[13] First, the transmitter and receiver are set up at a location, in the absence of the shield, and the field level at the receiver measured for a given output level from the transmitting antenna. Next, the shield is inserted between the transmitter and receiver locations and the field at the receiver measured a second time with the same output level from the transmitting antenna. The first quantity measured would be the field level in the absence of the enclosure and the second quantity would be the field level within the enclosure. These are the two quantities needed to solve Equations 6.6 and 6.7, whichever is applicable. However, it is seldom practical to remove and then insert the shield between transmitter and receiver. Consequently, the following method has been adopted as the preferred technique.

A series of tables are first generated, for the given measurement system, with the output level from the transmitting antenna, frequency and distance between receiver and transmitter antennas as variables. The measured received field level is then entered into the table for each combination of the three measured variables. These measurements need to be made only once and are conducted at a location where there is minimum interference from reflected signals. These measured values now become look-up tables for the values of E_1 or H_1 for the specific output level from the transmitter, frequency and distance between receiver and transmitter antenna.

For each particular enclosure for which the SE is being determined the receiver antenna is located inside the shield and the transmitting antenna outside the shield, and measurements of transmitter output level, antenna separation, frequency and receiver response E_2 or H_2 are made. This measured receiver response value of E_2 or H_2 can then be used with the appropriate E_1 or

H_1 value associated with the receiver frequency, transmitter output level and antenna separation distance and Equations 6.6 and 6.7 to compute the electric or magnetic insertion loss at that particular location.

In the radiated measurements the transmitting dipoles are replaced by a top-loaded monopole capable of operating over the frequency band from 10 kHz to 100 MHz. Response measurements are then made inside and outside the facility with $\bar{B}$ and $\bar{D}$ sensors and the measured amplitudes used to compute the ratios of electric and magnetic fields inside and outside the facility in order to assess the influence of penetrations and apertures on the overall facility shielding effectiveness.

In order to implement the measurement procedure for measuring electric and magnetic field shielding effectiveness using electric and magnetic dipoles, the system shown in a functional block diagram form in Figure 6.16 was used.

The system can be described in terms of two major and completely separate subsystems, namely the transmitter and receiver. The transmitter consists of a highly stable frequency synthesizer, power amplifier (100 watts), antenna matching network and either a small-loop magnetic dipole or short electric dipole transmitting antenna. The receiver employs similar antennas and associated matching networks in conjunction with a synchronous detection scheme to detect both in-phase and quadrature components of the received signal.

The system is intended to implement measurements similar to the "small-loop," "short dipole" tests presently employed[14,15] but with substantially greater sensitivity than presently available systems.

The system shown in Figure 6.16 has three basic operational configurations:

- o Low frequency H-field configuration
- o Low frequency E-field configuration
- o High frequency E-field configuration

and these are shown in Figures 16A, B, and C, respectively. The basic differences in these configurations lie in the required antennas and associated matching network for the high and low frequency E-field measurements and in the availability of two different size diameter loops for the H-field measurements. These two loops are one meter and 0.305 meters in diameter; the smaller, however, has a built-in matching network and consequently can be connected directly to the attenuator bypassing the capacitor box as shown by the dashed line in Figure 6.16A.

The CW radiated measurements were conducted using the CW system described in detail in Section 6.1.2 and shown schematically in Figure 6.3, where the antenna used was the top-loaded monopole shown

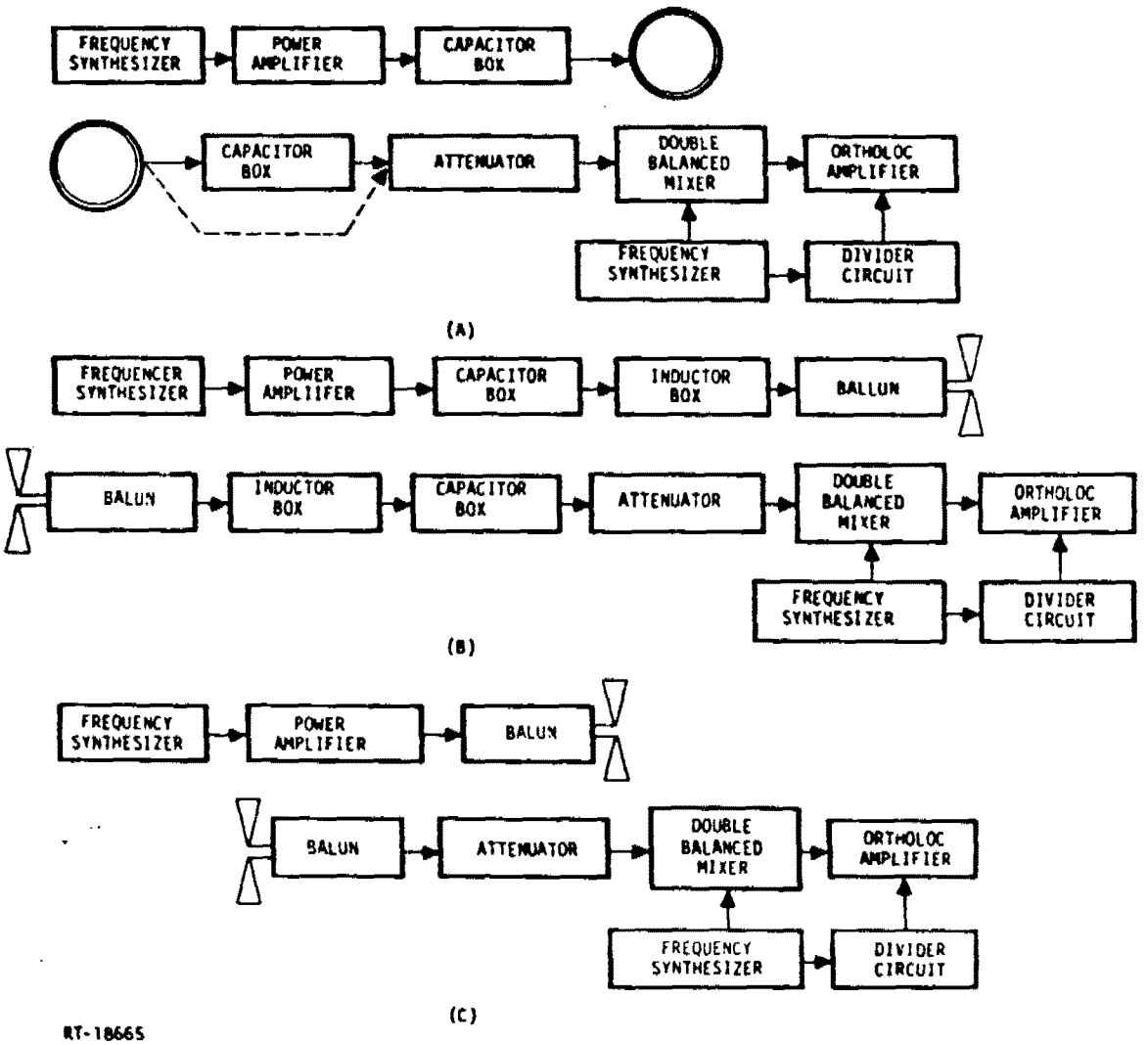

Figure 6.16. Preferred Equipment Configuration for Making Shielding Effectiveness Measurements

in Figure 6.17. This antenna, was designed by the Boeing Company for use on the APACHE (DNA/CINCPAC) Program and a typical calibration curve, at 20 MHz, is shown in Figure 6.18 and 6.19. Detailed calculations for the calibration curves at frequencies from 100 kHz to 100 MHz are available.[16]

6.4.2 Results of Facility Insertion Loss Using Small Electric and Magnetic Dipoles. The measurements were made at five locations within the facility as shown in Figure 6.20. The measure- ments were made at 15 kHz, 45 kHz, 90 kHz, and 1.5 MHz. The two wall thicknesses measured were 92 cm and 33 cm.

A summary of the results are presented in Table 6.7 and are shown plotted in Figure 6.21.

Table 6.7.

Summary of Facility Insertion Loss Measurements

	15 kHz	45 kHz	90 kHz	1.5 MHz	
AVG ATT(H)*	19.3 dB	28 dB	33 dB		92 cm Wall
AVG ATT(E)†				80 dB	Thickness
SE ATT(H)	6.8 dB	11.4 dB	11.3 dB		33 cm Wall
AVG ATT(E)				44.6 dB	Thickness

6.4.3 Results of Measurements Using Radiating Top Loaded Monopole. The location of the antenna for the radiated CW measurements is shown schematically in Figure 6.22 as positions A and B. The position of the reference sensor (B and D) with respect to the measurement points A, B and C is also shown.

The ratios of the interior and exterior electric and magnetic fields for antenna position B, test point A as a function of frequency are shown in Figure 6.23.

For test point B (antenna position B), which lies deeper within the facility the ratios are substantially greater, and are shown as function of frequency in Figure 6.24.

6.4.4 Coupling to Seismic Supports and Cable Trays. During the course of the measurements an attempt was made to determine if significant coupling existed between the building exterior and cable trays or seismic supports in the facility interior.

---

* Average of measurements at three locations.
† Average of horizontal and vertical polarizations at three locations.

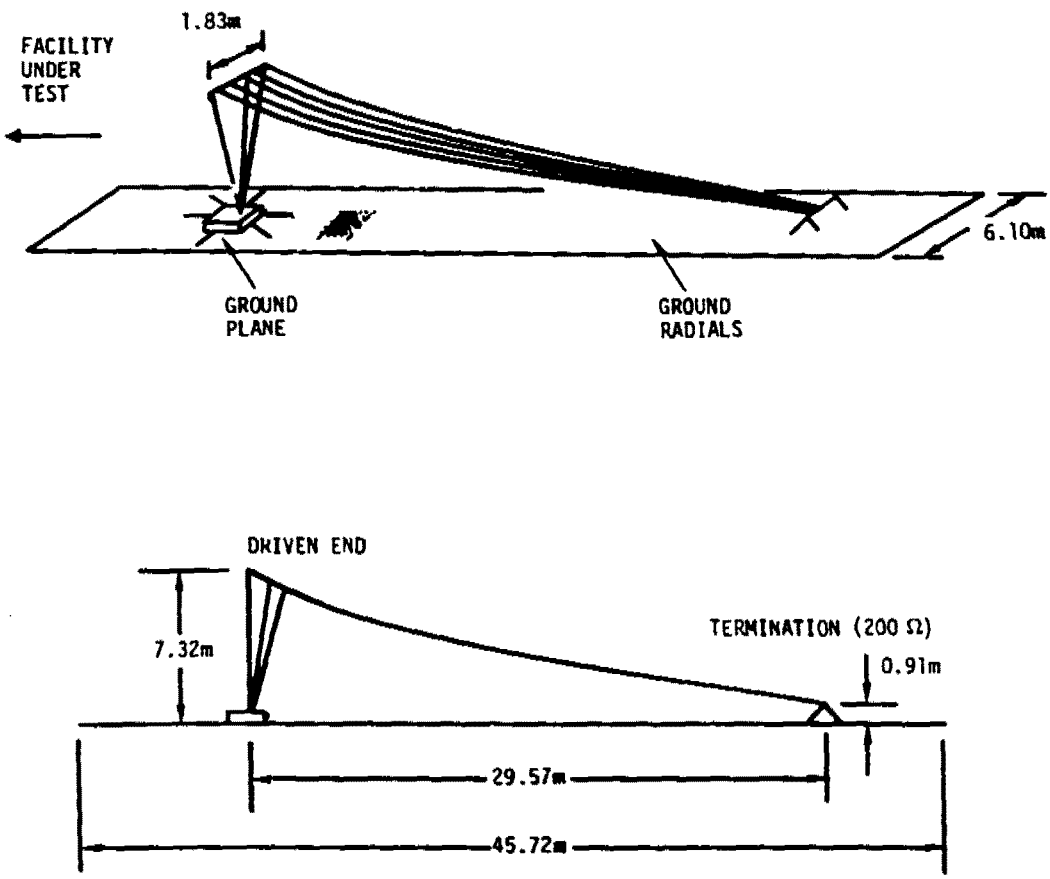

Figure 6.17. Radiated CW Vertically Polarized Antenna

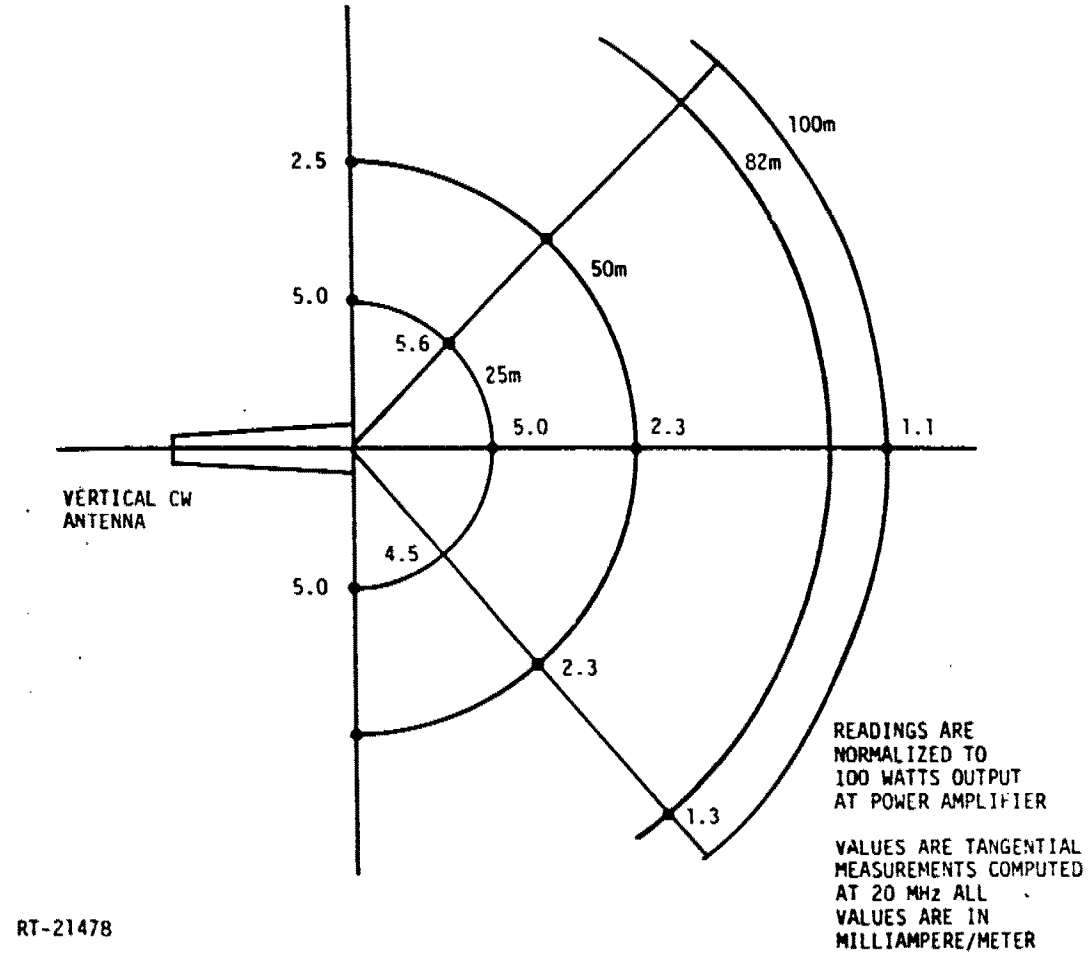

Figure 6.18. Vertical CW Antenna Field Distribution

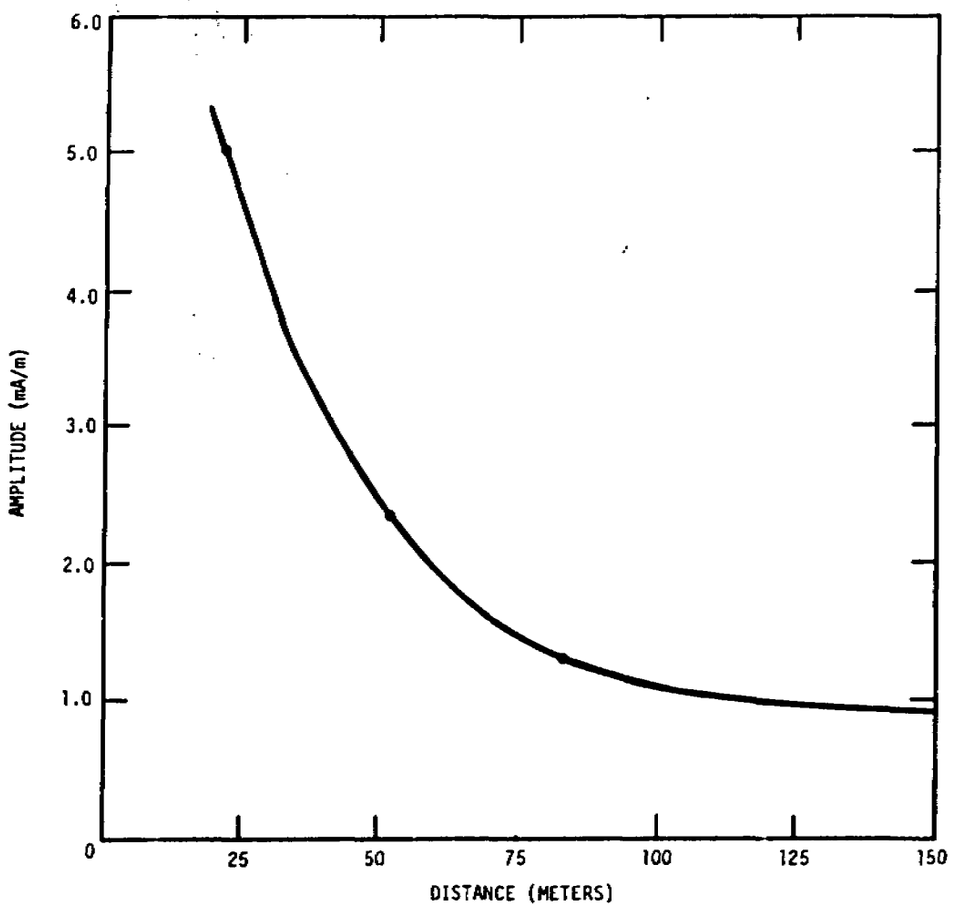

Figure 6.19. Vertical Antenna Field Strength vs Distance (On Axis)

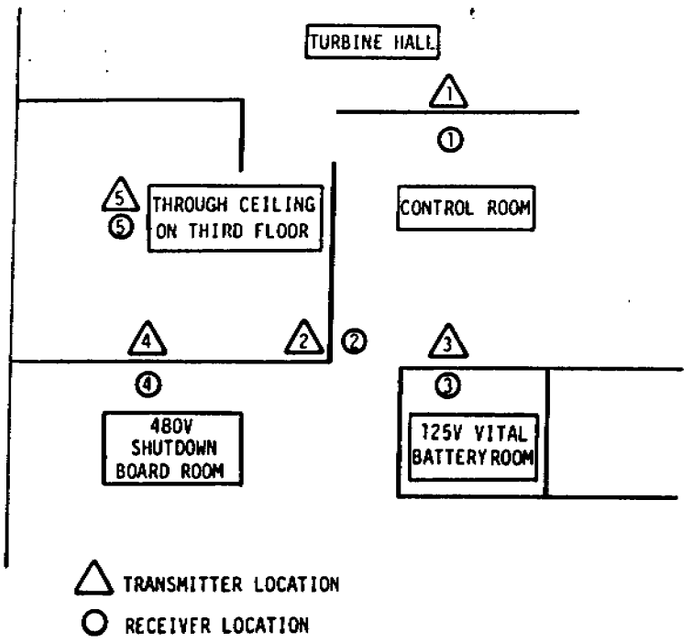

RT-21480

Figure 6.20. Location of Insertion Loss Measurements Within the Facility

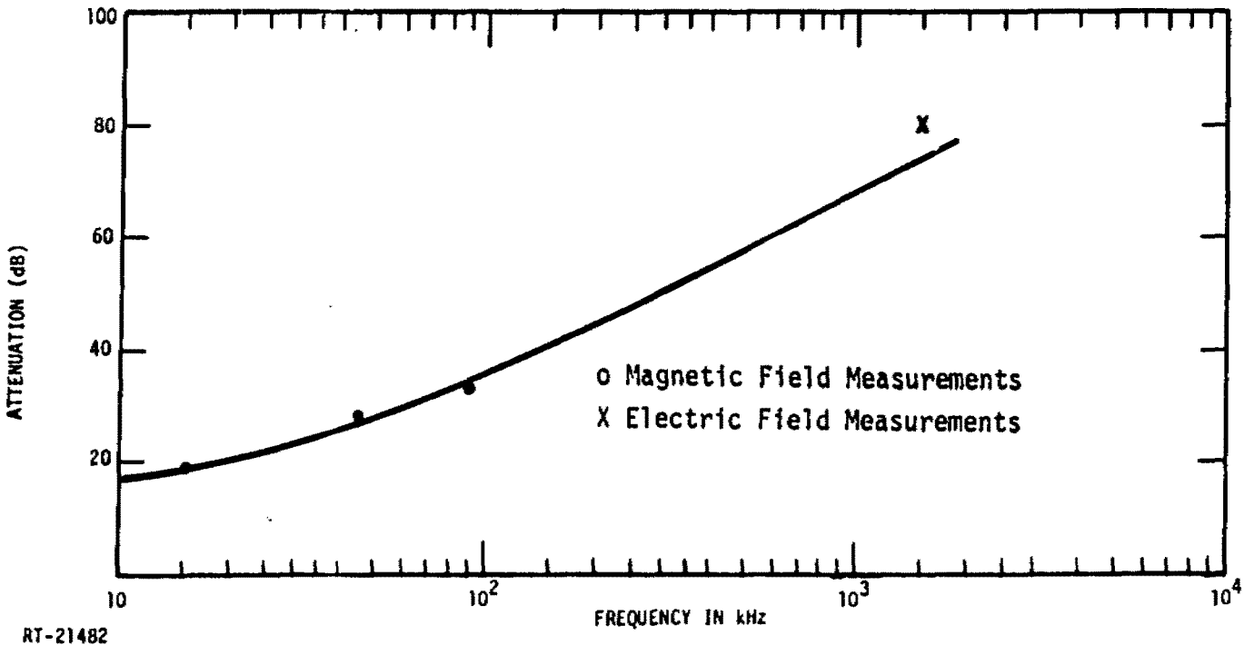

Figure 6.21. Magnetic and Electric Field Insertion Loss as a Function of Frequency (92 cm Wall Thickness)

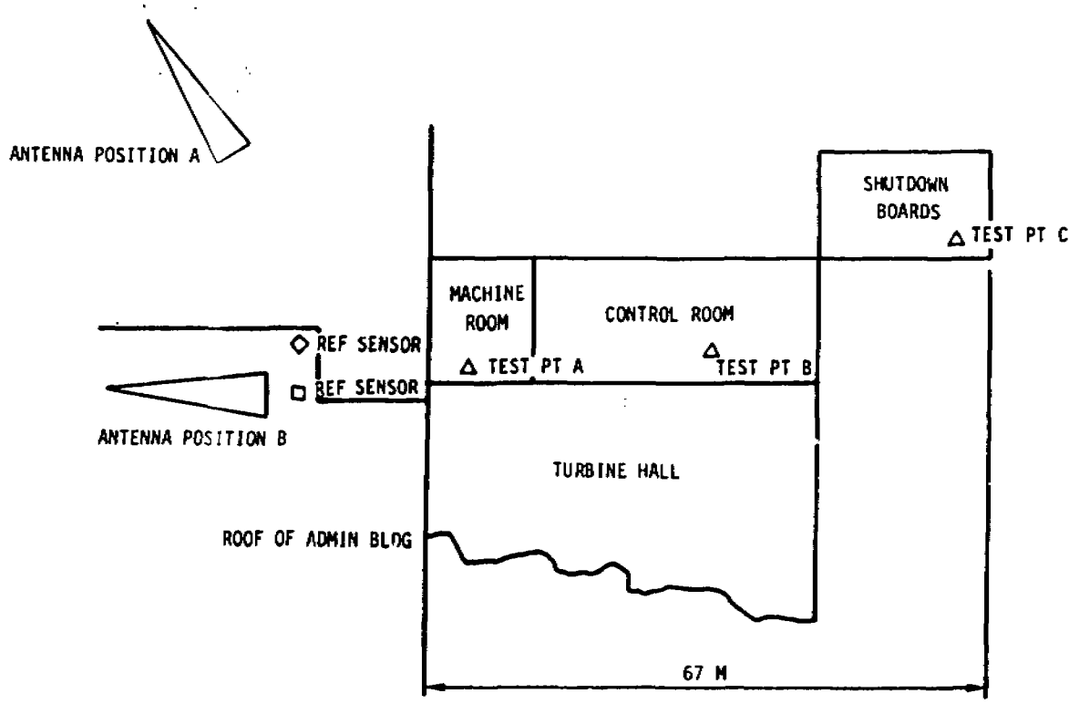

Figure 6.22. Antenna Location for Radiated CW Measurements

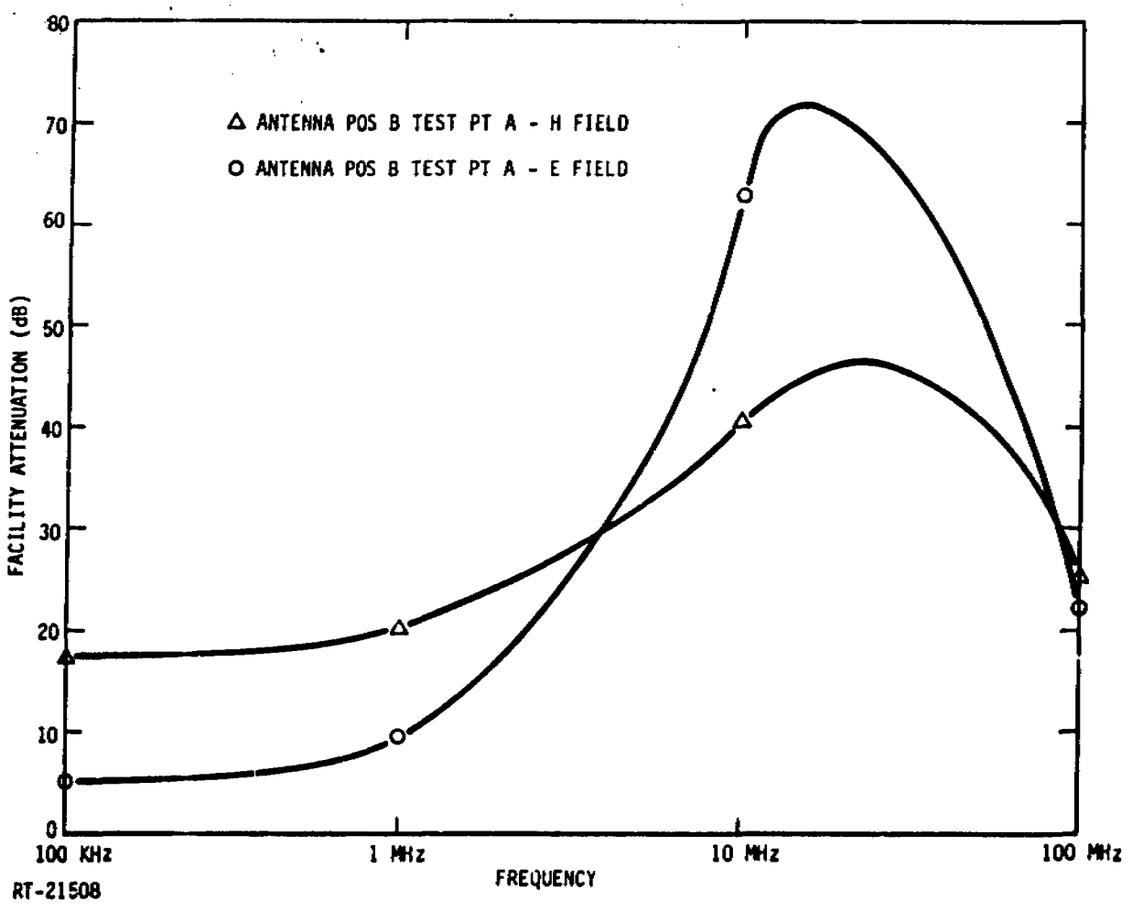

Figure 6.23. Ratios of Interior and Exterior Electric and Magnetic Fields vs Frequency, Antenna Position B, Test Point A

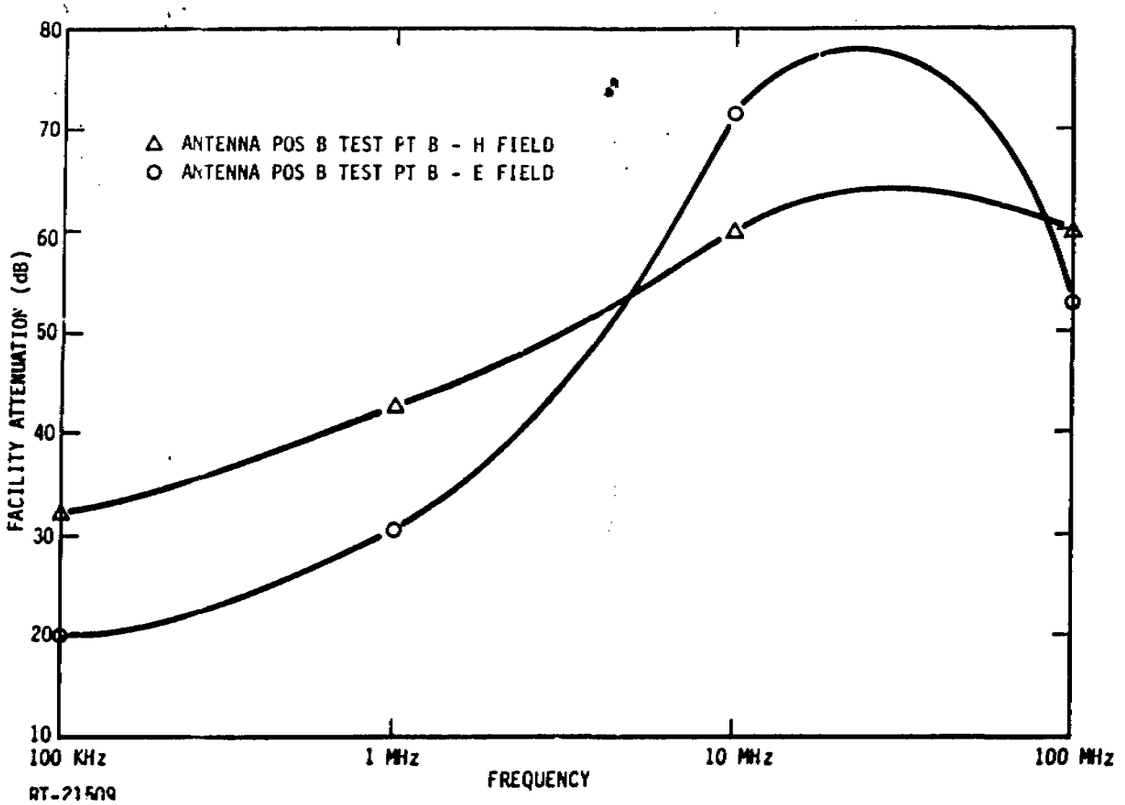

Figure 6.24. Ratios of Interior and Exterior Electric and Magnetic Fields vs Frequency, Antenna Position B, Test Point B